Title

Role of Adaptor Protein AP-3 in Biogenesis of the Regulated Secretory Pathway

Permalink

https://escholarship.org/uc/item/8sx2179c

Author

Sirkis, Daniel Wesley

Publication Date

2012

Peer reviewed|Thesis/dissertation

Role of Adaptor Protein AP-3 in Biogenesis
of the Regulated Secretory Pathway

by

Daniel Wesley Sirkis

DISSERTATION

Submitted in partial satisfaction of the requirements for the degree of

DOCTOR OF PHILOSOPHY

in

Pharmaceutical Sciences and Pharmacogenomics

in the

GRADUATE DIVISION

Acknowledgements

My dissertation work at UCSF was funded by a variety of sources. In my first year of graduate school, I was funded by an award from the UCSF graduate division and a training grant from the National Institute of General Medical Sciences (NIGMS), awarded to the PSPG graduate program. In 2009, I accepted a Ruth L. Kirschstein National Research Service Award (NRSA) predoctoral fellowship from the National Institute of Mental Health (NIMH) that provided funding for tuition, fees, stipend, travel and supplies that has lasted through the end of 2012. I was also given a one-time fellowship incentive award sponsored by Merck and disbursed by the PSPG program, upon my acceptance of the NIMH fellowship. This award enabled me to retain the honorific *Merck scholar*, which I, unfortunately, have not yet forced anyone to address me by. Throughout my time at UCSF, gaps in the funding were filled by a variety of grants awarded to my advisor, Robert Edwards.

Judith Klumperman, of the Utrecht University Medical Center, generously offered her lab space and the Department of Cell Biology's immense expertise in electron microscopy (EM), so that I could learn the techniques required for successful implementation of the Tokoyasu method of immuno-EM. Utrecht University awarded me a generous three-month fellowship that provided for living expenses during my stay in the Netherlands. I would like to thank my sister, Amber, for coming to hang out with me in Holland, even on that ill-fated evening on the Oudegracht. I will not soon forget our journeys to the Prinsengracht, Rotterdam, Den Haag and the beach at Scheveningen.

I would like to thank Kurt Thorn of the UCSF Nikon Imaging Center (NIC), who generously provided, over the course of several years, his redoubtable expertise in microscopy and digital

image analysis. Kurt's helpful advice and the NIC's resources proved to be essential for our studies of regulated secretion from adrenal chromaffin cells.

Greg Szot of the UCSF Diabetes Center provided critical assistance for our analysis of peptide hormone secretion from pancreatic islets. Greg isolated mouse islets, stimulated the release of insulin, and offered helpful advice on the measurement of secreted and cellular insulin.

Jeff Johnson and Nevan Krogan have been essential collaborators in our quantitative proteomic analysis of large dense-core vesicles. Jeff and Nevan have world-class expertise in mass spectrometry and quantitative proteomics, and it has been a pleasure to work with them.

Special thanks are due to Mark von Zastrow, an enthusiastic member of both my qualifying exam and thesis committees, who always asked insightful questions about my dissertation work, starting prior to my qualifying exam in 2008, and continuing over the years during my annual committee meetings. During a conversation in 2008, Mark introduced me to the work of Hsiao-Ping Moore, an investigator whose collaborative work with Lelio Orci on the regulated secretory pathway is highlighted in Chapter 1 of this dissertation.

I became truly interested in basic cell biological questions in 2007 during my spring-quarter lab rotation with Frances Brodsky's group. Although I ultimately chose to pursue a project focused on neuroendocrine secretion in the Edwards lab, my initial excitement about cell biology can be traced to my early days working in the Hooper Foundation. I first met Frances during my PSPG interview in February 2006, and have respected her as a scientist and mentor ever since. Frances' advice throughout my graduate career, spanning from my lab rotation, to my qualifying exam preparations, to four committee meetings, as well as a number of times in between, has proved to be consistently thoughtful, realistic and helpful.

I would like to thank Randy Schekman for giving me a chance to interview for a postdoctoral position in his lab despite the dearth of publications on my CV. I suspect that my interview request was granted based in no small part on the recommendations I received from Mark, Frances and Robert. I would further like to thank Randy for offering me a spot in his lab starting in 2013, so that I can continue to conduct exciting research in cell biology, in addition to picking up some much-needed skills in the field of biochemistry.

Many thanks are due to members of the Edwards lab past and present. During my 2006 lab rotation, I learned the ropes with Zhaolin Hua and Becky Seal. Becky later allowed me to submit some artistically Photoshopped renditions of the Organ of Corti to the journal *Neuron*, which ended up on the cover of the issue containing her first paper describing *VGLUT3* knockout mice. Susan Voglmaier and Tom Hnasko were friendly Wisconsin faces in what was, at the time, a new and strange place for me. Venu Nemani and Germaine Goh frequently provided helpful advice from a grad-student perspective.

Immense thanks are due to Cédric Asensio. Cédric generously agreed to have me join his project when I started in the Edwards lab in July 2007, and over the years, he taught me a variety of techniques and methods of analysis. In addition, we also worked out a number of experimental procedures together, such as TIRF microscopy and chromaffin cell isolation. With respect to the latter procedure, I should note that my early frustration—stemming from my maladroit attempts to cleanly dissect the mouse adrenal medulla—was mitigated by virtue of working it out with a friendly colleague. Near-daily conversations about our ongoing experiments, both before and after the 2010 publication of our paper in the *Journal of Cell Biology*, provided a rich opportunity for brainstorming, thinking about the meaning of experimental results, and, for me, remembering to always think clearly about the question being addressed in any given experiment. Finally, I

would like to add that Cédric is the model of a productive and thoughtful scientist who also happens to be a great family man.

I have always been amazed by the ability of my advisor, Robert Edwards, to keep under control the always-unwieldy array of projects being conducted in the lab. Robert is an MD and a practicing physician, but he is a basic scientist at heart, and his work over the years is a testament to the fact that by asking basic biological questions, your research can have a big impact on scientists' thinking about the mechanisms of disease. I would like to thank Robert for teaching me to articulate scientific questions more clearly, and to pursue them not only with more rigor, but also more vigor.

I am forever grateful to my parents-in-law, Leila and Bill, for offering me their abundant kindness and the comfort of a place to call home in California. Several years ago, Bill told me that his paintings, once completed, never came out better or worse than he had first imagined them, only different. Sometimes I like to think about my experiments this way: rather than seeing the results as being better or worse than I had hoped for, it is helpful to remember that the real excitement of science lies in getting results that are *different* than anticipated.

I suppose my mom and dad got me interested in the natural world. From my mom, I became interested in catching butterflies circa 1989, and although I never became much of a lepidopterist, I still remember catching my first Monarch that was actually a Monarch, and not a lowly Viceroy impostor. From my dad I became interested in catching fish in both fresh and saltwater. At some point I received a poster featuring beautiful illustrations of dozens of different trout species, and I became entranced by the stunning diversity that existed within the *Salmo* genus. As I mentioned during my thesis seminar in November 2012, I would like to thank my dad for telling me exciting stories of drug discovery that he had heard about on NPR, and for helping me get that first lab job

in 2001. I would like to thank my stepmom, Trudy, for making studying for high-school tests on genetics and the cell cycle more fun. I think I probably know less about the cell cycle now (at least in terms of nomenclature) than I did back then, if only because I had it down so well in high school—thanks to Trudy—and have simply forgotten the details in the intervening years.

I dedicate this dissertation to my wife, Jen, without whose pushing and prodding, and—let's face it—cajoling, I might not have finished this work in 2012, or possibly at all. If one were to take the ratio of a person's time spent thinking of and doing for others, to that spent on oneself, I am quite confident that Jen's ratio would be without much rival when compared with a universe of other ratios. She also happens to be a talented scientist, a prolific publisher, and an enthusiastic explicator of genetics to the public at large. Simply put, I am a lucky man to have moved out to San Francisco when I did, and to have met Jen when I did, regardless of whether it happened in the first or second half of 2006.

And now a remembrance of two people who are no longer with me: my mom, Linda Matthews, and my father-in-law, William Yokoyama, who both reminded me to think on these things:

> *...whatsoever things are true, whatsoever things are honest, whatsoever things are just, whatsoever things are pure, whatsoever things are lovely, whatsoever things are of good report; if there be any virtue, and if there be any praise, think on these things.*

And, on the lighter side, a thank you to Richard Axel for reminding us that:

> *The work of the righteous is done by others.*

Statement on published material and co-authorship

A portion of the text of this dissertation is a reformatted reprint of the material as it appears in the following published manuscript:

Chapter 3.

Asensio CS, **Sirkis DW**, Edwards RH. RNAi screen identifies a role for adaptor protein AP-3 in sorting to the regulated secretory pathway. *J. Cell Biol.* 2010; 191(6):1173-87.

Statement of work performed by Daniel W. Sirkis with regard to material included in this dissertation from the above published manuscript by advisor, Dr. Robert H. Edwards:

As the second author of this paper, Daniel Sirkis carried out portions of the RNAi screen in *Drosophila* cells, conducted a variety of experiments in mammalian neuroendocrine PC12 cells, and performed the work involving *mocha* mice. Daniel was also involved in the development of particular experimental procedures, participated in discussions involving data interpretation, and was involved in editing the manuscript prior to submission and during revision.

Abstract

Role of Adaptor Protein AP-3 in Biogenesis of the Regulated Secretory Pathway

Daniel Wesley Sirkis

The regulated secretion of peptide hormones, neuropeptides and many growth factors depends on their sorting into large dense-core vesicles (LDCVs) capable of regulated exocytosis. LDCVs form at the *trans*-Golgi network, but the mechanisms that sort proteins to this regulated secretory pathway and the cytosolic machinery that produces LDCVs remain poorly understood. Recently, we used RNAi to identify a role for heterotetrameric adaptor protein AP-3 in regulated secretion and LDCV formation. Indeed, *mocha* mice lacking AP-3 have a severe neurological and behavioral phenotype, but this has been attributed to a role for AP-3 in the endolysosomal pathway, and the contribution of dysregulated peptide hormone secretion has not been investigated. We now find that adrenal chromaffin cells from *mocha* animals show increased constitutive exocytosis of both soluble and membrane LDCV cargo, reducing the extent of stimulation. We also observe increased basal release of insulin and glucagon from AP-3-deficient pancreatic islet cells, suggesting a widespread disturbance in the release of peptide hormones. AP-3 exists as both ubiquitous and neuronal isoforms, but we find that loss of both is required to impair LDCV production. In addition, we show that loss of the related adaptor protein AP-1 has no effect on regulated secretion but greatly exacerbates the effect of AP-3 RNAi, indicating distinct roles for the two adaptors in formation of the regulated secretory pathway. Finally, quantitative proteomic analysis of LDCVs reveals a number of functionally important membrane proteins whose levels are significantly altered by the loss of AP-3. In particular, ectopic localization of the t-SNARE, syntaxin-1A, to LDCVs may account for the impairment in regulated secretion observed after loss of AP-3. Taken together, these results support the notion that AP-3-directed sorting maintains the normal complement of LDCV membrane proteins, thus ensuring the proper regulation of secretion.

TABLE OF CONTENTS

CHAPTER 3: RNAi SCREEN IDENTIFIES A ROLE FOR ADAPTOR PROTEIN AP-3 IN SORTING TO THE REGULATED SECRETORY PATHWAY

CHAPTER 4: WIDESPREAD DYSREGULATION OF PEPTIDE HORMONE RELEASE IN MICE LACKING ADAPTOR PROTEIN AP-3

CHAPTER 6: CONCLUSIONS AND FUTURE DIRECTIONS

PUBLISHING AGREEMENT   171

LIST OF TABLES

LIST OF FIGURES

CHAPTER 4

CHAPTER 5

CHAPTER 6

CHAPTER 1: BIOGENESIS OF THE REGULATED SECRETORY PATHWAY

REGULATED SECRETION IN PHYSIOLOGY, BEHAVIOR AND DISEASE

The physiological action of peptide hormones, neural peptides and growth factors depends on their sorting to vesicles capable of undergoing regulated exocytosis upon an appropriate stimulus. Secretion of the peptide hormone insulin, for example, is crucial for maintaining glycemia and is thus essential for life. Neural peptides such as opioids are intimately involved in the perception of pain as well as the reward pathway subverted by drugs of addiction, and the growth factor brain-derived neurotrophic factor plays a critical role in learning and memory.

Vesicles of the regulated secretory pathway (RSP), which are generally referred to as large dense-core vesicles (LDCVs) or secretory granules (SGs)[1], form at the *trans*-Golgi network (TGN) and are trafficked to the plasma membrane whereupon they dock, awaiting a physiological signal to secrete their contents into the extracellular space. Despite the incredibly broad importance of the various molecules secreted by the RSP for physiology and disease, and despite the fact that LDCV formation at the TGN has been appreciated for more than half a century, surprisingly little is understood about the molecular mechanisms involved in the selective sorting of proteins into vesicles capable of regulated release, as opposed to those which fuse constitutively (i.e., immediately and indiscriminately) with the cell surface.

---

[1] The nomenclature used varies considerably among investigators, but regulated secretory vesicles are generally referred to as LDCVs in neurons, SGs in endocrine cells, and interchangeably in neuroendocrine cells, such as chromaffin cells.

MODERN STUDY OF THE REGULATED SECRETORY PATHWAY:
MORPHOLOGICAL ORIGINS

The modern era of study of the RSP can be traced to the pioneering work of the great morphologists, Marilyn Farquhar, George Palade and Lelio Orci. Farquhar, notably, appears to have been the first to observe that the LDCVs of neuroendocrine and exocrine cells are formed at the Golgi apparatus, while working on her doctoral dissertation at the University of California, San Francisco (Farquhar and WELLINGS, 1957). Subsequent electron microscopic (EM) work by Farquhar extended these observations to the LDCVs found in neutrophils (Fig. 1), eosinophils and monocytes (Bainton and Farquhar, 1966; 1970; Nichols et al., 1971). Work in the same era by Palade using both traditional thin-section EM and autoradiographic pulse-chase analysis established the general itinerary that secretory proteins take within eukaryotic cells, and in particular demonstrated that pulse-labeled proteins in exocrine cells move from the endoplasmic reticulum to the Golgi, and from the TGN to so-called condensing vacuoles (i.e., immature secretory granules) (CARO and Palade, 1964; JAMIESON and Palade, 1967).
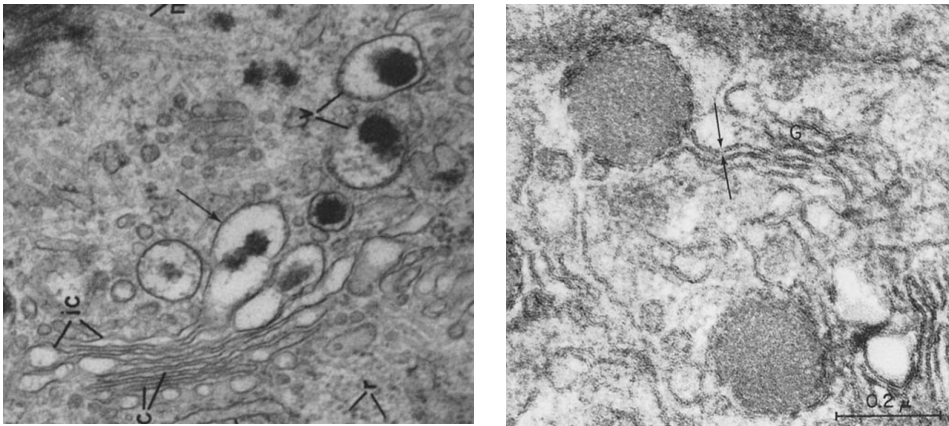
Figure 1. Left, condensing neutrophil azurophilic granules shown budding off the *trans* face of the Golgi apparatus, X 50,000 (Bainton and Farquhar, 1966). Right, a budding heart atrial granule is shown with its membrane still continuous with that of the Golgi, X 120,000 (JAMIESON and Palade, 1964). Reproduced under the noncommercial third-party reuse licensing agreement of the Rockefeller University Press.

Meanwhile, Orci's pioneering morphological studies on the pancreatic β cell resulted in a number of classic observations. In particular, he provided the first unequivocal morphological evidence that insulin secretion occurs by fusion of secretory granules with the plasma membrane (Orci et al., 1973). Second, using the techniques of immuno-EM, Orci demonstrated that proinsulin is sorted from the TGN to clathrin-coated immature SGs, where it is then converted to mature insulin (Fig. 2) (Orci et al., 1985; 1987b).
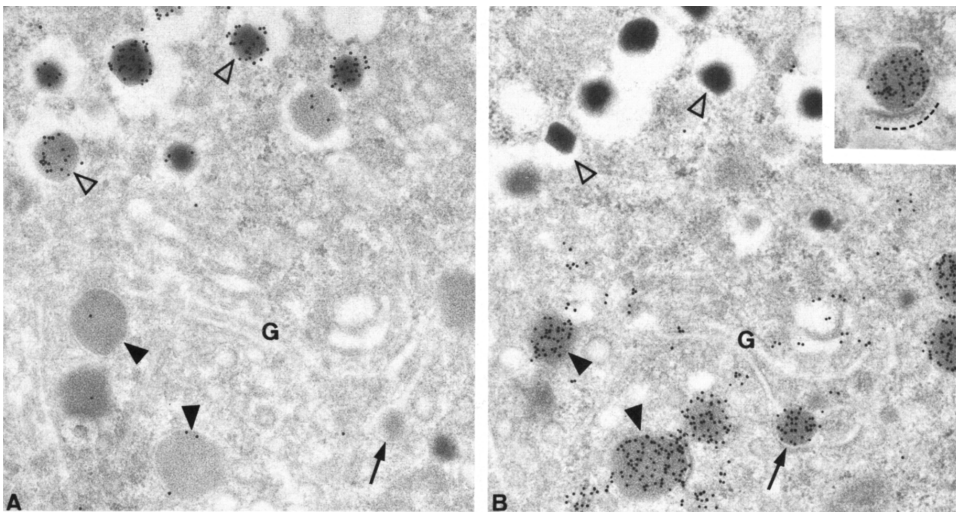
Figure 2. Immunolabeling of consecutive sections through the Golgi region of a β cell. (A) A monoclonal antibody (mAb) specific for insulin labels mature secretory granules, but not the Golgi or immature granules. (B) A proinsulin mAb labels the Golgi and immature granules, but not mature granules. The upper right inset depicts a clathrin coat on an immature granule (Orci et al., 1987b). Reproduced with permission from Elsevier.

Finally, working with Hsiao-Ping Moore, Orci demonstrated that while the constitutive protein hemagglutinin (HA) and proinsulin could be detected together within the Golgi cisternae of pancreatic β cells, these two proteins diverged at the TGN. Specifically, proinsulin was found to be concentrated in nascent SGs, while HA was found in other regions of the TGN and also in small, clear, constitutive secretory vesicles distributed throughout the cytoplasm (Orci et al., 1987a). Thus, at this point there was compelling morphological evidence for separation of the two pathways at the level of the TGN, but it was still unclear how such separation was achieved.

BIOCHEMICAL DISSECTION OF REGULATED SECRETORY PATHWAY BIOGENESIS

After the ground was laid by the morphologists, a number of biochemical studies began providing further insight into the formation of the RSP. For example, a landmark study from Regis Kelly's lab established for the first time the presence of constitutive *and* regulated secretory pathways operating in the same cell. This was demonstrated, first, by the absence of an endogenously expressed viral glycoprotein from adrenocorticotropic hormone (ACTH)-containing LDCVs despite the fact that this protein was glycosylated (and thus trafficked through the Golgi) in a manner similar to ACTH, and, second, by the fast, secretagogue-independent plasma membrane delivery of the glycoprotein, and stimulus-dependent secretion of ACTH (Gumbiner and Kelly, 1982). This finding was later confirmed and extended by Moore in her collaboration with Orci [see above; (Orci et al., 1987a)]. Next, Moore and Kelly demonstrated the pH-dependence of selective sorting to the RSP by showing that alkalinization by chloroquine treatment could shift newly synthesized ACTH from the regulated to constitutive secretory pathway (Moore et al., 1983). Given the later finding that aggregation of the chromogranin family of proteins within the lumen of the TGN was dependent on low pH and high levels of calcium, it eventually became clear that aggregation was an important and general mechanism for sorting of soluble cargo into the RSP (Chanat and Huttner, 1991). In addition, a groundbreaking paper by Tooze and Huttner demonstrated budding from the TGN of constitutive and regulated cargo into distinct vesicles in a cell-free system, and this *in vitro* preparation later enabled the identification of a number of proteins involved the budding process (Tooze and Huttner, 1990).

In the era following the morphological elucidation of RSP biogenesis at the TGN and the ultrastructural and biochemical demonstrations that constitutive and regulated secretory cargoes diverge upon exit from the Golgi, investigators began trying to understand the nature of the

driving force for LDCV formation, as well as how proteins are selectively sorted into one pathway or the other.

LUMENAL INTERACTIONS AS A SORTING MECHANISM

I. The Role of chromogranin B

As described above, it was known that the chromogranin family of proteins aggregated at the low-pH and high-calcium environment of the TGN. Furthermore, one such family member, chromogranin B (CgB), was found to exist in two states in neuroendocrine PC12 cells: a soluble form which was released into the medium upon secretion, and a membrane-associated form that stuck to the plasma membrane after exocytosis (Pimplikar and Huttner, 1992). Since it was known that CgB could self-associate, the membrane-associated form was hypothesized to act as an anchor point between the lumenal membrane leaflet and the aggregated dense core. CgB was also shown to have a conserved N-terminal disulfide-bonded loop that was essential for its targeting to the RSP (Chanat et al., 1993). Interestingly, although addition of reducing agent was sufficient to reroute CgB to the constitutive secretory pathway, this treatment had no effect on the related protein secretogranin II (SgII), which has no comparable disulfide bonds. On the other hand, moderate overexpression of CgB in the pituitary AtT-20 cell line significantly enhanced the retention of ACTH within the RSP, suggesting that the innate aggregative properties of CgB are capable of 'trapping' some peptide hormones within the dense core (Natori and Huttner, 1996). Although the N-terminal disulfide-bonded loop was known to be essential for CgB sorting to the RSP (Chanat et al., 1993), an exogenously expressed mutant CgB lacking the loop was only mis-sorted when endogenous granin synthesis was inhibited, implying that homophilic CgB interactions are sufficient to mediate sorting to the RSP (Krömer et al., 1998). The CgB disulfide-bonded loop was next demonstrated to be sufficient for sorting to the RSP, since it was capable of rerouting of constitutive protein, α_1-antitrypsin, to the RSP. Interestingly, the α_1-antitrypsin fusion

protein did not aggregate in the TGN, but did bind to TGN membranes, suggesting that aggregation of lumenal proteins is not required for sorting to the RSP (Glombik et al., 1999).

II. Secretogranin III and cholesterol

Further work demonstrated a requirement for cholesterol in the budding of LDCVs from the TGN, although constitutive vesicles were found to be similarly dependent on cholesterol, so it is unlikely that this finding is informative with respect to a selective sorting mechanism (Wang et al., 2000). More-recent work has suggested that another granin protein, SgIII, is capable of binding cholesterol and may thus act as a bridge between the membrane and granin-containing aggregates (Hosaka and Watanabe, 2010). This model, however, does not explain why dense-cored aggregates end up in vesicles containing the proper complement of membrane proteins—that is, those that confer upon the vesicle the ability to undergo regulated exocytosis.

III. Carboxypeptidase E

Several high-profile papers from the lab of Peng Loh have put forth ideas similar to those advanced for CgB and SgIII. For example, Loh claimed that the LDCV-resident protein carboxypeptidase E (CPE) existed in both a soluble and membrane-associated form, with the latter capable of interacting with prohormones (e.g., pro-opiomelanocortin [POMC] and proinsulin) but not constitutively secreted proteins (Cool et al., 1997). Furthermore, CPE knockdown inhibited regulated secretion of POMC-derived peptides, and CPE-mutant mice were found to have dysregulated ACTH secretion. However, this finding remains contentious, since a paper published later that year demonstrated normal targeting of pro-insulin in CPE-mutant mice (Irminger et al., 1997).

IV. Chromogranin A as an "on/off" switch

Next, Loh's lab published another prominent yet controversial paper claiming that chromogranin A (CgA) represented an "on/off" switch for RSP biogenesis (Kim et al., 2001). This paper claimed that loss of CgA by potent knockdown was associated with loss of other granule proteins such as CgB and CPE, in addition to synaptotagmin, the calcium sensor for regulated release. The loss of these proteins was associated with a loss of neuropeptide secretion, which could be restored by reintroduction of CgA. However, as with the finding that CPE could act as a sorting receptor, a paper published several years later claimed that CgA knockdown in a variety of clonal PC12 cell lines resulted in no clear correlation with CgB levels, thus contradicting the central claim by Loh's group that CgA sits atop the hierarchy of proteins involved in RSP biogenesis (Malosio et al., 2004). The most plausible explanation for the apparently conflicting results is that Loh's lab might have inadvertently selected for clones lacking a robust RSP by relying heavily on the use of stable transformants isolated after transfection with CgA antisense plasmids—clonal PC12 cell lines lacking regulated secretion have been extensively characterized by others (Corradi et al., 1996; Malosio et al., 1999).

V. Role of lumenal interactions tested in knockout mice

Several groups have independently generated CgA knockout (KO) mice over the last several years (Mahapatra et al., 2005; Hendy et al., 2006; Montesinos et al., 2008). While there were significant discrepancies among the reported phenotypes, including whether the KOs had normal numbers of chromaffin granules and whether their size was altered, several changes were consistently observed: (i) coordinate upregulation of other granins, including CgB and SgII, in neuroendocrine tissue, (ii) decreased adrenal catecholamine levels, and (iii) increased serum or urinary catecholamine levels. While these findings are consistent with a role for CgA in chromaffin granule monoamine storage, the only paper that looked directly at regulated secretion by amperometry found the KO mice to have an ~30% reduction in catecholamine secreted per

exocytotic event, but no reduction in the frequency of events (Montesinos et al., 2008). Taken together, these results cast considerable doubt on the hypothesis that CgA acts as an "on/off" switch for RSP formation *in vivo*. In addition, the reported phenotype for CgB KO mice was remarkably similar, with an ~30% reduction in monoamine stored and released per chromaffin granule (Díaz-Vera et al., 2010). Further, the CgA/B double KOs reported last year were found to be viable and fertile, and still had chromaffin granules with an electron-dense core. These double KOs were reported to have a slightly more remarkable ~50% reduction in adrenal monoamine content, although regulated secretion appeared to be largely intact (Díaz-Vera et al., 2011). The results of these *in vivo* studies thus make it quite unlikely that the granins act at the top of the hierarchy of factors involved in the biogenesis of the RSP, although it is clear that they do play a role in the vesicular retention of monoamines. A plausible explanation for the relatively mild phenotypes reported—besides the obvious one that the conclusions from the earlier, cell-based CgA studies were overstated—is that there are many granin-related proteins, and at least several of these appear to be significantly upregulated in response to the loss of CgA and/or CgB, thus potentially moderating the KO phenotype.

THE ROLE OF CYTOSOLIC FACTORS

I. Arf

A handful of cytosolic factors have been implicated in the formation of secretory vesicles from the TGN in both neuroendocrine and non-neuroendocrine cells. However, all of the proteins identified thus far in neuroendocrine cells have been shown to be involved in the formation of vesicles of both the constitutive *and* regulated pathways. Huttner and Tooze were the first to explore this issue, and they initially demonstrated a requirement for GTP hydrolysis in the formation of secretory vesicles at the TGN (Tooze et al., 1990). Brefeldin A was next demonstrated to block the formation of both types of vesicles, and the defect appeared to arise

from a block in TGN budding *per se*, rather than simply from disassembly of the Golgi (Rosa et al., 1992; Fernandez et al., 1997). Thus, an Arf-dependent GTP hydrolysis step appeared to be required for formation of secretory vesicles, as was known to be the case for COPI-dependent budding reactions in other regions of the Golgi (Tanigawa et al., 1993). Subsequently, purified Arf1 was shown to stimulate secretory vesicle formation (Chen and Shields, 1996), even when added to COPI-depleted cytosol (Barr and Huttner, 1996), demonstrating that the budding process involved was distinct from the intra-Golgi, coatomer-dependent budding reaction.

II. Heterotrimeric G proteins and lipid-modifying enzymes

Heterotrimeric G protein subunits have also been found to stimulate formation of both types of secretory vesicles (Barr et al., 1991; Leyte et al., 1992). In addition, a similar stimulatory effect on budding was identified for phosphatidylinositol transfer protein (PITP), and, remarkably, the yeast PITP, Sec14p, had comparable activity in the budding reaction, despite having no sequence homology to mammalian PITP (Ohashi et al., 1995). Phospholipase D was similarly found to promote formation of both types of secretory vesicles (Chen et al., 1997), and was shown to potentiate the effect of PITP, thus implicating phosphoinositides and phosphatidic acid in the TGN budding reaction (Tüscher et al., 1997; Siddhanta and Shields, 1998).

III. Protein kinase D

A host of other cytoplasmic factors has been implicated in secretory vesicle formation, albeit in non-neural cells. For example, Vivek Malhotra's lab has uncovered an important role for protein kinase D (PKD) in this process (Bossard et al., 2007), but it is currently unknown what role PKD plays in LDCV formation. Thus, we are left with a varied and incomplete list of cytosolic factors, all of which seem to be equally important for formation of constitutive and regulated vesicles, and the main investigators involved in elucidating their role have moved on to other fields. It remains possible that the cytosolic machinery involved in secretory vesicle budding and fission are

identical for the two pathways, but at the very least, there must be a mechanism to concentrate the relevant membrane proteins onto one vesicle class or the other, thus conferring upon them their respective secretory behavior. However, judging from the chromogranin KO and CPE-mutant mouse data produced thus far, aggregation within the lumen of the TGN is not sufficient to trap functionally important membrane proteins (e.g., synaptotagmin) into nascent LDCVs—if it were, one would expect these mice to have severe deficiencies in regulated secretion, but this is not the case.

IS THERE A ROLE FOR COAT PROTEINS IN LDCV FORMATION?

Nearly all membrane budding events other than secretory vesicle formation have been proposed to involve cytoplasmic coat proteins which deform the donor membrane into a bud prior to fission and vesicle formation. Prior to such bud formation, cytosolic adaptor proteins interact with the tails of membrane proteins anchored in the donor membrane such that the proteins to be transported are selected for inclusion within the nascent bud. Processes such as this have been described for COPII-mediated exit from the endoplasmic reticulum, COPI-mediated vesicle formation in the Golgi, as well as endocytosis and transport from one class of endosomes to another.

No coat proteins are currently known to be involved in the biogenesis of neuroendocrine LDCVs, but several recent papers have identified a requirement for such coats in the formation of endothelial and exocrine granules. First, the secretory granule of endothelial cells, the Weibel-Palade body (WPB), has been shown to require the adaptor protein AP-1 and clathrin for its biogenesis (Metcalf et al., 2008). Interestingly, the AP-1-interacting proteins aftiphilin and γ-synergin were later found to play a role specifically in conferring secretagogue sensitivity to WPBs, although these proteins are not required for the formation of WPBs *per se* (Lui-Roberts et

al., 2008). In addition, the salivary gland mucin-type glue granules of *Drosophila* have recently been shown to require an AP-1/clathrin coat for their formation at the TGN (Burgess et al., 2011). The requirement for AP-1 in the biogenesis of both WPBs and glue granules appeared to be relatively specific, in that loss of the related adaptor protein, AP-3 (whose function will be discussed in greater detail in Chapter 2), did not appear to affect biogenesis. In contrast, recent findings from our lab have demonstrated an important role for AP-3 in sorting proteins to the RSP in neuroendocrine cells (to be described in Chapters 3 and 4). Interestingly, our findings are somewhat analogous to those of the Cutler lab's on aftiphilin and γ-synergin, in that the loss of AP-3 in neuroendocrine cells does not abolish LDCV formation *per se*, but instead affects the regulation of secretion (Asensio et al., 2010). In addition, since clathrin, and thus AP-1, have been shown to be dispensable for the biogenesis of insulin granules (Molinete et al., 2001), the reported roles for these proteins in endothelial and exocrine cells serves to highlight differences in the biogenesis of distinct types of LDCVs—that is, the formation of WPBs and exocrine granules appears to differ in important ways from that of neuroendocrine LDCVs.

SORTING OF MEMBRANE PROTEINS INTO THE RSP

It is clear from the available data that aggregation plays a role in the sorting of some soluble cargo proteins, such as the granins, to the RSP. In addition, it is understood that an array of cytosolic factors are involved in the budding of multiple types of secretory vesicles from the TGN. But how are membrane proteins sorted into one pathway versus the other? The following section highlights findings for three well-characterized RSP membrane proteins.

I. Peptidylglycine α-amidating monooxygenase

Peptidylglycine α-amidating monooxygenase (PAM) is concentrated on LDCVs, where it catalyzes the C-terminal amidation of many peptide hormones, a modification that is often crucial for biological activity (Eipper et al., 1992). Early experiments on PAM trafficking indicated that its cytosolic tail was important for efficient sorting to the RSP. For example, pulse-labeled PAM is barely detected at the cell surface after a one-hour chase, but a significant fraction of PAM lacking the cytosolic tail reached the cell surface in this time period, suggesting re-routing to the constitutive pathway (Milgram et al., 1993; 1994). These experiments implied that simple trapping of the lumenal domain of PAM by aggregation was not sufficient to retain this protein within the RSP. Somewhat surprisingly, though, subsequent studies by this group indicated that the lumenal enzymatic domains of PAM, when expressed heterologously in AtT-20 cells, contained targeting information sufficient for their incorporation into LDCVs (Milgram et al., 1996). However, newer experiments done in primary anterior pituitary cells, rather than the AtT-20 pituitary cell line, demonstrated that a form of PAM completely lacking the lumenal domain still trafficked efficiently to the RSP, while an irrelevant membrane protein, Tac, did not (Meskini et al., 2001). In addition, phosphorylation of the PAM cytoplasmic domain was shown to increase the efficiency of its trafficking to the RSP (Steveson et al., 2001). Thus, a variety of experiments have demonstrated that the cytoplasmic domain of PAM is sufficient and possibly required for efficient targeting to the RSP. The PAM literature described above thus shows that it is important to consider potential discrepancies that may arise regarding the trafficking of a given protein in primary neuroendocrine cells versus in their corresponding tumor-derived cell lines (e.g., AtT-20 and PC12) which produce many fewer LDCVs than their primary counterparts (Meskini et al., 2001) and may thus have more limited sorting capacity.

II. P-selectin

The cell-adhesion molecule P-selectin is an endothelially-expressed protein that localizes to WPBs, a type of regulated secretory granule that has some hallmarks of LDCVs, but is in some respects a lysosome-related organelle (see below for a comparative discussion of these two types of organelle). Daniel Cutler's lab has characterized in detail the trafficking of P-selectin, both in heterologous systems and, more recently, in primary endothelial cells. Early trafficking studies in PC12 cells using P-selectin chimeras in which the lumenal domain was replaced with horseradish peroxidase as a reporter resulted in the identification of a cytoplasmic sorting signal required for trafficking to LDCVs (Blagoveshchenskaya et al., 1999). Heterologous expression of von Willebrand factor (vWF), the main soluble component of WPBs, in AtT-20 cells was later shown to be sufficient to recruit membrane proteins such as CD63 and P-selectin—both of which normally localize to WPBs in endothelial cells—to wWF-containing "pseudogranules" (formed due to the expression of vWF). If the cytoplasmic trafficking signal in P-selectin was mutated, however, vWF co-expression was no longer sufficient to retain P-selectin within the pseudogranules (Blagoveshchenskaya et al., 2002). This finding suggested that both lumenal and cytosolic interactions were at play in the targeting of P-selectin, but that cytosolic interactions were at the top of the sorting hierarchy.

This model was thrown out several years later, though, when Cutler's lab began trafficking studies in human umbilical vein endothelial cells (HUVECs). Using this system, they found that the lumenal domain of P-selectin alone was sufficient to direct sorting to WPBs, and that the previously-identified cytosolic motifs were important for retrieval of P-selectin from the cell surface to WPBs (Harrison-Lavoie et al., 2006). Thus, as in the situation described above regarding discrepancies in PAM trafficking in cells lines versus primary cells, the dependence on particular sorting signals for P-selectin's trafficking varies depending on the cell type being studied. However, in the case of PAM, the use of primary cells underscored the importance of

cytosolic trafficking interactions, while in the case of P-selectin, the use of primary cells revealed the primacy of lumenal interactions. Taken together, it is thus apparent that different membrane proteins rely on different types of interactions to sort to the RSP, and that investigators should be mindful of the limitations of their chosen model system, as well as judicious in generalizing their conclusions to other RSP proteins.

III. The vesicular monoamine transporter

A series of papers from our lab has demonstrated that the vesicular monoamine transporter[2], VMAT, localizes to LDCVs in neuroendocrine cells (Liu et al., 1994). When compared with VMAT, the closely related vesicular acetylcholine transporter, VAChT, was found to traffic differentially in neuroendocrine PC12 cells, but not in non-neural CHO cells (Liu and Edwards, 1997). This suggested that in cells with a regulated pathway, factors exist which are capable of recognizing a motif in VMAT and directing it to the RSP, while proteins (e.g., VAChT) without such a motif will sort to the constitutive pathway, and subsequently be directed to endosomes and synaptic vesicles. The first trafficking signals in VAChT and VMAT to be identified were of the acidic dileucine type, specifically RS<u>E</u>RDV<u>LL</u> for VAChT and K<u>EE</u>KMA<u>IL</u> for VMAT. Alanine-scanning mutagenesis identified the pair of dileucine residues to be critical for efficient endocytosis (Tan et al., 1998), and subsequent work on VAChT found that phosphorylation (or phosphomimetic mutation) of the serine residue five positions upstream of the dileucine partially routed VAChT to LDCVs (Krantz et al., 2000). Interestingly, this addition of negative charge at the -5 position rendered the VAChT motif more similar to that in VMAT, thus giving a further clue to VMAT's ability to sort to the RSP. As predicted from this finding, mutation of VMAT's upstream acidic residues to alanine (K<u>EE</u>KMAIL → K<u>AA</u>KMAIL) reduced its localization to

---

[2] There are two mammalian isoforms of VMAT, with VMAT1 being expressed in adrenal chromaffin cells and VMAT2 expressed in neurons (Peter et al., 1995). Both isoforms sort efficiently to LDCVs when expressed in neuroendocrine cells, while endogenous VMAT2 localizes to both synaptic vesicles and LDCVs in neurons (Nirenberg et al., 1996). The cytoplasmic dileucine motif is essentially identical in VMAT1 and 2.

LDCVs (Krantz et al., 2000). Further, metabolic labeling studies showed that wild type VMAT does not appear at the cell surface before entering LDCVs, while the EE/AA mutant reaches the cell surface shortly after labeling. Importantly, the EE/AA mutant is internalized from the cell surface with kinetics comparable to wild type VMAT (Li et al., 2005). Thus, this motif appears to act in the biosynthetic pathway, presumably at the level of the TGN, where LDCVs form. In addition to the work described above on PAM and P-selectin, these findings provided some of the first evidence for a cytosolic motif involved in membrane protein targeting to the RSP.

Hence, it is clear that a sorting motif in the C-terminal cytoplasmic tail of VMAT is required for its sorting to the RSP. But is this motif sufficient? Work from another lab independently confirmed the requirement of VMAT's cytoplasmic tail for RSP targeting, but demonstrated that replacement of VAChT's cytoplasmic tail with VMAT's was not sufficient to reroute the chimeric protein to LDCVs (Yao and Hersh, 2007). Rather, only a chimeric protein that contained both VMAT's large, N-terminal, lumenal loop in addition to the C-terminal cytoplasmic tail efficiently sorted to LDCVs. Further, treatment of cells with an inhibitor of N-linked glycosylation was sufficient to inhibit sorting of VMAT to LDCVs, but had no effect on VAChT localization (Yao and Hersh, 2007). Taken together, these findings suggest that although VMAT's cytoplasmic tail is required for sorting to the RSP, VMAT normally relies on a combination of both lumenal and cytoplasmic interactions for proper sorting.

THE ROLE OF SORTING RECEPTORS

The basic concept of a sorting receptor involves a transmembrane protein with a lumenal domain capable of recognizing and interacting with soluble cargo in the originating organelle, and a cytoplasmic domain capable of interacting with vesicle budding machinery, often in the form of heterotetrameric adaptor proteins. Sorting receptors such as the mannose 6-phosphate receptors

(MPRs) have been understood to operate within TGN for many years. These proteins interact with lysosomal hydrolases on the lumenal side and the AP-1 and GGA adaptors on the cytoplasmic side (Saftig and Klumperman, 2009). This interaction enables the concentration of hydrolases within transport vesicles bound for endosomes, with the end result being the delivery of hydrolases to lysosomes.

I. CgB and CPE as sorting receptors

What is the evidence for sorting receptors being involved in the delivery of cargo to the RSP? Membrane-associated forms of CgB and CPE were discussed above for their potential role in forming 'anchor points' for association between a lumenal aggregate and the inner membrane leaflet of a nascent LDCV. However, the relative importance of these two proteins in sorting cargo has been called into question with the mild phenotype reported in the CgB-null mice (Díaz-Vera et al., 2010) and the conflicting data on CPE's importance *in vivo* (Irminger et al., 1997). In addition, CgB is a strictly soluble secretory protein, and CPE exists mostly as a soluble protein as well, although a small fraction of the total pool may adopt a transmembrane form with a short cytoplasmic tail (Dhanvantari et al., 2002). Thus, it is difficult to envision either of these proteins fulfilling the role of a canonical sorting receptor.

II. Sortilin as a BDNF sorting receptor

One well-characterized transmembrane protein, the Vps10 domain-containing protein sortilin, has been proposed to act as a sorting receptor for BDNF within the RSP (Chen et al., 2005). The single study to explore this possibility mapped interaction domains between the two proteins and demonstrated that co-expression of mutant proteins unable to interact resulted in reduced regulated and increased constitutive secretion of pro-BDNF in neurons. However, this finding has not been explored further, and sortilin is also known to act as a cell surface receptor for secreted pro-BDNF (Teng et al., 2005). Further, sortilin was more recently shown to aid in the sorting of

pro-BDNF to lysosomes rather than the secretory pathway (Evans et al., 2011). Thus, it is currently unclear which of these modes of interaction (extracellular vs. lumenal) as well as which trafficking pathway (secretory vs. endocytic) predominates in neurons.

SECRETORY GRANULE MATURATION

In addition to the formation of LDCVs at the TGN, it has been appreciated for many years that newly formed LDCVs undergo a process of maturation. Indeed, the great morphologists Palade and Farquhar, using traditional thin-section EM as well as EM autoradiography, and Orci, using immuno-EM labeling, distinguished between immature and mature secretory granules (Smith and Farquhar, 1966; Orci et al., 1987b), which they showed were distinct in terms of shape, size and content, including the presence of small patches of a clathrin associating with immature, but not mature, granules. For years after these observations, though, a basic biochemical understanding of the process of maturation was lacking. The development of a TGN budding assay (both cell-free and cell-intact) using PC12 cells or derived membranes greatly expanded the ability to study the process of maturation at the molecular level (Tooze and Huttner, 1990). This assay relied on (i) the selective labeling of a RSP protein, SgII, and a constitutively secreted protein, heparin sulfate proteoglycan (HSPG), with $[^{35}S]$-sulfate by sulfotransferases present only in the TGN, and (ii) the ability to separate the TGN from budded vesicles, as well as immature LDCVs from constitutive secretory vesicles, by sequential velocity and equilibrium sedimentation. The development of this assay was important for a number of reasons, including the support it lent to the *sorting for entry* hypothesis (see below), but also because it enabled a detailed characterization of LDCV maturation. Using this assay, Tooze and Huttner confirmed Farquhar's morphological observation that maturation entails an increase in LDCV size, and also demonstrated that immature LDCVs are capable of undergoing regulated release (Smith and Farquhar, 1966; Tooze et al., 1991). The latter finding was particularly significant since the ability of immature LDCVs to undergo

regulated exocytosis immediately after forming implied the sorting of specific membrane proteins (i.e., those that confer regulated release) into nascent LDCVs at the level of the TGN.

I. Proteins involved in LDCV maturation

Subsequent experiments based on variations of Tooze and Huttner's assay demonstrated the Arf1•GTP-dependent recruitment of the adaptor protein AP-1 and clathrin to immature, but not mature LDCVs (Dittie et al., 1996; Austin et al., 2000). The recruitment of AP-1 was next suggested to play a role in the removal from immature LDCVs of proteins which normally reside in other compartments, for example the TGN-resident protease furin (Dittie et al., 1997), and cation-independent MPR (Dittie et al., 1999). The increase in LDCV size during maturation suggested the possibility of homotypic fusion, and an elegant assay devised by Tooze's lab confirmed this possibility (Urbé et al., 1998). In particular, the assay utilized one population of immature LDCVs labeled with [^{35}S]-sulfated SgII, and another containing a heterologously expressed prohormone convertase enzyme, PC2, which is not normally present in PC12 cells. Upon mixing of the two vesicle populations, the radiolabeled SgII was proteolytically processed in a reaction that was eventually shown to depend on the proteins NSF, α-SNAP, syntaxin 6 and synaptotagmin IV (Urbé et al., 1998; Wendler et al., 2001; Ahras et al., 2006).

II. What is the significance of maturation?

Despite the now-extensive characterization of the LDCV maturation process in PC12 and other cells, it remains unclear what the functional or physiological consequences are of inhibiting maturation. To cite one example, overexpression of a dominant-negative clathrin hub fragment in primary pancreatic β cells resulted in no defects in the sorting or processing of proinsulin, nor in the regulated exocytosis of pro- or mature insulin, indicating that insulin granule biogenesis was essentially unaffected in the absence of functional clathrin (Molinete et al., 2001). However, expression of the hub domain was associated with increased degradation of C-peptide, the

fragment which results from the proteolytic conversion of proinsulin to insulin. This finding was in line with earlier immuno-EM observations that AP-1/clathrin patches on immature insulin granules are associated with the removal of MPRs and their associated lysosomal hydrolases (Kuliawat et al., 1997; Klumperman et al., 1998), and further suggested that clathrin is needed to remove from immature granules lysosomal proteases which evaded the initial AP-1-dependent sorting process at the level of the TGN.

SORTING FOR ENTRY VS. SORTING BY RETENTION

I. Sorting for entry

Over the years two major hypotheses have been proposed to explain the sorting of proteins into LDCVs (Arvan and Castle, 1998). The *sorting for entry* model involves directed sorting into nascent LDCVs, with all other secretory proteins in the TGN sorting by default into the constitutive pathway (Kelly, 1985). Implicit in this model is the need for a sorting receptor that directs soluble cargo into the forming LDCV. As mentioned above, the membrane-associated form of CPE was proposed to play such a role (Cool et al., 1997), although this finding has remained controversial (Irminger et al., 1997). In addition, sortilin has more recently been proposed to act as a sorting receptor for BDNF (Chen et al., 2005). Despite the lack of identification of a 'universal' sorting receptor to date, the fact remains that several RSP membrane proteins have sorting information in their cytosolic tails required for their efficient entry into the regulated pathway, thus strongly suggesting a role for directed sorting.

II. Sorting by retention

Proponents of the *sorting by retention* model, on the other hand, claim that sorting to the RSP occurs by default, either by the nonspecific trapping of proteins during aggregation or by the uniform partitioning of soluble content throughout the TGN lumen. In this model, proteins

destined for other organelles are removed during LDCV maturation (i.e., after budding), while those strongly associated with the condensed core will be retained in the maturing LDCV. Implicit in this model is that the immature secretory granule acts as a functional extension of the TGN (Arvan and Castle, 1998). The studies that inspired this model were carried out in exocrine secretory cells in the 1980s, and provided evidence of a third form of secretion which was kinetically and compositionally distinct from the classical constitutive and regulated pathways (Arvan and Castle, 1987; Zastrow and Castle, 1987). These studies suggested the novel form of secretion was taking place via the removal of a specific set of proteins from already-budded immature granules. Later immuno-EM studies in both exocrine and pancreatic β cells provided a morphological correlate of this process, with the observation that MPRs and lysosomal hydrolases were concentrated within clathrin-coated patches on immature granules (Kuliawat et al., 1997; Klumperman et al., 1998). However, the validity of this model has been called into question, at least for endocrine cells, with the finding that a mutant proinsulin that cannot be processed, and therefore does not associate with the condensed core, is still sorted and stored very efficiently in primary β cells (Halban and Irminger, 2003).

III. Weighing the evidence

Investigators in the field have long debated the veracity and significance of these two models, while they are, in fact, not mutually exclusive. Indeed, it is important to be mindful of the fact that many of the landmark studies supporting one model or the other were carried out in one particular cell type, and thus may not necessarily be generalizable to all cells with a RSP. Some of the strongest arguments in favor of *sorting for entry* include the following findings: (i) Orci and Moore showed by immuno-EM that while proinsulin and the constitutive membrane protein HA are seen together in Golgi cisternae, they diverge at the TGN; (ii) Tooze and Huttner demonstrated that LDCVs containing SgII and constitutive vesicles containing HSPG could be separated by density immediately after budding from the TGN; and (iii) several membrane

proteins have cytosolic sorting motifs which direct their efficient sorting into the RSP. In support of *sorting by retention*, the morphological observations from Orci and Klumperman provide clear evidence for removal of selected proteins from immature granules, thus suggesting that sorting at that level of the TGN is not completely efficient. Further, secretory GFP (i.e., GFP fused to a signal sequence) has been found to sort efficiently to the RSP in an insulin-secreting cell line, suggesting that specific sorting mechanisms are not always required for entry into LDCVs (Molinete et al., 2000). It is important to remember, however, that attempts to inhibit clathrin's involvement in the removal of 'incorrect' proteins from the RSP resulted in only modest changes in insulin granule content, thus raising questions about the physiological relevance of this type of sorting event.

IV. Reconciliation

On balance, it is apparent that a wealth of data from a variety of systems provides support for various aspects of both models. It seems clear, then, that a combination of multilayered interactions is at play. One can imagine a hierarchy of interactions starting with aggregation of soluble proteins in the TGN, followed by interaction of the aggregate with a specialized membrane domain and/or membrane proteins associated with such a domain, and finally interaction of the cytosolic domains of transmembrane proteins with the vesicle budding machinery. After LDCV formation, small amounts of contaminating proteins could be removed during the subsequent maturation process.

Thus, the field has come a long way since Farquhar and Palade's initial descriptions of LDCV formation over half a century ago, but there are still many fundamental, unanswered questions. In addition to the basic mysteries surrounding the selective sorting of proteins to the RSP in neuroendocrine cells, there are additional questions about the relatedness of canonical LDCVs to other dense-cored granules that have traditionally been referred to as lysosome-related organelles

(LROs). A basic description of LROs, their biogenesis, and their potential relationship to LDCVs is given below.

LDCVS VS. LYSOSOME-RELATED ORGANELLES

LROs are diverse and specialized cellular compartments which have some of the hallmark features of lysosomes, such as an acidic pH and hydrolytic activity, but which also carry out unique, cell-type-dependent functions (Raposo et al., 2007). LROs are found in a wide variety of cells, including melanocytes, platelets, endothelial cells, renal tubular cells, as well as in a host of leukocytes, including cytotoxic T cells, natural killer cells, neutrophils and mast cells (Raposo et al., 2007). In some ways, LROs also resemble LDCVs in that they are often electron-dense, many of them undergo regulated secretion, and they are thought be to derived, in part, from the TGN (Blott and Griffiths, 2002). Unlike LDCVs, however, they often contain intralumenal vesicles and/or internal laminar membranes and receive significant input from the endocytic pathway, which can be demonstrated by their efficient labeling with fluid-phase endocytic tracers (Clark et al., 2003; Sitaram and Marks, 2012). How related are these two organelles?

To discuss one exemplar in more detail, endothelial WPBs have traditionally been considered LDCVs, and they are known to form at the TGN, but the finding that the lysosomal membrane protein CD63 is delivered to WPBs by AP-3-directed sorting from an endosomal intermediate has raised new questions about the nature of this organelle (Harrison-Lavoie et al., 2006). Does this finding imply that WPBs should be considered more of a LRO? Or rather does it suggest the possibility that many 'canonical' LDCVs receive some fraction of their membrane protein complement from the endosomal system, rather than directly from the TGN, where LDCVs form? It is known that LDCV membrane proteins can be recycled from the cell surface to newly formed LDCVs, but it has generally been assumed that such recycling proceeds through the TGN as an

intermediary, rather than via a direct, endosome-to-LDCV route (Farquhar, 1978; Patzak and Winkler, 1986; Bäck et al., 2010). However, our lab's recent finding that AP-3, an adaptor protein traditionally thought to operate within the endosomal system, controls the sorting of proteins to LDCVs (Asensio et al., 2010), raises the distinct possibility that there is a direct, endosome-to-LDCV pathway. If such a pathway exists, it could be considered analogous to the AP-3-dependent, endosome-to-LRO route that many membrane proteins are known to take, and would provide further evidence for the relatedness of LDCVs and LROs. Alternatively, AP-3 might act at the TGN to concentrate membrane proteins directly at the site of LDCV formation. The next chapter will describe the discovery of AP-3 and discuss the progress that has been made on understanding its role in vesicular trafficking in the approximately 15 years since it was first characterized.

References

Ahras, M., Otto, G.P., and Tooze, S.A. (2006). Synaptotagmin IV is necessary for the maturation of secretory granules in PC12 cells. J Cell Biol *173*, 241–251.

Arvan, P., and Castle, D. (1998). Sorting and storage during secretory granule biogenesis: looking backward and looking forward. Biochem J *332 (Pt 3)*, 593–610.

Arvan, P., and Castle, J.D. (1987). Phasic release of newly synthesized secretory proteins in the unstimulated rat exocrine pancreas. J Cell Biol *104*, 243–252.

Asensio, C.S., Sirkis, D.W., and Edwards, R.H. (2010). RNAi screen identifies a role for adaptor protein AP-3 in sorting to the regulated secretory pathway. J Cell Biol *191*, 1173–1187.

Austin, C., Hinners, I., and Tooze, S.A. (2000). Direct and GTP-dependent interaction of ADP-ribosylation factor 1 with clathrin adaptor protein AP-1 on immature secretory granules. J Biol Chem *275*, 21862–21869.

Bainton, D.F., and Farquhar, M.G. (1966). Origin of granules in polymorphonuclear leukocytes. Two types derived from opposite faces of the Golgi complex in developing granulocytes. J Cell Biol *28*, 277–301.

Bainton, D.F., and Farquhar, M.G. (1970). Segregation and packaging of granule enzymes in eosinophilic leukocytes. J Cell Biol *45*, 54–73.

Barr, F.A., and Huttner, W.B. (1996). A role for ADP-ribosylation factor 1, but not COP I, in secretory vesicle biogenesis from the trans-Golgi network. FEBS Lett *384*, 65–70.

Barr, F.A., Leyte, A., Mollner, S., Pfeuffer, T., Tooze, S.A., and Huttner, W.B. (1991). Trimeric G-proteins of the trans-Golgi network are involved in the formation of constitutive secretory vesicles and immature secretory granules. FEBS Lett *294*, 239–243.

Bäck, N., Rajagopal, C., Mains, R.E., and Eipper, B.A. (2010). Secretory granule membrane protein recycles through multivesicular bodies. Traffic *11*, 972–986.

Blagoveshchenskaya, A.D., Hannah, M.J., Allen, S., and Cutler, D.F. (2002). Selective and signal-dependent recruitment of membrane proteins to secretory granules formed by heterologously expressed von Willebrand factor. Mol Biol Cell *13*, 1582–1593.

Blagoveshchenskaya, A.D., Hewitt, E.W., and Cutler, D.F. (1999). A complex web of signal-dependent trafficking underlies the triorganellar distribution of P-selectin in neuroendocrine PC12 cells. J Cell Biol *145*, 1419–1433.

Blott, E.J., and Griffiths, G.M. (2002). Secretory lysosomes. Nat Rev Mol Cell Biol *3*, 122–131.

Bossard, C., Bresson, D., Polishchuk, R.S., and Malhotra, V. (2007). Dimeric PKD regulates membrane fission to form transport carriers at the TGN. J Cell Biol *179*, 1123–1131.

Burgess, J., Jauregui, M., Tan, J., Rollins, J., Lallet, S., Leventis, P.A., Boulianne, G.L., Chang, H.C., Le Borgne, R., Krämer, H., et al. (2011). AP-1 and clathrin are essential for secretory granule biogenesis in Drosophila. Mol Biol Cell *22*, 2094–2105.

CARO, L.G., and Palade, G.E. (1964). PROTEIN SYNTHESIS, STORAGE, AND DISCHARGE IN THE PANCREATIC EXOCRINE CELL. AN AUTORADIOGRAPHIC STUDY. J Cell Biol *20*, 473–495.

Chanat, E., and Huttner, W.B. (1991). Milieu-induced, selective aggregation of regulated secretory proteins

in the trans-Golgi network. J Cell Biol *115*, 1505–1519.

Chanat, E., Weiss, U., Huttner, W.B., and Tooze, S.A. (1993). Reduction of the disulfide bond of chromogranin B (secretogranin I) in the trans-Golgi network causes its missorting to the constitutive secretory pathways. Embo J *12*, 2159–2168.

Chen, Y.G., and Shields, D. (1996). ADP-ribosylation factor-1 stimulates formation of nascent secretory vesicles from the trans-Golgi network of endocrine cells. J Biol Chem *271*, 5297–5300.

Chen, Y.G., Siddhanta, A., Austin, C.D., Hammond, S.M., Sung, T.C., Frohman, M.A., Morris, A.J., and Shields, D. (1997). Phospholipase D stimulates release of nascent secretory vesicles from the trans-Golgi network. J Cell Biol *138*, 495–504.

Chen, Z.-Y., Ieraci, A., Teng, H., Dall, H., Meng, C.-X., Herrera, D.G., Nykjaer, A., Hempstead, B.L., and Lee, F.S. (2005). Sortilin controls intracellular sorting of brain-derived neurotrophic factor to the regulated secretory pathway. J Neurosci *25*, 6156–6166.

Clark, R.H., Stinchcombe, J.C., Day, A., Blott, E., Booth, S., Bossi, G., Hamblin, T., Davies, E.G., and Griffiths, G.M. (2003). Adaptor protein 3-dependent microtubule-mediated movement of lytic granules to the immunological synapse. Nat Immunol *4*, 1111–1120.

Cool, D.R., Normant, E., Shen, F., Chen, H.C., Pannell, L., Zhang, Y., and Loh, Y.P. (1997). Carboxypeptidase E is a regulated secretory pathway sorting receptor: genetic obliteration leads to endocrine disorders in Cpe(fat) mice. Cell *88*, 73–83.

Corradi, N., Borgonovo, B., Clementi, E., Bassetti, M., Racchetti, G., Consalez, G.G., Huttner, W.B., Meldolesi, J., and Rosa, P. (1996). Overall lack of regulated secretion in a PC12 variant cell clone. J Biol Chem *271*, 27116–27124.

Dhanvantari, S., Arnaoutova, I., Snell, C.R., Steinbach, P.J., Hammond, K., Caputo, G.A., London, E., and Loh, Y.P. (2002). Carboxypeptidase E, a prohormone sorting receptor, is anchored to secretory granules via a C-terminal transmembrane insertion. Biochemistry *41*, 52–60.

Dittie, A.S., Hajibagheri, N., and Tooze, S.A. (1996). The AP-1 adaptor complex binds to immature secretory granules from PC12 cells, and is regulated by ADP-ribosylation factor. J Cell Biol *132*, 523–536.

Dittie, A.S., Klumperman, J., and Tooze, S.A. (1999). Differential distribution of mannose-6-phosphate receptors and furin in immature secretory granules. J Cell Sci *112 (Pt 22)*, 3955–3966.

Dittie, A.S., Thomas, L., Thomas, G., and Tooze, S.A. (1997). Interaction of furin in immature secretory granules from neuroendocrine cells with the AP-1 adaptor complex is modulated by casein kinase II phosphorylation. Embo J *16*, 4859–4870.

Díaz-Vera, J., Camacho, M., Machado, J.D., Domínguez, N., Montesinos, M.S., Hernández-Fernaud, J.R., Luján, R., and Borges, R. (2011). Chromogranins A and B are key proteins in amine accumulation, but the catecholamine secretory pathway is conserved without them. Faseb J.

Díaz-Vera, J., Morales, Y.G., Hernández-Fernaud, J.R., Camacho, M., Montesinos, M.S., Calegari, F., Huttner, W.B., Borges, R., and Machado, J.D. (2010). Chromogranin B gene ablation reduces the catecholamine cargo and decelerates exocytosis in chromaffin secretory vesicles. J Neurosci *30*, 950–957.

Eipper, B.A., Stoffers, D.A., and Mains, R.E. (1992). The biosynthesis of neuropeptides: peptide alpha-amidation. Annu. Rev. Neurosci. *15*, 57–85.

Evans, S.F., Irmady, K., Ostrow, K., Kim, T., Nykjaer, A., Saftig, P., Blobel, C., and Hempstead, B.L.

(2011). Neuronal brain-derived neurotrophic factor is synthesized in excess, with levels regulated by sortilin-mediated trafficking and lysosomal degradation. J Biol Chem *286*, 29556–29567.

Farquhar, M.G. (1978). Recovery of surface membrane in anterior pituitary cells. Variations in traffic detected with anionic and cationic ferritin. J Cell Biol *77*, R35–R42.

Farquhar, M.G., and WELLINGS, S.R. (1957). Electron microscopic evidence suggesting secretory granule formation within the Golgi apparatus. J Biophys Biochem Cytol *3*, 319–322.

Fernandez, C.J., Haugwitz, M., Eaton, B., and Moore, H.-P. (1997). Distinct molecular events during secretory granule biogenesis revealed by sensitivities to brefeldin A. Mol Biol Cell *8*, 2171–2185.

Glombik, M.M., Krömer, A., Salm, T., Huttner, W.B., and Gerdes, H.H. (1999). The disulfide-bonded loop of chromogranin B mediates membrane binding and directs sorting from the trans-Golgi network to secretory granules. Embo J *18*, 1059–1070.

Gumbiner, B., and Kelly, R.B. (1982). Two distinct intracellular pathways transport secretory and membrane glycoproteins to the surface of pituitary tumor cells. Cell *28*, 51–59.

Halban, P.A., and Irminger, J.-C. (2003). Mutant proinsulin that cannot be converted is secreted efficiently from primary rat beta-cells via the regulated pathway. Mol Biol Cell *14*, 1195–1203.

Harrison-Lavoie, K.J., Michaux, G., Hewlett, L., Kaur, J., Hannah, M.J., Lui-Roberts, W.W.Y., Norman, K.E., and Cutler, D.F. (2006). P-selectin and CD63 use different mechanisms for delivery to Weibel-Palade bodies. Traffic *7*, 647–662.

Hendy, G.N., Li, T., Girard, M., Feldstein, R.C., Mulay, S., Desjardins, R., Day, R., Karaplis, A.C., Tremblay, M.L., and Canaff, L. (2006). Targeted ablation of the chromogranin a (Chga) gene: normal neuroendocrine dense-core secretory granules and increased expression of other granins. Mol Endocrinol *20*, 1935–1947.

Hosaka, M., and Watanabe, T. (2010). Secretogranin III: a bridge between core hormone aggregates and the secretory granule membrane. Endocrine Journal *57*, 275–286.

Irminger, J.C., Verchere, C.B., Meyer, K., and Halban, P.A. (1997). Proinsulin targeting to the regulated pathway is not impaired in carboxypeptidase E-deficient Cpefat/Cpefat mice. J Biol Chem *272*, 27532–27534.

JAMIESON, J.D., and Palade, G.E. (1964). SPECIFIC GRANULES IN ATRIAL MUSCLE CELLS. J Cell Biol *23*, 151–172.

JAMIESON, J.D., and Palade, G.E. (1967). Intracellular transport of secretory proteins in the pancreatic exocrine cell. II. Transport to condensing vacuoles and zymogen granules. J Cell Biol *34*, 597–615.

Kelly, R.B. (1985). Pathways of protein secretion in eukaryotes. Science *230*, 25–32.

Kim, T., Tao-Cheng, J.H., Eiden, L.E., and Loh, Y.P. (2001). Chromogranin A, an "on/off" switch controlling dense-core secretory granule biogenesis. Cell *106*, 499–509.

Klumperman, J., Kuliawat, R., Griffith, J.M., Geuze, H.J., and Arvan, P. (1998). Mannose 6-phosphate receptors are sorted from immature secretory granules via adaptor protein AP-1, clathrin, and syntaxin 6-positive vesicles. J Cell Biol *141*, 359–371.

Krantz, D.E., Waites, C.L., Oorschot, V., Liu, Y., Wilson, R.I., Tan, P.K., Klumperman, J., and Edwards, R.H. (2000). A phosphorylation site regulates sorting of the vesicular acetylcholine transporter to dense

core vesicles. J Cell Biol *149*, 379–396.

Krömer, A., Glombik, M.M., Huttner, W.B., and Gerdes, H.H. (1998). Essential role of the disulfide-bonded loop of chromogranin B for sorting to secretory granules is revealed by expression of a deletion mutant in the absence of endogenous granin synthesis. J Cell Biol *140*, 1331–1346.

Kuliawat, R., Klumperman, J., Ludwig, T., and Arvan, P. (1997). Differential sorting of lysosomal enzymes out of the regulated secretory pathway in pancreatic beta-cells. J Cell Biol *137*, 595–608.

Leyte, A., Barr, F.A., Kehlenbach, R.H., and Huttner, W.B. (1992). Multiple trimeric G-proteins on the trans-Golgi network exert stimulatory and inhibitory effects on secretory vesicle formation. Embo J *11*, 4795–4804.

Li, H., Waites, C.L., Staal, R.G., Dobryy, Y., Park, J., Sulzer, D.L., and Edwards, R.H. (2005). Sorting of vesicular monoamine transporter 2 to the regulated secretory pathway confers the somatodendritic exocytosis of monoamines. Neuron *48*, 619–633.

Liu, Y., and Edwards, R.H. (1997). Differential localization of vesicular acetylcholine and monoamine transporters in PC12 cells but not CHO cells. J Cell Biol *139*, 907–916.

Liu, Y., Schweitzer, E.S., Nirenberg, M.J., Pickel, V.M., Evans, C.J., and Edwards, R.H. (1994). Preferential localization of a vesicular monoamine transporter to dense core vesicles in PC12 cells. J Cell Biol *127*, 1419–1433.

Lui-Roberts, W.W.Y., Ferraro, F., Nightingale, T.D., and Cutler, D.F. (2008). Aftiphilin and gamma-synergin are required for secretagogue sensitivity of Weibel-Palade bodies in endothelial cells. Mol Biol Cell *19*, 5072–5081.

Mahapatra, N.R., O'Connor, D.T., Vaingankar, S.M., Hikim, A.P.S., Mahata, M., Ray, S., Staite, E., Wu, H., Gu, Y., Dalton, N., et al. (2005). Hypertension from targeted ablation of chromogranin A can be rescued by the human ortholog. J Clin Invest *115*, 1942–1952.

Malosio, M.L., Benfante, R., Racchetti, G., Borgonovo, B., Rosa, P., and Meldolesi, J. (1999). Neurosecretory cells without neurosecretion: evidence of an independently regulated trait of the cell phenotype. J. Physiol. (Lond.) *520 Pt 1*, 43–52.

Malosio, M.L., Giordano, T., Laslop, A., and Meldolesi, J. (2004). Dense-core granules: a specific hallmark of the neuronal/neurosecretory cell phenotype. J Cell Sci *117*, 743–749.

Meskini, El, R., Galano, G.J., Marx, R., Mains, R.E., and Eipper, B.A. (2001). Targeting of membrane proteins to the regulated secretory pathway in anterior pituitary endocrine cells. J Biol Chem *276*, 3384–3393.

Metcalf, D.J., Nightingale, T.D., Zenner, H.L., Lui-Roberts, W.W., and Cutler, D.F. (2008). Formation and function of Weibel-Palade bodies. J Cell Sci *121*, 19–27.

Milgram, S.L., Eipper, B.A., and Mains, R.E. (1994). Differential trafficking of soluble and integral membrane secretory granule-associated proteins. J Cell Biol *124*, 33–41.

Milgram, S.L., Mains, R.E., and Eipper, B.A. (1993). COOH-terminal signals mediate the trafficking of a peptide processing enzyme in endocrine cells. J Cell Biol *121*, 23–36.

Milgram, S.L., Mains, R.E., and Eipper, B.A. (1996). Identification of routing determinants in the cytosolic domain of a secretory granule-associated integral membrane protein. J Biol Chem *271*, 17526–17535.

Molinete, M., Dupuis, S., Brodsky, F.M., and Halban, P.A. (2001). Role of clathrin in the regulated secretory pathway of pancreatic beta-cells. J Cell Sci *114*, 3059–3066.

Molinete, M., Lilla, V., Jain, R., Joyce, P.B., Gorr, S.U., Ravazzola, M., and Halban, P.A. (2000). Trafficking of non-regulated secretory proteins in insulin secreting (INS-1) cells. Diabetologia *43*, 1157–1164.

Montesinos, M.S., Machado, J.D., Camacho, M., Diaz, J., Morales, Y.G., Alvarez de la Rosa, D., Carmona, E., Castañeyra, A., Viveros, O.H., O'Connor, D.T., et al. (2008). The crucial role of chromogranins in storage and exocytosis revealed using chromaffin cells from chromogranin A null mouse. J Neurosci *28*, 3350–3358.

Moore, H.P., Gumbiner, B., and Kelly, R.B. (1983). Chloroquine diverts ACTH from a regulated to a constitutive secretory pathway in AtT-20 cells. Nature *302*, 434–436.

Natori, S., and Huttner, W.B. (1996). Chromogranin B (secretogranin I) promotes sorting to the regulated secretory pathway of processing intermediates derived from a peptide hormone precursor. Proc Natl Acad Sci USA *93*, 4431–4436.

Nichols, B.A., Bainton, D.F., and Farquhar, M.G. (1971). Differentiation of monocytes. Origin, nature, and fate of their azurophil granules. J Cell Biol *50*, 498–515.

Ohashi, M., Jan de Vries, K., Frank, R., Snoek, G., Bankaitis, V., Wirtz, K., and Huttner, W.B. (1995). A role for phosphatidylinositol transfer protein in secretory vesicle formation. Nature *377*, 544–547.

Orci, L., Amherdt, M., Malaisse-Lagae, F., Rouiller, C., and Renold, A.E. (1973). Insulin release by emiocytosis: demonstration with freeze-etching technique. Science *179*, 82–84.

Orci, L., Ravazzola, M., Amherdt, M., Madsen, O., Vassalli, J.D., and Perrelet, A. (1985). Direct identification of prohormone conversion site in insulin-secreting cells. Cell *42*, 671–681.

Orci, L., Ravazzola, M., Amherdt, M., Perrelet, A., Powell, S.K., Quinn, D.L., and Moore, H.P. (1987a). The trans-most cisternae of the Golgi complex: a compartment for sorting of secretory and plasma membrane proteins. Cell *51*, 1039–1051.

Orci, L., Ravazzola, M., Storch, M.J., Anderson, R.G., Vassalli, J.D., and Perrelet, A. (1987b). Proteolytic maturation of insulin is a post-Golgi event which occurs in acidifying clathrin-coated secretory vesicles. Cell *49*, 865–868.

Patzak, A., and Winkler, H. (1986). Exocytotic exposure and recycling of membrane antigens of chromaffin granules: ultrastructural evaluation after immunolabeling. J Cell Biol *102*, 510–515.

Pimplikar, S.W., and Huttner, W.B. (1992). Chromogranin B (secretogranin I), a secretory protein of the regulated pathway, is also present in a tightly membrane-associated form in PC12 cells. J Biol Chem *267*, 4110–4118.

Raposo, G., Marks, M.S., and Cutler, D.F. (2007). Lysosome-related organelles: driving post-Golgi compartments into specialisation. Curr Opin Cell Biol *19*, 394–401.

Rosa, P., Barr, F.A., Stinchcombe, J.C., Binacchi, C., and Huttner, W.B. (1992). Brefeldin A inhibits the formation of constitutive secretory vesicles and immature secretory granules from the trans-Golgi network. Eur J Cell Biol *59*, 265–274.

Saftig, P., and Klumperman, J. (2009). Lysosome biogenesis and lysosomal membrane proteins: trafficking meets function. Nat Rev Mol Cell Biol *10*, 623–635.

Siddhanta, A., and Shields, D. (1998). Secretory vesicle budding from the trans-Golgi network is mediated by phosphatidic acid levels. J Biol Chem *273*, 17995–17998.

Sitaram, A., and Marks, M.S. (2012). Mechanisms of protein delivery to melanosomes in pigment cells. Physiology (Bethesda) *27*, 85–99.

Smith, R.E., and Farquhar, M.G. (1966). Lysosome function in the regulation of the secretory process in cells of the anterior pituitary gland. J Cell Biol *31*, 319–347.

Steveson, T.C., Zhao, G.C., Keutmann, H.T., Mains, R.E., and Eipper, B.A. (2001). Access of a membrane protein to secretory granules is facilitated by phosphorylation. J Biol Chem *276*, 40326–40337.

Tan, P.K., Waites, C.L., Liu, Y., Krantz, D.E., and Edwards, R.H. (1998). A leucine-based motif mediates the endocytosis of vesicular monoamine and acetylcholine transporters. J Biol Chem *273*, 17351–17360.

Tanigawa, G., Orci, L., Amherdt, M., Ravazzola, M., Helms, J.B., and Rothman, J.E. (1993). Hydrolysis of bound GTP by ARF protein triggers uncoating of Golgi-derived COP-coated vesicles. J Cell Biol *123*, 1365–1371.

Teng, H.K., Teng, K.K., Lee, R., Wright, S., Tevar, S., Almeida, R.D., Kermani, P., Torkin, R., Chen, Z.-Y., Lee, F.S., et al. (2005). ProBDNF induces neuronal apoptosis via activation of a receptor complex of p75NTR and sortilin. J Neurosci *25*, 5455–5463.

Tooze, S.A., and Huttner, W.B. (1990). Cell-free protein sorting to the regulated and constitutive secretory pathways. Cell *60*, 837–847.

Tooze, S.A., Flatmark, T., Tooze, S.A., and Huttner, W.B. (1991). Characterization of the immature secretory granule, an intermediate in granule biogenesis. J Cell Biol *115*, 1491–1503.

Tooze, S.A., Weiss, U., and Huttner, W.B. (1990). Requirement for GTP hydrolysis in the formation of secretory vesicles. Nature *347*, 207–208.

Tüscher, O., Lorra, C., Bouma, B., Wirtz, K.W., and Huttner, W.B. (1997). Cooperativity of phosphatidylinositol transfer protein and phospholipase D in secretory vesicle formation from the TGN--phosphoinositides as a common denominator? FEBS Lett *419*, 271–275.

Urbé, S., Page, L.J., and Tooze, S.A. (1998). Homotypic fusion of immature secretory granules during maturation in a cell-free assay. J Cell Biol *143*, 1831–1844.

Wang, Y., Thiele, C., and Huttner, W.B. (2000). Cholesterol is required for the formation of regulated and constitutive secretory vesicles from the trans-Golgi network. Traffic *1*, 952–962.

Wendler, F., Page, L., Urbé, S., and Tooze, S.A. (2001). Homotypic fusion of immature secretory granules during maturation requires syntaxin 6. Mol Biol Cell *12*, 1699–1709.

Yao, J., and Hersh, L.B. (2007). The vesicular monoamine transporter 2 contains trafficking signals in both its N-glycosylation and C-terminal domains. J Neurochem *100*, 1387–1396.

Zastrow, von, M., and Castle, J.D. (1987). Protein sorting among two distinct export pathways occurs from the content of maturing exocrine storage granules. J Cell Biol *105*, 2675–2684.

CHAPTER 2: THE ADAPTOR PROTEIN AP-3

PREAMBLE

The adaptor protein AP-3 is a conserved heterotetrameric protein complex involved in the trafficking of membrane proteins within the biosynthetic and endocytic pathways of a strikingly wide range of eukaryotic cells. In addition to sorting membrane proteins, there is strong evidence that AP-3 participates directly in the formation of certain classes of transport vesicles that ferry cargo from one organelle to another. While it is clearly involved in sorting proteins to lysosomes, and is also important for targeting selected proteins to synaptic vesicles, its most conspicuous and well-characterized role appears to be that of targeting proteins to so-called lysosome-related organelles (LROs), thus contributing to their biogenesis. The latter role is most clearly illustrated in mutant organisms lacking functional AP-3. Defects in lysosome and LRO biogenesis have now been observed in a broad array of AP-3-deficient organisms including *Leishmania*, *Trypanosoma*, *Arabidopsis*, *S. cerevisiae*, *C. elegans*, *Drosophila*, mice, dogs and humans (Ooi et al., 1997; Cowles et al., 1997a; Kantheti et al., 1998; Dell Angelica et al., 1999; Benson et al., 2003; Hermann et al., 2005; Besteiro et al., 2008; Huang et al., 2011; Zwiewka et al., 2011). Finally, as will become apparent in the subsequent chapters, recent work from our lab has begun to uncover a new and unexpected role for AP-3 in the biogenesis of the regulated secretory pathway of neuroendocrine cells (Asensio et al., 2010).

PRELUDE TO THE DISCOVERY OF AP-3

Of the four AP-3 subunits, the medium or μ3 subunit was the first to be cloned, and was initially isolated from the electric lobe of the ray *Discopyge ommata* (Pevsner et al., 1994). Subsequent screening of rat spinal cord and cerebral cortex cDNA libraries using the *D. ommata* clone as a probe yielded the first mammalian AP-3 subunits, μ3A and μ3B (referred to as p47A and p47B)

(Pevsner et al., 1994). At the time of cloning, only the AP-1 and AP-2 adaptor complexes had been characterized, although the authors speculated that the isolated μ3 subunits may have been components of a third adaptor-related complex. The next AP-3 subunit to be identified was β3B. This large subunit with homology to β-adaptin from the AP-1 and -2 complexes as well as to β-COP, was cloned from a human cerebellar cDNA library by screening with antiserum from a patient with autoimmune cerebellar degeneration (Darnell et al., 1991; Newman et al., 1995). The authors went on to show that β3B (referred to as β-NAP) was expressed exclusively in the nervous system, localized to both neuronal cell bodies and nerve terminals, was found in both cytosolic and membrane-associated fractions, and associated with synaptic vesicles.

ISOLATION OF THE INTACT AP-3 COMPLEX

I. The complex begins to assemble

The first direct evidence for a third heterotetrameric adaptor protein complex homologous to AP-1 and -2 came in 1996 from Margaret Robinson's group (Simpson et al., 1996). This paper demonstrated that the previously identified μ3 and β3B proteins could co-immunoprecipitate each other along with two other proteins, one of 160 kDa, and another of 25 kDa. Consistent with the previously reported properties of β3B, μ3 was found in both cytosolic and membrane-associated fractions, but was not enriched in clathrin-coated vesicles (Simpson et al., 1996). Biochemical analysis indicated that μ3's membrane association was enhanced by incubation with the non-hydrolyzable GTP analog GTPγS and blocked by incubation with the fungal metabolite brefeldin A. These data thus suggested that the newly identified adaptor-related complex could be reversibly recruited to membranes in an Arf-dependent manner.

II. AP-3 gets its name

The next year, Juan Bonifacino's lab gave the AP-3 complex its current name, after isolating the

small and highly related σ3A and σ3B subunits, homologs of the AP-1 and -2 σ subunits (Dell Angelica et al., 1997a). The authors provided biochemical evidence that the σ3 subunits were part of a large complex by size-exclusion chromatography (Stokes radius, 85 Å). Furthermore, using an antiserum directed against β3B, they immunoisolated a complex consisting of σ3, μ3 and a non-neuronal form of β3 (i.e., β3A). Yeast two-hybrid analysis provided the first evidence that the μ3 subunit could bind tyrosine-based sorting signals of the form YXXΦ, where Φ is an amino acid with a bulky, hydrophobic side chain. Finally, the authors showed by immunofluorescence that AP-3 localized both to perinuclear punctate structures that partially overlapped with markers of the *trans*-Golgi network (TGN), as well as to more peripheral structures overlapping with a marker of recycling endosomes (Dell Angelica et al., 1997a).

III. Identification of the first AP-3 mutant animal

Following closely on the heels of the Bonifacino lab's characterization of the ubiquitous form of AP-3, the Robinson lab further characterized the complex, cloning the largest subunit, δ, homologous to AP-1 γ and AP-2 α (Simpson et al., 1997). As with the other initial papers on AP-3, the immunofluorescence-based localization reported here provides a rather ambiguous picture. In particular, staining for the δ subunit showed partial and rather unconvincing overlap with markers of TGN as well as early endosomes. Finally, using database searching, the authors showed that the mammalian δ subunit was homologous to the *Drosophila garnet* gene. *garnet* was first identified as a *Drosophila* eye-color mutant in 1916, and was cloned and partially sequenced in 1995 [discussed in (Simpson et al., 1997)]. Robinson's group reported that *garnet* mutants had defects in eye pigment-granule formation, thus providing the first evidence that AP-3 is important for the biogenesis of LROs (Simpson et al., 1997).

32

IV. Tying up loose ends

Subsequent papers from the Bonifacino lab reported the cloning of the ubiquitous AP-3 β subunit, β3A (Dell Angelica et al., 1997b), as well as the δ subunit (Ooi et al., 1997). Among other findings, these papers demonstrated that at steady state, the β3A subunit exists as a phosphoprotein, similar to the original report of β3B (Newman et al., 1995), and provided further confirmation that AP-3 was not enriched in clathrin-coated vesicles. Interestingly, a recent report has suggested that phosphorylation of the β3A hinge region influences the complex's ability to bind a kinesin family member (Azevedo et al., 2009), although the role of AP-3 phosphorylation has otherwise not been explored in much detail.

IDENTIFICATION OF THE YEAST AP-3 COMPLEX

I. Discovery

Around the same time the mammalian AP-3 complex was being described, several groups independently identified yeast orthologs to subunits of the metazoan complex. These orthologs were originally identified as suppressors of lethality in strains lacking casein kinases Yck1 and Yck2 (Panek et al., 1997). Shortly after this initial report, the labs of Sandra Lemmon and Scott Emr independently reported that yeast AP-3 is required for the direct, Golgi-to-vacuole transport of the membrane protein alkaline phosphatase (ALP) (Stepp et al., 1997; Cowles et al., 1997a). Following these papers, transport of ALP within this pathway was shown to depend on a dileucine-like motif within its cytoplasmic tail. Notably, this motif was related to mammalian dileucine signals known to interact with other adaptor proteins, such as AP-2 (Vowels and Payne, 1998). In addition, further work from the Emr lab showed that the vacuolar t-SNARE, Vam3p, contained an acidic dileucine motif similar to ALP's, which was required for this protein's trafficking via the AP-3-dependent, direct, Golgi-to-vacuole route (Darsow et al., 1998).

II. Vps41 is an essential component of the yeast AP-3 pathway

The next major advance in our understanding of the yeast AP-3 pathway came in an elegant paper

from Emr's lab demonstrating the existence of AP-3-coated transport vesicles derived from the

Golgi apparatus, *en route* to the vacuole (Rehling et al., 1999). The isolation of these transport

intermediates was made possible by the use of a temperature-sensitive *vam3^{tsf}* mutant, which

blocked docking and fusion at the vacuole (Darsow et al., 1997), and thus enabled accumulation

of AP-3-decorated vesicles. An earlier report had shown that another protein, Vps41, was also

involved in Golgi-to-vacuole transport of ALP (Cowles et al., 1997b), so the authors used a

vps41^{tsf} mutant to assess the effect on the AP-3 transport vesicles. They found, in contrast to the

vam3^{tsf} cells, that loss of Vps41 function led to an apparent accumulation of AP-3 on Golgi

membranes and blocked formation of AP-3-coated transport vesicles. Finally, the authors

demonstrated interactions between Vps41 and the AP-3 δ subunit both *in vitro* and *in vivo*, with a

predicted C-terminal coiled-coil domain in δ (i.e., in the appendage domain) shown to be required

for interaction (Rehling et al., 1999).

Additional genetic screens in yeast added new insight into the AP-3 pathway by identifying two

novel point mutations in Vps41—specifically, an N-terminal mutation that blocked binding to

AP-3 δ, and a C-terminal mutation within the clathrin heavy-chain repeat (CHCR) domain that

interfered with Vps41's ability to self-associate (Darsow et al., 2001). Size-exclusion studies

done on recombinant Vps41 protein produced both in *E. coli* and yeast yielded a high-molecular-

weight complex estimated to consist of six Vps41 molecules, and deletion of the CHCR domain

abrogated this elution profile. Importantly, both the N- and C-terminal point mutations interfered

with the formation of ALP transport intermediates derived from the Golgi, suggesting that a

homo-oligomeric form of Vps41, interacting with AP-3, is required for the biogenesis of this

pathway. Notably, a recent paper has shown that a functional interaction exists between AP-3 and

Vps41 in metazoan cells as well (Swetha et al., 2011).

III. Vps41 in the HOPS complex

Shortly after the discovery of Vps41's role in the AP-3 pathway, Vps41 was shown to be a subunit of the homotypic fusion and vacuole protein sorting (HOPS) complex (Seals et al., 2000), a vacuole-localized hexameric complex involved in vesicle tethering and fusion, and this latter role was assumed to be independent of its function in AP-3 vesicle formation at the *trans*-Golgi. Thus, the next question to be addressed lay in discerning Vps41's function at the vacuole versus its known role at the Golgi. Specifically, how Vps41 switched from its HOPS-incorporated to HOPS-independent configurations remained unknown. The first clue to regulation of this process came with the realization that Vps41 could be phosphorylated by the casein kinase Yck3, a modification that was proposed to release Vps41 from the HOPS complex (LaGrassa and Ungermann, 2005). Consistent with this idea, a genome-wide screen for additional regulators of the AP-3 / ALP pathway yielded the kinase Yck3, which was found to be required for the formation of ALP transport intermediates (Anand et al., 2009). In addition, expression of a Vps41 mutant unable to be phosphorylated by Yck3 led to hyper-accumulation of the mutant protein at the vacuole, but impaired delivery of AP-3 cargo to the vacuole. Conversely, a Vps41 phosphomimetic mutant localized less efficiently to the vacuole, while still enabling effective delivery of an AP-3 cargo protein (Cabrera et al., 2009).

IV. Which form of Vps41 operates in the AP-3 pathway?

A recent paper has attempted to challenge the idea that Vps41 is required for AP-3-dependent vesicle formation at the Golgi, and asserts instead that Vps41 interacts with AP-3-coated transport vesicles at the vacuole, thus enabling their fusion (Angers and Merz, 2009). This model, however, rests almost entirely on the use of live-cell imaging in yeast, and specifically on the observations that: (i) AP-3 but not Vps41 colocalized with a Golgi marker protein, (ii) AP-3 accumulates on punctate structures in a Vps41-null background, some of which do not colocalize with a Golgi marker (and thus could be transport vesicles), and (iii) AP-3 could be observed transiently

35

colocalizing with HOPS complex members at the vacuole membrane. Thus, due to the fact that different groups have used different mutants (temperature-sensitive alleles versus deletions) and utilized different techniques (biochemistry versus imaging), it is currently unclear whether Vps41 interacts with AP-3 primarily at the *trans*-Golgi, the vacuole, or both, and whether the interaction with AP-3 occurs primarily in a HOPS-associated or -disassociated form.

EXPANDING MAMMALIAN AP-3'S REPERTOIRE

I. The contentious role of clathrin in AP-3 function

Subsequent work on the mammalian AP-3 complex complicated matters by providing biochemical evidence for an interaction with the clathrin heavy chain, as well as localization to clathrin-labeled membranes by immuno-electron microscopy (EM) (Dell Angelica et al., 1998). However, work published several years later showed that heterologous expression of a β3A subunit lacking the clathrin box motif (SLLDLD)—known to be required for binding clathrin *in vitro*—was sufficient to rescue a LAMP-1 cell surface sorting phenotype in β3A-deficient fibroblasts (Peden et al., 2002). Thus, although there was evidence that mammalian AP-3 was capable of interacting with clathrin *in vitro*, the weight of evidence thus far indicated that an interaction with clathrin *in vivo* was not required for the complex's then-known functions.

II. Arfs and dileucine motifs as interactors

In addition to the conflicting data on AP-3's potential interaction with clathrin, an expanding number of other AP-3 interactors were being identified in the late 1990s. For example, Bonifacino's lab demonstrated that purified Arf1•GTP could recruit AP-3 to membranes, and that such recruitment required the presence of membrane proteins, since pretreatment of the membranes with trypsin blocked recruitment (Ooi et al., 1998). The first description of mammalian AP-3 cargo proteins came the same year with the demonstration that the cytoplasmic

36

tails of two membrane proteins, LIMP-II and tyrosinase, were capable of interacting with AP-3

(Höning et al., 1998). Both proteins have acidic dileucine motifs of the form (D/E)XXXL(L/I),

which are related to those found in the yeast proteins ALP and Vam3p. Notably, it had been

previously demonstrated that the upstream acidic residues were important for LIMP-II sorting to

the lysosome, and these residues were now shown to be required for binding to AP-3 (Höning et

al., 1998). Furthermore, because tyrosinase was an established melanosomal protein, the

demonstration of this interaction linked the earlier findings of defective pigment granule

biogenesis in *Drosophila garnet* mutants to a potential role for mammalian AP-3 in sorting

proteins to melanosomes. Direct evidence to this effect came several years later when AP-3 was

found to be required for proper sorting of tyrosinase in human melanocytes (Huizing et al., 2001).

Evidence for AP-3-dependent sorting of the lysosomal membrane proteins LAMP-I and LIMP-II

came shortly thereafter, with results indicating that AP-3 knockdown increased cell surface

trafficking of these proteins, with no effect on the sorting of cation-independent mannose 6-

phosphate receptor (MPR), which relies on AP-1 for sorting from the TGN to late endosomes (Le

Borgne et al., 1998).

III. Differential recognition of dileucine motifs among the adaptor proteins

Although the adaptor protein complexes AP-1 through AP-4 are all known to bind dileucine

motifs, relatively little is understood about how these motifs are recognized differentially among

the four adaptors. A recently published and detailed interaction study using the yeast three-hybrid

system was carried out to provide a better understanding of such interactions (Mattera et al.,

2011). The authors found that the overall mechanism of dileucine signal binding was conserved

between AP-1, -2 and -3, but subtle differences in recognition mode were observed. In particular,

conserved basic residues in both subunits of the AP-2 and -3 hemicomplexes, α-σ2 and δ-σ3, are

important for an electrostatic interaction with the acidic residues at the -4 and -5 positions of

dileucine motifs. For AP-1, however, only a conserved basic residue in γ but not σ1 is crucial for

this interaction. Interestingly, for each of the adaptors, certain mutations were found to strongly impair binding to one cargo protein while having little effect on another. Overall, binding to dileucine signals appears to be mediated by a combination of basic and hydrophobic residues on the small subunits (σ1, σ2, σ3) as well as a single, conserved basic residue on the large, σ-associated subunits (γ, α, δ) (Mattera et al., 2011).

IV. P-selectin and CD63 as cargo molecules

AP-3 has also been claimed to sort the cell-adhesion molecule P-selectin to Weibel-Palade bodies (WPBs), a type of regulated secretory organelle found in endothelial cells (Daugherty et al., 2001). However, this finding was called into question with the demonstration that the lumenal domain of P-selectin was sufficient to direct sorting into WPBs, and the fact that AP-3-deficient cells showed normal levels of P-selectin-dependent leukocyte rolling (Harrison-Lavoie et al., 2006). Interestingly, though, the authors of the latter paper found that targeting of the tetraspanin CD63, previously shown to interact with AP-3, relied on this adaptor for targeting to WPBs. They went on to speculate that some proteins, such as P-selectin, are added directly to WPBs budding from the TGN, while others, such as CD63, are added to already-formed WPBs from an endosomal compartment, although their data supporting this model are somewhat wanting.

V. Proteomics approaches identify new cargoes and regulators

Starting almost a decade after the discovery of AP-3, several groups began to apply the techniques of biological mass spectrometry to the problem of characterizing the AP-3 interactome. The first such effort was carried out by Victor Faundez' lab, and utilized a PC12 synaptic-like microvesicle fraction enriched in the known AP-3 cargo ZnT3 (Salazar et al., 2005). Proteomic analysis identified one novel component, phosphatidylinositol 4-kinase type IIα (PI4KIIα), which was explored further. Interestingly, PI4KIIα appeared to be both a cargo and a regulator of AP-3, as depletion of either component altered the subcellular distribution of the

38

other (Craige et al., 2008). Further proteomics work by the same group relied on a chemical crosslinking strategy rather than vesicle isolation to identify other AP-3 interactors. This approach revealed a tripartite interaction between AP-3, PI4KIIα and the BLOC-1 complex (see below for a discussion of the BLOC complexes), with loss of the latter component impairing the interaction between AP-3 and PI4KIIα (Salazar et al., 2009).

An alternative proteomics approach involved recruiting AP-3 to phosphatidylinositol 3-phosphate (PI3P)-containing liposomes decorated with the cytoplasmic tail of the AP-3 cargo protein, LIMP-II (Baust et al., 2008). This strategy enabled the recruitment of several previously established AP-3 interactors (e.g., AGAP1), as well as many novel candidates. Although most of the identified proteins did not overlap with those identified by the Faundez lab, the authors demonstrated that knockdown of several of their identified proteins led to a reduction in AP-3 levels and a concomitant increase in cell surface trafficking of LAMP-1 (Baust et al., 2008). It is particularly striking that knockdown of Big1, a Sec7-related Arf1 guanine nucleotide exchange factor (GEF) (Togawa et al., 1999), resulted in a marked reduction in overall AP-3 levels (Baust et al., 2008). It has recently been shown that the small GTPase, Arl1, recruits Big1 to the TGN where it, in turn, recruits and activates Arf1 (Christis and Munro, 2012). The finding that depletion of a TGN-localized Arf GEF destabilizes AP-3 is thus highly suggestive of AP-3 being involved in traffic originating from the TGN. Interestingly, although PI3P-containing liposomes were used for the proteomics, the authors demonstrated that PI4P-containing liposomes could also recruit AP-3, suggesting that mammalian AP-3 has affinity for both endosome- and TGN-enriched phosphoinositides.

THE STRUCTURAL BASIS FOR ADAPTOR PROTEIN–CARGO INTERACTIONS

Although there is relatively little structural information on AP-3 itself, detailed structural studies of AP-2, as well as coatomer (COPI), have provided many insights that are likely to be relevant to understanding AP-3's function. As noted above, detailed mutagenesis studies guided by the AP-2 structure have demonstrated the overall conservation of the dileucine-binding pocket in AP-1, -2 and -3 (Mattera et al., 2011). A series of elegant structural studies published by David Owen's group over the last ~15 years has established the structural basis for the binding of YXXΦ motifs to the medium μ2 subunit (Owen and Evans, 1998), of acidic dileucine motifs binding to basic and hydrophobic patches at the interface of the α and σ2 subunits (Kelly et al., 2008), and most recently, of a large-scale conformational rearrangement the complex undergoes upon binding to phosphatidylinositol 4,5-bisphosphate [PI(4,5)P$_2$], which appears to enable simultaneous binding of YXXΦ- and dileucine-containing cargoes to the complex (Jackson et al., 2010). In addition to these canonical AP-cargo interactions, several novel binding modes have been elucidated in recent years, including, for example, a recent structure demonstrating interaction of the AP-3 δ hinge domain with the so-called longin domain of the SNARE protein VAMP7 (Kent et al., 2012). Such interactions appear to occur independently of canonical cargo interactions with the AP 'core' domain, suggesting that a single AP complex may be capable of simultaneously binding three or more cargo proteins. Finally, recent structural work on Arf and coatomer by Jonathan Goldberg's lab has revealed that the Arf-binding sites on coatomer are spatially related to the PI(4,5)P$_2$-binding sites on AP-2, thus suggesting that membrane recruitment of COPI and APs 1-4 occurs in a conserved manner (Yu et al., 2012).

MEMBRANE RECRUITMENT OF AP-3

While the number of cargo molecules interacting with AP-3 has been steadily increasing since the complex's discovery, comparatively little is understood about the mechanism and regulation of

AP-3's recruitment to the membrane. The first regulator to be identified, other than Arf1, was an Arf GTPase-activating protein (GAP) (Nie et al., 2003). This particular Arf GAP, known as AGAP1, was shown to interact with the so-called δ-σ3A hemicomplex, which is a modular subcomplex of AP-3 (Figure 1). Overexpression of AGAP1 in cells was found to disrupt AP-3's association with the membrane, while siRNA knockdown conferred BFA resistance to AP-3, presumably due to AP-3's interaction with a GTP-locked form of Arf1 in the absence of specific GAP activity. The next mechanistic insight into AP-3 membrane recruitment came from detailed intra-complex interaction studies from Bonifacino's group. They demonstrated that the C-terminal 'ear' or 'appendage' domain of δ is capable of binding σ3, located within the 'core' domain of the complex. This interaction was shown to block AP-3's interaction with Arf1•GTP, and consequently, overexpression of the δ ear domain reduced endogenous AP-3's association with membranes and led to an increase in cell surface expression of several AP-3 cargo molecules (Lefrançois et al., 2004).
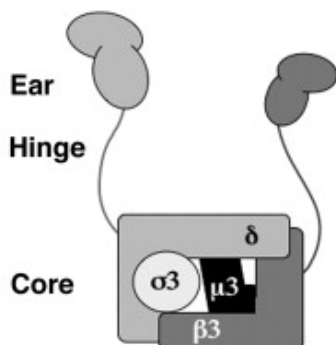
Figure 1. The heterotetrameric AP-3 complex is depicted as having a central 'core' domain consisting of the N-terminal portions of the δ and β3 subunits, as well as their associated σ3 and μ3 subunits. The δ and β3 subunits also contain long, unstructured 'hinge' segments followed by 'ear' or 'appendage' domains. Studies from Bonifacino's lab have demonstrated interactions within the δ-σ3 hemicomplex which occur by means of the δ ear domain folding back to bind σ3, thus regulating the complex's recruitment to membranes. Reproduced from (Lefrançois et al., 2004) with permission from Elsevier.

A ROLE FOR AP-3 IN SYNAPTIC VESICLE FORMATION

I. In vitro reconstitution

Essentially contemporaneous with the early characterization of AP-3 in yeast, Regis Kelly's lab at

UCSF reported that AP-3 was involved in a new pathway of synaptic vesicle formation (Faundez

et al., 1998; Lichtenstein et al., 1998). Specifically, they showed that synaptic-like microvesicles

(SLMVs) could be formed *in vitro* by incubating endosomes with brain cytosol in a reaction that

could be inhibited by immunodepletion of AP-3. Moreover, addition of recombinant Arf1•GTP

plus biochemically enriched fractions of AP-3 were sufficient to promote SLMV budding from

washed endosomal membranes *in vitro* (Faundez et al., 1998). The Kelly lab later demonstrated a

requirement for the protein VAMP2 in the AP-3-dependent biogenesis of SLMVs from

endosomes (Salem et al., 1998), and, interestingly, VAMP2 has a dileucine-like motif embedded

within a predicted amphipathic helix that has been shown to be important for its SLMV targeting

(Grote et al., 1995; Grote and Kelly, 1996). However, AP-3 has not been demonstrated to interact

with this motif, and thus the significance of this observation remains unclear. Further adaptation

of the SLMV budding system demonstrated the presence of two distinct pathways of SLMV

biogenesis: one derived from endosomes that was Arf1- and AP-3-dependent, and thus sensitive

to brefeldin A (BFA), and another derived from the plasma membrane that was dependent on

clathrin and AP-2, and thus BFA-insensitive (Shi et al., 1998).

II. Does AP-3 form SVs in vivo?

The growing evidence that AP-3 participated in an alternative synaptic vesicle (SV) formation

pathway suggested the intriguing possibility that compositionally distinct SVs might exist. In

support of this possibility, SV sorting of the zinc and chloride transporters, ZnT3 and ClC-3, is

perturbed in AP-3-deficient-mice, while cargoes that take the AP-2-dependent pathway are

unaffected (Salazar et al., 2004a; 2004b). In addition, several papers have demonstrated that AP-3

is involved in sorting the tetanus toxin-insensitive v-SNARE, VAMP7, in both neural (Scheuber et al., 2006) and non-neural cells (Martinez-Arca et al., 2003). Indeed, *mocha* mice lacking AP-3 display a specific loss of VAMP7 at hippocampal mossy fiber terminals, and it was suggested that the observed increase in spontaneous SV release and decrease in asynchronous release were due to loss of VAMP7 at the nerve terminal (Scheuber et al., 2006). Moreover, work from our lab has suggested that AP-3 is involved in forming the so-called resting pool of SVs, which are recalcitrant to evoked exocytosis (Voglmaier et al., 2006). Indeed, more recent work from our lab has suggested that VAMP7 is sorted preferentially to the resting pool of SVs, providing further evidence that AP-3-dependent sorting contributes to the biogenesis of a particular class of SVs with distinct properties (Hua et al., 2011).

AP-3 MUTATIONS DISCOVERED IN METAZOANS

AP-3 mutations have now been identified in a wide range of metazoans, including *Drosophila*, mice and humans. The resultant phenotypes will be described below, and the potential cell biological abnormalities responsible will be discussed. As will become apparent, there is remarkable phenotypic conservation across species—with the most conspicuous attribute being pigmentation defects—suggesting a conserved role for AP-3 in pigment-granule biogenesis. In addition, the bleeding phenotypes found in AP-3-deficient vertebrates suggest a conserved role in platelet dense-granule formation, and more broadly, in LRO biogenesis.

I. AP-3 mutations in Drosophila eye-color mutants

As mentioned previously, early work on AP-3 led to the identification of a mutation in the δ subunit in *Drosophila garnet* mutants. Subsequent work implicated the μ3 subunit in *carmine* mutants (Mullins et al., 1999) as well as the β3 subunit in *ruby* mutants (Kretzschmar et al., 2000), with both papers reporting the expected defects in pigment granules. Interestingly, the

latter paper also reported some behavioral alterations in both *ruby* and *garnet* flies, including abnormal visual fixation and increased walking speed. Bonifacino's group subsequently identified a lesion in the σ3 gene in *orange* mutant flies, and independently linked β3 to *ruby* (Mullins et al., 2000). No behavioral abnormalities were reported in this paper, although the only paradigm tested was a larval motility assay. In addition, around the same period of time the *light* gene of *Drosophila* was found to be a homolog of Vps41, and a genetic interaction between *light* and *garnet*, with respect to the eye-pigment phenotype, was reported (Warner et al., 1998). Notably, this finding foreshadowed the genetic and physical interactions between yeast AP-3 and Vps41 reported the following year by Emr's group (Rehling et al., 1999).

II. AP-3 subunits identified in spontaneous mouse coat-color mutants

Less than a year before the discovery that AP-3 was linked to Hermansky Pudlak Syndrome (HPS), a team led by Margit Burmeister discovered a null mutation in the AP-3 δ subunit in the classical coat-color mutant mouse, *mocha* (Kantheti et al., 1998). The *mocha* mutation was generated spontaneously on a C57BL/6J background at Jackson Laboratory in 1963. The first paper published on the mice appeared in 1974, and reported eye and hair pigmentation defects, inner-ear degeneration with defects in otolith formation, hyperactive or nervous behavior, head tilt at weaning in some mice, as well as reduced survival of pups within several days of birth (Lane and Deol, 1974). Of note, the authors pointed out that *mocha* mice shared many characteristics of another spontaneous mouse mutant, *pallid*, now known to harbor a mutation in the pallidin gene, which is a component of the BLOC-1 complex [described in more detail below; (Huang et al., 1999)]. In addition to showing that *mocha* mice have a null mutation in the AP-3 δ subunit—which leads to loss of both ubiquitous and neuronal AP-3—Burmeister's team also provided the first *in vivo* evidence for altered synaptic vesicle composition in these mice. Specifically, they showed a loss of staining for the vesicular zinc transporter, ZnT3, in the hippocampus and neocortex, with a striking and corresponding loss of vesicular zinc in the same

regions, detected histologically by Timm's stain (Kantheti et al., 1998). The alterations in the neocortex were remarkable due to a report a decade earlier showing persistent neocortical hypersynchronization in *mocha* mice, detected by electrocorticography (Noebels and Sidman, 1989). Interestingly, a study prior to the molecular elucidation of the *mocha* mutation had already established this mutant as a model for HPS, showing that *mocha* mice had defective and less-abundant platelet dense granules, reduced platelet aggregation in response to collagen, greatly increased bleeding time, as well as decreased secretion of lysosomal enzymes from kidney proximal tubule cells (Swank et al., 1991).

Around the same time the *mocha* mutation was mapped to the δ subunit, Richard Swank's group mapped two different alleles of the *pearl* mouse, another model for HPS, to the AP-3 β3A gene (Feng et al., 1999). Loss of β3A in *pearl* mice does not lead to loss of the entire complex (as in *mocha*), but rather leads only to a moderate reduction in the levels of δ (Zhen et al., 1999). However, the mutation is associated with a change in the δ subunit's appearance by immunofluorescence from the typical punctate pattern to a more diffuse, cytoplasmic appearance, suggesting loss of normal function. Finally, EM analysis has shown that *pearl* kidney proximal tubule cells had enlarged and abnormally multilamellar lysosomes, a finding which could be a morphological correlate of the previously reported abnormal lysosomal enzyme secretion phenotype (Novak and Swank, 1979; Swank et al., 1991; Lyerla et al., 2003). Interestingly, the Swank lab was one of the earliest to note the interrelatedness of lysosomes, melanosomes, and platelet dense granules after consistently observing a similar constellation of cellular and physiological abnormalities in multiple spontaneous coat-color mutants [e.g., *pearl, pallid, pale ear*; (Novak et al., 1984)] now known to be bona fide models for HPS.

III. Engineered AP-3-null mice

In addition to the spontaneous mouse coat-color mutants, *pearl* and *mocha*, several knockout

(KO) animals have been generated by homologous recombination. Specifically, the β3A, β3B and μ3B alleles have been targeted (Yang et al., 2000; Nakatsu et al., 2004; Seong et al., 2005). As expected, β3A KO mice have coat-color dilution like *pearl* (lacking ubiquitous AP-3) and *mocha* (lacking ubiquitous and neuronal AP-3). In contrast, the β3B KOs have no coat-color dilution, but are hyperactive like *mocha* mice, suggesting that this phenotype is mediated by neuronal AP-3 (Seong et al., 2005). Interestingly, in β3B KO neurons, staining for total AP-3 showed a selective loss of the complex in processes, but not in the cell body, while β3A KO neurons showed no change in staining. This indicates that ubiquitous AP-3 is restricted to the cell body, while neuronal AP-3 localizes to both the cell body and processes. Some in the field have speculated that the ubiquitous form of the complex may thus carry out AP-3's 'non-specialized' functions (e.g., sorting to lysosomes) in neurons, although this has not been directly tested. Finally, the observation that the β3A KOs had *increased* hippocampal zinc staining with concomitantly increased ZnT3 sorting to SVs (Seong et al., 2005), provides further evidence that the neuron-specific trafficking of ZnT3 to SVs is mediated by the neuronal, β3B-containing, form of the complex.

The only report on the neuronal μ3B subunit KO (Nakatsu et al., 2004) focused predominantly on phenotypes that have not been assessed in either *mocha* mice or β3B KOs, so a comprehensive comparison is not possible. As expected, the μ3B KOs were susceptible to spontaneous epileptic seizures, as are the β3B KOs and *mocha* mice (Kantheti et al., 1998; Nakatsu et al., 2004; Seong et al., 2005). Unexpectedly, though, μ3B-deficient mice were shown to have slight reductions in the levels of the vesicular GABA transporter, VGAT, and, consequently, reduced inhibitory transmission in the hippocampus, resulting in abnormal excitatory transmission from the entorhinal cortex to CA1 pyramidal cells. Perhaps most interestingly, though, was the authors' claim that neither vesicular zinc nor ZnT3 were altered in the μ3B KOs, a finding that stands in contrast to what has been reported for both *mocha* mice and the β3B KOs (Kantheti et al., 1998;

Seong et al., 2005). This suggests that μ3A might be able to compensate for loss of μ3B, while, at least for the zinc phenotype, the β3 subunits appear to be non-redundant. Moreover, this suggests the possibility that there is not just one 'neuronal' AP-3 complex but rather several potential combinations of neuronal complexes (e.g., δ-σ3-β3B-**μ3A**).

IV. AP-3 is implicated in Hermansky-Pudlak syndrome

Less than three years after the initial characterization of AP-3 (Simpson et al., 1996), a collaborative effort by the labs of William Gahl and Juan Bonifacino resulted in the identification of mutations in the β3A subunit in two patients with HPS (Dell Angelica et al., 1999). This syndrome is an autosomal recessive disorder characterized by symptoms such as platelet storage pool deficiency, oculocutaneous albinism and pulmonary fibrosis (HERMANSKY and PUDLAK, 1959), as well as severe neutropenia, which was noted in the third patient identified with a β3A-subunit mutation (Zhen et al., 1999; Huizing et al., 2001; Feng et al., 2002; Benson et al., 2003; Lyerla et al., 2003). These symptoms are thought to arise, respectively, from specific defects in the biogenesis of platelet dense granules, melanosomes, lung surfactant-containing lamellar bodies, and neutrophil azurophil granules (Zhen et al., 1999; Huizing et al., 2001; Feng et al., 2002; Benson et al., 2003; Lyerla et al., 2003). As the β3A subunit was the second gene identified to contain causative mutations in HPS, patients with this form of the disease are now classified as having HPS type 2. Interestingly, the original sibling pair reported to have this form of HPS are actually compound heterozygotes, having inherited a deletion allele from their father and a point mutation from their mother (Dell Angelica et al., 1999). These mutations both fall within the N-terminal 'trunk' or 'core' domain, and thus probably inhibit assembly of the heterotetrameric complex. Supporting this hypothesis, metabolic labeling studies demonstrated large reductions in the half lives of both the mutated subunit, β3A, and a non-mutated subunit, σ3A (Dell Angelica et al., 1999). Finally, this study confirmed and extended findings from other systems on the trafficking of lysosomal membrane proteins by showing increased cell surface

trafficking of the proteins CD63, LAMP-1 and LAMP-2 in cells derived from the HPS patients, in addition to demonstrating interactions between AP-3 and the tyrosine-based sorting signals from these proteins.

AP-3 FUNCTION IN THE IMMUNE SYSTEM: THE ROLE OF LEUKOCYTIC LROS

AP-3-dependent trafficking has now been implicated in a wide variety of immune cell functions. Some HPS patients are known to be susceptible to recurrent infection (DePinho and Kaplan, 1985), and studies of AP-3-deficient cells in recent years have led to the identification of functional defects in both the myeloid and lymphoid cell lineages. Strikingly, these deficits consistently appear to involve aberrant trafficking of membrane proteins to the various types of leukocytic LROs. Several examples will be discussed below to convey the broad range of functions that have been described to date.

I. CD1 trafficking

The first evidence for a role of AP-3 in the immune system came from Michael Brenner's lab with the demonstration that the lipid-antigen presenting protein CD1b, but not other CD1 isoforms, was trafficked improperly in immune cells from HPS type 2 patients (Sugita et al., 2002). In particular, CD1b, which normally resides in a lysosome-like compartment at steady state, was found to be trapped in transferrin-receptor-labeled endosomes. Furthermore, CD1b was shown to interact with the AP-3 μ3A subunit by yeast two-hybrid analysis. This defect in trafficking resulted in a profound deficit in lipid-antigen presentation, but not in antigen presentation by CD1c, whose localization to early endosomes was not affected by loss of AP-3 (Sugita et al., 2002). These findings were particularly notable due to the fact that some HPS patients are susceptible to recurrent bacterial infection, even though HPS cells were known to have normal MHC class II trafficking (Caplan et al., 2000).

II. T cell lytic-granule biogenesis

Shortly after the findings on CD1 were published, Gillian Griffiths' lab reported the identification of another HPS type 2 patient and characterized a defect in the sorting of the tetraspanin CD63 to a type of LRO found in cytotoxic T lymphocytes (CTLs) known as the lytic granule (Clark et al., 2003). Morphologically, the HPS type 2 lytic granules appeared markedly larger by EM, and contained significantly more intraluminal vesicles relative to control cells. In terms of functional consequences, the lack of AP-3 was associated with defective lytic granule polarization at the immunological synapse, and, consequently, decreased killing ability of the CTLs.

III. Neutrophil azurophil granule biogenesis

The same year saw the identification of a β3A subunit mutation in a cohort of inbred dogs displaying coat-color dilution and cyclic hematopoiesis, a disorder wherein the levels of neutrophils and other leukocytes oscillate in weekly phases. In humans this disorder is associated with mutations in neutrophil elastase (NE), and the authors showed that AP-3 is capable of interacting with NE, while loss of AP-3 in the mutant dogs led to impaired trafficking of NE to azurophil granules, a type of LRO (Benson et al., 2003).

IV. Toll-like receptor trafficking

Two recent studies have independently reported roles for AP-3 (Sasai et al., 2010) as well as the BLOC-1 and -2 complexes (Blasius et al., 2010) in toll-like receptor (TLR)-induced interferon responses specifically from plasmacytoid dendritic cells (pDCs). These papers raise the possibility that HPS patients might be compromised in their ability to respond to viral infection (in addition to bacterial infection), as pDCs are responsible for the majority of interferon produced after infection. The findings also suggest that pDCs may contain a hitherto uncharacterized LRO specialized for TLR signaling.

V. HIV protein trafficking

Several papers have described interactions between AP-3 and HIV proteins. The first demonstration of such an interaction gave general insight into how dileucine signals are recognized by AP-3. In particular, Bonifacino's group demonstrated that a dileucine signal from HIV-1 Nef interacts with the AP-3 δ-σ3 hemicomplex (Janvier et al., 2003). In addition, HIV-1 Gag was shown to interact with the hinge region of AP-3 δ, and this interaction was suggested to mediate Gag trafficking to multivesicular bodies, thus enabling HIV particle formation (Dong et al., 2005). The physiological implications of these AP-3–HIV protein interactions remain unknown.

THE BIOGENESIS OF LYSOSOME-RELATED ORGANELLES COMPLEXES

I. Basic characterization of BLOC-1

The years 2002-2004 saw the identification of three new cytoplasmic protein complexes involved in the biogenesis of LROs, known as the BLOC complexes, and containing subunits mutated in various spontaneous coat-color mutant mice. The first hints of a novel cytoplasmic complex came from Esteban Dell'Angelica's lab with the demonstration that the pallidin and muted proteins, from *pallid* and *muted* mice, respectively, interacted with each other and were part of an ~200 kDa complex (Falcon-Perez et al., 2002). The next subunit from BLOC-1 to be identified was cappuccino, from the mutant mouse of the same name (Ciciotte et al., 2003). The fourth subunit, dysbindin, was identified in the same year, and was shown to be mutated in both the *sandy* mouse and in a HPS patient (now referred to as HPS type 7) (Li et al., 2003). This was the first demonstration that loss of a BLOC component could cause HPS. Further work from Dell'Angelica's lab demonstrated the presence of four more members of the BLOC-1 complex, including the t-SNARE-interacting protein snapin, and three previously uncharacterized proteins

they named BLOS1 through 3, with BLOS3 being mutated in the *reduced pigmentation* mouse (Starcevic and Dell Angelica, 2004). Additional genetic studies have identified novel mutations in other BLOC subunits, for example, with the recent identification of a mutation in pallidin in HPS type 9 (Cullinane et al., 2011). Finally, a recent study has furthered our understanding of the mechanism of BLOC-1 function in LRO biogenesis by showing that trafficking of the copper transporter, ATP7A, to the melanosome is dependent on BLOC-1. Importantly, the presence of copper in the melanosome, which is enabled by ATP7A transport, is required for tyrosinase activity, without which melanin cannot be formed (Setty et al., 2008).

II. Discovery of BLOC-2 and -3

The BLOC-2 complex was initially characterized as being comprised of three novel proteins, HPS3, HPS5 and HPS6—all genetically linked to HPS subtypes of the same number—to form an ~340 kDa complex (Di Pietro et al., 2004; Gautam et al., 2004). The ~175 kDa BLOC-3 complex was isolated around the same time and found to be made up of two more HPS-associated proteins, HPS1 and HPS4 (Chiang et al., 2003; Martina et al., 2003; Nazarian et al., 2003). Interestingly, clinical studies have demonstrated phenotypic differences among some HPS subtypes, including the presence of granulomatous colitis and pulmonary fibrosis in some patients with HPS types 1 and 4 (i.e., BLOC-3 deficiency) (Nazarian et al., 2003; Carmona-Rivera et al., 2011) as well as type 2 (i.e., AP-3 deficiency) (Gochuico et al., 2011). Thus, although little is known about the BLOC complexes' molecular functions, we can surmise from the clinical data that BLOC-3 and AP-3 might serve tissue-specific functions in which BLOC-1 and -2 are not involved.

III. The BLOC complexes and AP-3

After the discovery and initial characterization of the three BLOC complexes, questions arose as to their interdependence and functional relationship with AP-3. Studies showed that the

51

trafficking of some AP-3-dependent cargo molecules, such as LAMP-1 and the v-SNARE, VAMP7, was similarly altered in BLOC-1-deficient cells (Salazar et al., 2006), and there is some evidence that BLOC-1 and AP-3 can interact physically (Di Pietro et al., 2006). However, until further elucidation of BLOC complex molecular function, it will be difficult to understand the precise relationship between these hetero-oligomeric protein complexes.

IV. BLOC-1 is associated with schizophrenia and involved in neurotransmission

The BLOC complex gained wider interest after genetic variants in two of its constituents, dysbindin and muted, were shown to be significantly associated with risk for schizophrenia (Morris et al., 2008). At the time this association was made, it was unclear how the BLOC complex could be involved in schizophrenia pathogenesis, but recently the dysbindin and snapin subunits have been implicated in the presynaptic, homeostatic modulation of neurotransmission (Dickman and Davis, 2009; Dickman et al., 2012), thus providing a new avenue of research.

DOES AP-3 ACT AT THE GOLGI, ENDOSOME, OR BOTH?

I. Early characterizations

At the time of its isolation and initial characterization in mammalian cells, AP-3 was considered to localize primarily to a perinuclear compartment, most likely either TGN or early endosomes (Simpson et al., 1997; Dell Angelica et al., 1997a). However, the initial, inconclusive immunofluorescence efforts actually showed that AP-3 did not co-localize particularly strongly with markers of either TGN or early endosomes, nor with clathrin or AP-1. On the other hand, yeast genetic and biochemical evidence strongly supported a primary role for AP-3 acting at the TGN, findings which to this day are not disputed (Cowles et al., 1997a; Rehling et al., 1999). How has the picture changed for mammalian AP-3 over the last decade?

II. Immuno-EM studies

Several years after AP-3's discovery, careful immuno-EM studies by Judith Klumperman suggested a predominant role for mammalian AP-3 in concentrating certain membrane proteins at the tips of tubular early endosomes, with ~10-fold less AP-3 found associated with TGN membranes (Peden et al., 2004). It should be noted, though, that these studies were limited to the HepG2 hepatic cancer cell line and δ-subunit-rescued *mocha* fibroblasts. In addition, some limited, non-quantitative immuno-EM for AP-3 has been reported in neuroendocrine PC12 cells, and in this case labeling could be observed in the vicinity of the Golgi, although the precise origin of the membranes was not defined (Dell Angelica et al., 1998). A modest amount of TGN labeling was observed in immuno-EM studies done on the melanocytic cell line Melan-a, in this case amounting to ~10% of the total label (Theos et al., 2005). Considering the above observations, it appears that in non-neural cells AP-3 localizes to a greater extent to early endosomes. On the other hand, the AP-3 cargo protein VAMP7 becomes trapped in the cell body of *mocha* neurons and, in particular, appears to accumulate in the TGN by immuno-EM (Scheuber et al., 2006)—strongly suggesting a role for AP-3 at the Golgi in neurons. It is currently not known how AP-3 might localize in other specialized secretory cells, such as adrenal chromaffin cells or pancreatic β cells.

III. Additional evidence for metazoan AP-3 at the TGN

While a number of investigators in the field now consider metazoan AP-3 to be primarily an endosomal adaptor, a variety of papers have presented data supporting a role for this complex in sorting particular proteins directly from the TGN. For instance, the lab of J. Paul Luzio has suggested that AP-3 sorts some proteins, such as CD63, from the TGN to late endosomes, while sorting others, such as endolyn, from early endosomes to late (Rous et al., 2002; Ihrke et al., 2004). In another example, efficient exit of the vesicular stomatitis virus glycoprotein (VSVG) from the TGN into secretory vesicles has been proposed to involve AP-3 (Nishimura et al., 2002).

In addition, the lab of Stefan Höning has used an innovative TGN budding assay to demonstrate a requirement for AP-3 in the budding of LAMP-1 and tyrosinase carriers, but not in the budding of the cation-dependent MPR, which is known to depend on AP-1 (Chapuy et al., 2008). Moreover, several biochemical studies have shown that AP-3 can be readily recruited to isolated Golgi membranes or to liposomes containing phosphatidylinositol 4-phosphate, a lipid enriched in the TGN (Drake et al., 2000; Baust et al., 2008). Thus, the accumulated evidence suggests that metazoan AP-3 is capable of acting at early endosomes *and* the TGN, and the predominant role probably depends on cell-specific context.

AP-3 AND THE BLOC COMPLEX IN THE REGULATED SECRETORY PATHWAY

I. BLOC subunits modulate a late stage of large dense-core vesicle exocytosis

There are a few examples in the literature that suggest members of the BLOC complex might influence certain aspects of regulated exocytosis in neuroendocrine cells. In particular, the coiled-coil protein snapin, a member of the BLOC-1 complex, appears to modulate the size of the readily releasable pool (RRP) of large dense-core vesicles (LDCVs) in chromaffin cells (Tian et al., 2005). Specifically, snapin-null chromaffin cells showed a selective reduction in the "burst phase" of LDCV release after calcium uncaging, but normal sustained release. Since snapin had been known to interact with the fusion machinery (Chheda et al., 2001), and other parameters measured, including LDCV number and distribution (i.e., docking status), were unchanged, the authors suggested that snapin might contribute to the RRP by stabilizing LDCV priming (Tian et al., 2005).

The BLOC-1 member dysbindin has also been shown to play a role in regulated exocytosis. In particular, amperometric recording of dysbindin-null *sandy* chromaffin cells demonstrated a modest reduction in the number of depolarization-induced exocytotic events, with the average

event having slightly increased quantal size (Chen et al., 2008). In addition, capacitance measurements showed an ~50% reduction in RRP size in these mice, consistent with the phenotype of the snapin-null mice (Tian et al., 2005). Finally, by EM, the dysbindin-null chromaffin cells were found to have moderately reduced numbers of LDCVs, with a slight (~10%) increase in LDCV size, although the number of morphologically docked vesicles was unchanged. Although neither of the above papers was studying snapin or dysbindin in the context of their roles in the BLOC complex, the similar phenotypes reported suggest that the BLOC complex indeed plays a role in regulated neuroendocrine secretion (albeit a subtle one), possibly at the level of vesicle priming.

II. AP-3 regulates LDCV quantal size

In addition to the findings described above demonstrating a role for the BLOC complex in modulating regulated exocytosis, one paper from Aaron Fox's lab has suggested a role for AP-3 in controlling chromaffin granule size (Grabner et al., 2006). The methodology used in this study (direct application of calcium to permeabilized cells) prevented the authors from assessing the regulation of exocytosis, but they did find AP-3-deficient *mocha* mice to have significantly larger quantal events (i.e., amount of catecholamine released), and these findings were consistent with the observation that *mocha* chromaffin granule size was significantly increased, as seen by EM (Grabner et al., 2006).

III. AP-3 controls protein sorting to the regulated secretory pathway

Finally, our lab has recently demonstrated a role for AP-3 in sorting proteins to the regulated secretory pathway of neuroendocrine cells. In particular, depletion of AP-3 by RNAi results in a defect in the formation of LDCVs at TGN, and leads to dysregulated secretion of soluble and membrane proteins (Asensio et al., 2010), a phenotype which we have hypothesized occurs due to mis-sorting of functionally important LDCV membrane proteins. In addition, we find that loss of

55

AP-3 *in vivo* is sufficient to dysregulate LDCV exocytosis from adrenal chromaffin and pancreatic β cells. Furthermore, quantitative proteomic analysis has defined the set of LDCV proteins which are altered upon loss of AP-3, as well as provided clues as to the molecules responsible for the dysregulation of secretion. Taken together, our work suggests a surprising but crucial role for AP-3-directed sorting within the regulated secretory pathway, with potentially important implications for physiology and disease. Moreover, it underscores a potential metazoan adaptation of the ancient yeast AP-3 pathway for a neuroendocrine-specific function. Our findings on AP-3's role in the biogenesis of the regulated secretory pathway will be the focus of Chapters 3 and 4.

References

Anand, V.C., Daboussi, L., Lorenz, T.C., and Payne, G.S. (2009). Genome-wide analysis of AP-3-dependent protein transport in yeast. Mol Biol Cell *20*, 1592–1604.

Angers, C.G., and Merz, A.J. (2009). HOPS interacts with Apl5 at the vacuole membrane and is required for consumption of AP-3 transport vesicles. Mol Biol Cell *20*, 4563–4574.

Asensio, C.S., Sirkis, D.W., and Edwards, R.H. (2010). RNAi screen identifies a role for adaptor protein AP-3 in sorting to the regulated secretory pathway. J Cell Biol *191*, 1173–1187.

Azevedo, C., Burton, A., Ruiz-Mateos, E., Marsh, M., and Saiardi, A. (2009). Inositol pyrophosphate mediated pyrophosphorylation of AP3B1 regulates HIV-1 Gag release. Proc Natl Acad Sci USA *106*, 21161–21166.

Baust, T., Anitei, M., Czupalla, C., Parshyna, I., Bourel, L., Thiele, C., Krause, E., and Hoflack, B. (2008). Protein networks supporting AP-3 function in targeting lysosomal membrane proteins. Mol Biol Cell *19*, 1942–1951.

Benson, K.F., Li, F.-Q., Person, R.E., Albani, D., Duan, Z., Wechsler, J., Meade-White, K., Williams, K., Acland, G.M., Niemeyer, G., et al. (2003). Mutations associated with neutropenia in dogs and humans disrupt intracellular transport of neutrophil elastase. Nat Genet *35*, 90–96.

Besteiro, S., Tonn, D., Tetley, L., Coombs, G.H., and Mottram, J.C. (2008). The AP3 adaptor is involved in the transport of membrane proteins to acidocalcisomes of Leishmania. J Cell Sci *121*, 561–570.

Blasius, A.L., Arnold, C.N., Georgel, P., Rutschmann, S., Xia, Y., Lin, P., Ross, C., Li, X., Smart, N.G., and Beutler, B. (2010). Slc15a4, AP-3, and Hermansky-Pudlak syndrome proteins are required for Toll-like receptor signaling in plasmacytoid dendritic cells. Proc Natl Acad Sci USA *107*, 19973–19978.

Cabrera, M., Ostrowicz, C.W., Mari, M., LaGrassa, T.J., Reggiori, F., and Ungermann, C. (2009). Vps41 phosphorylation and the Rab Ypt7 control the targeting of the HOPS complex to endosome-vacuole fusion sites. Mol Biol Cell *20*, 1937–1948.

Caplan, S., Dell Angelica, E.C., Gahl, W.A., and Bonifacino, J.S. (2000). Trafficking of major histocompatibility complex class II molecules in human B-lymphoblasts deficient in the AP-3 adaptor complex. Immunol. Lett. *72*, 113–117.

Carmona-Rivera, C., Golas, G., Hess, R.A., Cardillo, N.D., Martin, E.H., O'Brien, K., Tsilou, E., Gochuico, B.R., White, J.G., Huizing, M., et al. (2011). Clinical, Molecular, and Cellular Features of Non-Puerto Rican Hermansky-Pudlak Syndrome Patients of Hispanic Descent. J Invest Dermatol.

Chapuy, B., Tikkanen, R., Mühlhausen, C., Wenzel, D., Figura, von, K., and Höning, S. (2008). AP-1 and AP-3 mediate sorting of melanosomal and lysosomal membrane proteins into distinct post-Golgi trafficking pathways. Traffic *9*, 1157–1172.

Chen, X.-W., Feng, Y.-Q., Hao, C.-J., Guo, X.-L., He, X., Zhou, Z.-Y., Guo, N., Huang, H.-P., Xiong, W., Zheng, H., et al. (2008). DTNBP1, a schizophrenia susceptibility gene, affects kinetics of transmitter release. J Cell Biol *181*, 791–801.

Chheda, M.G., Ashery, U., Thakur, P., Rettig, J., and Sheng, Z.H. (2001). Phosphorylation of Snapin by PKA modulates its interaction with the SNARE complex. Nat Cell Biol *3*, 331–338.

Chiang, P.-W., Oiso, N., Gautam, R., Suzuki, T., Swank, R.T., and Spritz, R.A. (2003). The Hermansky-Pudlak syndrome 1 (HPS1) and HPS4 proteins are components of two complexes, BLOC-3 and BLOC-4,

involved in the biogenesis of lysosome-related organelles. J Biol Chem *278*, 20332–20337.

Christis, C., and Munro, S. (2012). The small G protein Arl1 directs the trans-Golgi-specific targeting of the Arf1 exchange factors BIG1 and BIG2. J Cell Biol *196*, 327–335.

Ciciotte, S.L., Gwynn, B., Moriyama, K., Huizing, M., Gahl, W.A., Bonifacino, J.S., and Peters, L.L. (2003). Cappuccino, a mouse model of Hermansky-Pudlak syndrome, encodes a novel protein that is part of the pallidin-muted complex (BLOC-1). Blood *101*, 4402–4407.

Clark, R.H., Stinchcombe, J.C., Day, A., Blott, E., Booth, S., Bossi, G., Hamblin, T., Davies, E.G., and Griffiths, G.M. (2003). Adaptor protein 3-dependent microtubule-mediated movement of lytic granules to the immunological synapse. Nat Immunol *4*, 1111–1120.

Cowles, C.R., Odorizzi, G., Payne, G.S., and Emr, S.D. (1997a). The AP-3 adaptor complex is essential for cargo-selective transport to the yeast vacuole. Cell *91*, 109–118.

Cowles, C.R., Snyder, W.B., Burd, C.G., and Emr, S.D. (1997b). Novel Golgi to vacuole delivery pathway in yeast: identification of a sorting determinant and required transport component. Embo J *16*, 2769–2782.

Craige, B., Salazar, G., and Faundez, V. (2008). Phosphatidylinositol-4-kinase type II alpha contains an AP-3-sorting motif and a kinase domain that are both required for endosome traffic. Mol Biol Cell *19*, 1415–1426.

Cullinane, A.R., Curry, J.A., Carmona-Rivera, C., Summers, C.G., Ciccone, C., Cardillo, N.D., Dorward, H., Hess, R.A., White, J.G., Adams, D., et al. (2011). A BLOC-1 mutation screen reveals that PLDN is mutated in Hermansky-Pudlak Syndrome type 9. Am J Hum Genet *88*, 778–787.

Darnell, R.B., Furneaux, H.M., and Posner, J.B. (1991). Antiserum from a patient with cerebellar degeneration identifies a novel protein in Purkinje cells, cortical neurons, and neuroectodermal tumors. J Neurosci *11*, 1224–1230.

Darsow, T., Burd, C.G., and Emr, S.D. (1998). Acidic di-leucine motif essential for AP-3-dependent sorting and restriction of the functional specificity of the Vam3p vacuolar t-SNARE. J Cell Biol *142*, 913–922.

Darsow, T., Katzmann, D.J., Cowles, C.R., and Emr, S.D. (2001). Vps41p function in the alkaline phosphatase pathway requires homo-oligomerization and interaction with AP-3 through two distinct domains. Mol Biol Cell *12*, 37–51.

Darsow, T., Rieder, S.E., and Emr, S.D. (1997). A multispecificity syntaxin homologue, Vam3p, essential for autophagic and biosynthetic protein transport to the vacuole. J Cell Biol *138*, 517–529.

Daugherty, B.L., Straley, K.S., Sanders, J.M., Phillips, J.W., Disdier, M., McEver, R.P., and Green, S.A. (2001). AP-3 adaptor functions in targeting P-selectin to secretory granules in endothelial cells. Traffic *2*, 406–413.

Dell Angelica, E.C., Klumperman, J., Stoorvogel, W., and Bonifacino, J.S. (1998). Association of the AP-3 adaptor complex with clathrin. Science *280*, 431–434.

Dell Angelica, E.C., Ohno, H., Ooi, C.E., Rabinovich, E., Roche, K.W., and Bonifacino, J.S. (1997a). AP-3: an adaptor-like protein complex with ubiquitous expression. Embo J *16*, 917–928.

Dell Angelica, E.C., Ooi, C.E., and Bonifacino, J.S. (1997b). Beta3A-adaptin, a subunit of the adaptor-like complex AP-3. J Biol Chem *272*, 15078–15084.

Dell Angelica, E.C., Shotelersuk, V., Aguilar, R.C., Gahl, W.A., and Bonifacino, J.S. (1999). Altered trafficking of lysosomal proteins in Hermansky-Pudlak syndrome due to mutations in the beta 3A subunit of the AP-3 adaptor. Mol Cell *3*, 11–21.

DePinho, R.A., and Kaplan, K.L. (1985). The Hermansky-Pudlak syndrome. Report of three cases and review of pathophysiology and management considerations. Medicine (Baltimore) *64*, 192–202.

Di Pietro, S.M., Falcon-Perez, J.M., and Dell Angelica, E.C. (2004). Characterization of BLOC-2, a complex containing the Hermansky-Pudlak syndrome proteins HPS3, HPS5 and HPS6. Traffic *5*, 276–283.

Di Pietro, S.M., Falcon-Perez, J.M., Tenza, D., Setty, S.R.G., Marks, M.S., Raposo, G., and Dell Angelica, E.C. (2006). BLOC-1 interacts with BLOC-2 and the AP-3 complex to facilitate protein trafficking on endosomes. Mol Biol Cell *17*, 4027–4038.

Dickman, D.K., and Davis, G.W. (2009). The schizophrenia susceptibility gene dysbindin controls synaptic homeostasis. Science *326*, 1127–1130.

Dickman, D.K., Tong, A., and Davis, G.W. (2012). Snapin is Critical for Presynaptic Homeostatic Plasticity. J Neurosci *32*, 8716–8724.

Dong, X., Li, H., Derdowski, A., Ding, L., Burnett, A., Chen, X., Peters, T.R., Dermody, T.S., Woodruff, E., Wang, J.-J., et al. (2005). AP-3 directs the intracellular trafficking of HIV-1 Gag and plays a key role in particle assembly. Cell *120*, 663–674.

Drake, M.T., Zhu, Y., and Kornfeld, S. (2000). The assembly of AP-3 adaptor complex-containing clathrin-coated vesicles on synthetic liposomes. Mol Biol Cell *11*, 3723–3736.

Falcon-Perez, J.M., Starcevic, M., Gautam, R., and Dell Angelica, E.C. (2002). BLOC-1, a novel complex containing the pallidin and muted proteins involved in the biogenesis of melanosomes and platelet-dense granules. J Biol Chem *277*, 28191–28199.

Faundez, V., Horng, J.T., and Kelly, R.B. (1998). A function for the AP3 coat complex in synaptic vesicle formation from endosomes. Cell *93*, 423–432.

Feng, L., Novak, E.K., Hartnell, L.M., Bonifacino, J.S., Collinson, L.M., and Swank, R.T. (2002). The Hermansky-Pudlak syndrome 1 (HPS1) and HPS2 genes independently contribute to the production and function of platelet dense granules, melanosomes, and lysosomes. Blood *99*, 1651–1658.

Feng, L., Seymour, A.B., Jiang, S., To, A., Peden, A.A., Novak, E.K., Zhen, L., Rusiniak, M.E., Eicher, E.M., Robinson, M.S., et al. (1999). The beta3A subunit gene (Ap3b1) of the AP-3 adaptor complex is altered in the mouse hypopigmentation mutant pearl, a model for Hermansky-Pudlak syndrome and night blindness. Hum Mol Genet *8*, 323–330.

Gautam, R., Chintala, S., Li, W., Zhang, Q., Tan, J., Novak, E.K., Di Pietro, S.M., Dell Angelica, E.C., and Swank, R.T. (2004). The Hermansky-Pudlak syndrome 3 (cocoa) protein is a component of the biogenesis of lysosome-related organelles complex-2 (BLOC-2). J Biol Chem *279*, 12935–12942.

Gochuico, B.R., Huizing, M., Golas, G.A., Scher, C.D., Tsokos, M., Denver, S.D., Frei-Jones, M.J., and Gahl, W.A. (2011). Interstitial Lung Disease and Pulmonary Fibrosis in Hermansky-Pudlak Syndrome Type 2, an AP-3 Complex Disease. Mol Med.

Grabner, C.P., Price, S.D., Lysakowski, A., Cahill, A.L., and Fox, A.P. (2006). Regulation of large dense-core vesicle volume and neurotransmitter content mediated by adaptor protein 3. Proc Natl Acad Sci USA *103*, 10035–10040.

Grote, E., and Kelly, R.B. (1996). Endocytosis of VAMP is facilitated by a synaptic vesicle targeting signal. J Cell Biol *132*, 537–547.

Grote, E., Hao, J.C., Bennett, M.K., and Kelly, R.B. (1995). A targeting signal in VAMP regulating transport to synaptic vesicles. Cell *81*, 581–589.

Harrison-Lavoie, K.J., Michaux, G., Hewlett, L., Kaur, J., Hannah, M.J., Lui-Roberts, W.W.Y., Norman, K.E., and Cutler, D.F. (2006). P-selectin and CD63 use different mechanisms for delivery to Weibel-Palade bodies. Traffic *7*, 647–662.

Hermann, G.J.G., Schroeder, L.K.L., Priess, J.R.J., 8 (2005). Genetic analysis of lysosomal trafficking in Caenorhabditis elegans. Mol Biol Cell *16*, 3273–3288.

HERMANSKY, F., and PUDLAK, P. (1959). Albinism associated with hemorrhagic diathesis and unusual pigmented reticular cells in the bone marrow: report of two cases with histochemical studies. Blood *14*, 162–169.

Höning, S., Sandoval, I.V., and Figura, von, K. (1998). A di-leucine-based motif in the cytoplasmic tail of LIMP-II and tyrosinase mediates selective binding of AP-3. Embo J *17*, 1304–1314.

Hua, Z., Leal-Ortiz, S., Foss, S.M., Waites, C.L., Garner, C.C., Voglmaier, S.M., and Edwards, R.H. (2011). v-SNARE Composition Distinguishes Synaptic Vesicle Pools. Neuron *71*, 474–487.

Huang, G., Fang, J., Sant'anna, C., Li, Z., Wellems, D.L., Rohloff, P., and Docampo, R. (2011). Adaptor protein-3 (AP-3) complex mediates the biogenesis of acidocalcisomes and is essential for growth and virulence of Trypanosoma brucei. J Biol Chem.

Huang, L., Kuo, Y.M., and Gitschier, J. (1999). The pallid gene encodes a novel, syntaxin 13-interacting protein involved in platelet storage pool deficiency. Nat Genet *23*, 329–332.

Huizing, M., Sarangarajan, R., Strovel, E., Zhao, Y., Gahl, W.A., and Boissy, R.E. (2001). AP-3 mediates tyrosinase but not TRP-1 trafficking in human melanocytes. Mol Biol Cell *12*, 2075–2085.

Ihrke, G., Kyttälä, A., Russell, M.R.G., Rous, B.A., and Luzio, J.P. (2004). Differential use of two AP-3-mediated pathways by lysosomal membrane proteins. Traffic *5*, 946–962.

Jackson, L.P., Kelly, B.T., McCoy, A.J., Gaffry, T., James, L.C., Collins, B.M., Höning, S., Evans, P.R., and Owen, D.J. (2010). A large-scale conformational change couples membrane recruitment to cargo binding in the AP2 clathrin adaptor complex. Cell *141*, 1220–1229.

Janvier, K., Kato, Y., Boehm, M., Rose, J.R., Martina, J.A., Kim, B.-Y., Venkatesan, S., and Bonifacino, J.S. (2003). Recognition of dileucine-based sorting signals from HIV-1 Nef and LIMP-II by the AP-1 gamma-sigma1 and AP-3 delta-sigma3 hemicomplexes. J Cell Biol *163*, 1281–1290.

Kantheti, P., Qiao, X., Diaz, M.E., Peden, A.A., Meyer, G.E., Carskadon, S.L., Kapfhamer, D., Sufalko, D., Robinson, M.S., Noebels, J.L., et al. (1998). Mutation in AP-3 delta in the mocha mouse links endosomal transport to storage deficiency in platelets, melanosomes, and synaptic vesicles. Neuron *21*, 111–122.

Kelly, B.T., McCoy, A.J., Späte, K., Miller, S.E., Evans, P.R., Höning, S., and Owen, D.J. (2008). A structural explanation for the binding of endocytic dileucine motifs by the AP2 complex. Nature *456*, 976–979.

Kent, H.M., Evans, P.R., Schäfer, I.B., Gray, S.R., Sanderson, C.M., Luzio, J.P., Peden, A.A., and Owen, D.J. (2012). Structural Basis of the Intracellular Sorting of the SNARE VAMP7 by the AP3 Adaptor Complex. Dev Cell.

Kretzschmar, D., Poeck, B., Roth, H., Ernst, R., Keller, A., Porsch, M., Strauss, R., and Pflugfelder, G.O. (2000). Defective pigment granule biogenesis and aberrant behavior caused by mutations in the Drosophila AP-3beta adaptin gene ruby. Genetics *155*, 213–223.

LaGrassa, T.J., and Ungermann, C. (2005). The vacuolar kinase Yck3 maintains organelle fragmentation by regulating the HOPS tethering complex. J Cell Biol *168*, 401–414.

Lane, P.W., and Deol, M.S. (1974). Mocha, a new coat color and behavior mutation on chromosome 10 of the mouse. J Hered *65*, 362–364.

Le Borgne, R., Alconada, A., Bauer, U., and Hoflack, B. (1998). The mammalian AP-3 adaptor-like complex mediates the intracellular transport of lysosomal membrane glycoproteins. J Biol Chem *273*, 29451–29461.

Lefrançois, S., Janvier, K., Boehm, M., Ooi, C.E., and Bonifacino, J.S. (2004). An ear-core interaction regulates the recruitment of the AP-3 complex to membranes. Dev Cell *7*, 619–625.

Li, W., Zhang, Q., Oiso, N., Novak, E.K., Gautam, R., O'Brien, E.P., Tinsley, C.L., Blake, D.J., Spritz, R.A., Copeland, N.G., et al. (2003). Hermansky-Pudlak syndrome type 7 (HPS-7) results from mutant dysbindin, a member of the biogenesis of lysosome-related organelles complex 1 (BLOC-1). Nat Genet *35*, 84–89.

Lichtenstein, Y., Desnos, C., Faundez, V., Kelly, R.B., and Clift-O'Grady, L. (1998). Vesiculation and sorting from PC12-derived endosomes in vitro. Proc Natl Acad Sci USA *95*, 11223–11228.

Lyerla, T.A., Rusiniak, M.E., Borchers, M., Jahreis, G., Tan, J., Ohtake, P., Novak, E.K., and Swank, R.T. (2003). Aberrant lung structure, composition, and function in a murine model of Hermansky-Pudlak syndrome. Am. J. Physiol. Lung Cell Mol. Physiol. *285*, L643–L653.

Martina, J.A., Moriyama, K., and Bonifacino, J.S. (2003). BLOC-3, a protein complex containing the Hermansky-Pudlak syndrome gene products HPS1 and HPS4. J Biol Chem *278*, 29376–29384.

Martinez-Arca, S., Rudge, R., Vacca, M., Raposo, G., Camonis, J., Proux-Gillardeaux, V., Daviet, L., Formstecher, E., Hamburger, A., Filippini, F., et al. (2003). A dual mechanism controlling the localization and function of exocytic v-SNAREs. Proc Natl Acad Sci USA *100*, 9011–9016.

Mattera, R., Boehm, M., Chaudhuri, R., Prabhu, Y., and Bonifacino, J.S. (2011). Conservation and diversification of dileucine signal recognition by adaptor protein (AP) complex variants. J Biol Chem *286*, 2022–2030.

Morris, D.W., Murphy, K., Kenny, N., Purcell, S.M., McGhee, K.A., Schwaiger, S., Nangle, J.-M., Donohoe, G., Clarke, S., Scully, P., et al. (2008). Dysbindin (DTNBP1) and the biogenesis of lysosome-related organelles complex 1 (BLOC-1): main and epistatic gene effects are potential contributors to schizophrenia susceptibility. Biol Psychiatry *63*, 24–31.

Mullins, C., Hartnell, L.M., and Bonifacino, J.S. (2000). Distinct requirements for the AP-3 adaptor complex in pigment granule and synaptic vesicle biogenesis in Drosophila melanogaster. Mol Gen Genet *263*, 1003–1014.

Mullins, C., Hartnell, L.M., Wassarman, D.A., and Bonifacino, J.S. (1999). Defective expression of the mu3 subunit of the AP-3 adaptor complex in the Drosophila pigmentation mutant carmine. Mol Gen Genet *262*, 401–412.

Nakatsu, F., Okada, M., Mori, F., Kumazawa, N., Iwasa, H., Zhu, G., Kasagi, Y., Kamiya, H., Harada, A., Nishimura, K., et al. (2004). Defective function of GABA-containing synaptic vesicles in mice lacking the

AP-3B clathrin adaptor. J Cell Biol *167*, 293–302.

Nazarian, R., Falcon-Perez, J.M., and Dell Angelica, E.C. (2003). Biogenesis of lysosome-related organelles complex 3 (BLOC-3): a complex containing the Hermansky-Pudlak syndrome (HPS) proteins HPS1 and HPS4. Proc Natl Acad Sci USA *100*, 8770–8775.

Newman, L.S., McKeever, M.O., Okano, H.J., and Darnell, R.B. (1995). Beta-NAP, a cerebellar degeneration antigen, is a neuron-specific vesicle coat protein. Cell *82*, 773–783.

Nie, Z., Boehm, M., Boja, E.S., Vass, W.C., Bonifacino, J.S., Fales, H.M., and Randazzo, P.A. (2003). Specific regulation of the adaptor protein complex AP-3 by the Arf GAP AGAP1. Dev Cell *5*, 513–521.

Nishimura, N., Plutner, H., Hahn, K., and Balch, W.E. (2002). The delta subunit of AP-3 is required for efficient transport of VSV-G from the trans-Golgi network to the cell surface. Proc Natl Acad Sci USA *99*, 6755–6760.

Noebels, J.L., and Sidman, R.L. (1989). Persistent hypersynchronization of neocortical neurons in the mocha mutant of mouse. J Neurogenet *6*, 53–56.

Novak, E.K., and Swank, R.T. (1979). Lysosomal dysfunctions associated with mutations at mouse pigment genes. Genetics *92*, 189–204.

Novak, E.K., Hui, S.W., and Swank, R.T. (1984). Platelet storage pool deficiency in mouse pigment mutations associated with seven distinct genetic loci. Blood *63*, 536–544.

Ooi, C.E., Dell Angelica, E.C., and Bonifacino, J.S. (1998). ADP-Ribosylation factor 1 (ARF1) regulates recruitment of the AP-3 adaptor complex to membranes. J Cell Biol *142*, 391–402.

Ooi, C.E., Moreira, J.E., Dell Angelica, E.C., Poy, G., Wassarman, D.A., and Bonifacino, J.S. (1997). Altered expression of a novel adaptin leads to defective pigment granule biogenesis in the Drosophila eye color mutant garnet. Embo J *16*, 4508–4518.

Owen, D.J., and Evans, P.R. (1998). A structural explanation for the recognition of tyrosine-based endocytotic signals. Science *282*, 1327–1332.

Panek, H.R., Stepp, J.D., Engle, H.M., Marks, K.M., Tan, P.K., Lemmon, S.K., and Robinson, L.C. (1997). Suppressors of YCK-encoded yeast casein kinase 1 deficiency define the four subunits of a novel clathrin AP-like complex. Embo J *16*, 4194–4204.

Peden, A.A., Oorschot, V., Hesser, B.A., Austin, C.D., Scheller, R.H., and Klumperman, J. (2004). Localization of the AP-3 adaptor complex defines a novel endosomal exit site for lysosomal membrane proteins. J Cell Biol *164*, 1065–1076.

Peden, A.A., Rudge, R.E., Lui, W.W.Y., and Robinson, M.S. (2002). Assembly and function of AP-3 complexes in cells expressing mutant subunits. J Cell Biol *156*, 327–336.

Pevsner, J., Volknandt, W., Wong, B.R., and Scheller, R.H. (1994). Two rat homologs of clathrin-associated adaptor proteins. Gene *146*, 279–283.

Rehling, P., Darsow, T., Katzmann, D.J., and Emr, S.D. (1999). Formation of AP-3 transport intermediates requires Vps41 function. Nat Cell Biol *1*, 346–353.

Rous, B.A., Reaves, B.J., Ihrke, G., Briggs, J.A.G., Gray, S.R., Stephens, D.J., Banting, G., and Luzio, J.P. (2002). Role of adaptor complex AP-3 in targeting wild-type and mutated CD63 to lysosomes. Mol Biol Cell *13*, 1071–1082.

Salazar, G., Craige, B., Styers, M.L., Newell-Litwa, K.A., Doucette, M.M., Wainer, B.H., Falcon-Perez, J.M., Dell Angelica, E.C., Peden, A.A., Werner, E., et al. (2006). BLOC-1 complex deficiency alters the targeting of adaptor protein complex-3 cargoes. Mol Biol Cell *17*, 4014–4026.

Salazar, G., Craige, B., Wainer, B.H., Guo, J., De Camilli, P., and Faundez, V. (2005). Phosphatidylinositol-4-kinase type II alpha is a component of adaptor protein-3-derived vesicles. Mol Biol Cell *16*, 3692–3704.

Salazar, G., Love, R., Styers, M.L., Werner, E., Peden, A., Rodriguez, S., Gearing, M., Wainer, B.H., and Faundez, V. (2004a). AP-3-dependent mechanisms control the targeting of a chloride channel (ClC-3) in neuronal and non-neuronal cells. J Biol Chem *279*, 25430–25439.

Salazar, G., Love, R., Werner, E., Doucette, M.M., Cheng, S., Levey, A., and Faundez, V. (2004b). The zinc transporter ZnT3 interacts with AP-3 and it is preferentially targeted to a distinct synaptic vesicle subpopulation. Mol Biol Cell *15*, 575–587.

Salazar, G., Zlatic, S., Craige, B., Peden, A.A., Pohl, J., and Faundez, V. (2009). Hermansky-Pudlak syndrome protein complexes associate with phosphatidylinositol 4-kinase type II alpha in neuronal and non-neuronal cells. J Biol Chem *284*, 1790–1802.

Salem, N., Faundez, V., Horng, J.T., and Kelly, R.B. (1998). A v-SNARE participates in synaptic vesicle formation mediated by the AP3 adaptor complex. Nat Neurosci *1*, 551–556.

Sasai, M., Linehan, M.M., and Iwasaki, A. (2010). Bifurcation of Toll-like receptor 9 signaling by adaptor protein 3. Science *329*, 1530–1534.

Scheuber, A., Rudge, R., Danglot, L., Raposo, G., Binz, T., Poncer, J.-C., and Galli, T. (2006). Loss of AP-3 function affects spontaneous and evoked release at hippocampal mossy fiber synapses. Proc Natl Acad Sci USA *103*, 16562–16567.

Seals, D.F., Eitzen, G., Margolis, N., Wickner, W.T., and Price, A. (2000). A Ypt/Rab effector complex containing the Sec1 homolog Vps33p is required for homotypic vacuole fusion. Proc Natl Acad Sci USA *97*, 9402–9407.

Seong, E., Wainer, B.H., Hughes, E.D., Saunders, T.L., Burmeister, M., and Faundez, V. (2005). Genetic analysis of the neuronal and ubiquitous AP-3 adaptor complexes reveals divergent functions in brain. Mol Biol Cell *16*, 128–140.

Setty, S.R.G., Tenza, D., Sviderskaya, E.V., Bennett, D.C., Raposo, G., and Marks, M.S. (2008). Cell-specific ATP7A transport sustains copper-dependent tyrosinase activity in melanosomes. Nature *454*, 1142–1146.

Shi, G., Faundez, V., Roos, J., Dell Angelica, E.C., and Kelly, R.B. (1998). Neuroendocrine synaptic vesicles are formed in vitro by both clathrin-dependent and clathrin-independent pathways. J Cell Biol *143*, 947–955.

Simpson, F., Bright, N.A., West, M.A., Newman, L.S., Darnell, R.B., and Robinson, M.S. (1996). A novel adaptor-related protein complex. J Cell Biol *133*, 749–760.

Simpson, F., Peden, A.A., Christopoulou, L., and Robinson, M.S. (1997). Characterization of the adaptor-related protein complex, AP-3. J Cell Biol *137*, 835–845.

Starcevic, M., and Dell Angelica, E.C. (2004). Identification of snapin and three novel proteins (BLOS1, BLOS2, and BLOS3/reduced pigmentation) as subunits of biogenesis of lysosome-related organelles complex-1 (BLOC-1). J Biol Chem *279*, 28393–28401.

Stepp, J.D., Huang, K., and Lemmon, S.K. (1997). The yeast adaptor protein complex, AP-3, is essential for the efficient delivery of alkaline phosphatase by the alternate pathway to the vacuole. J Cell Biol *139*, 1761–1774.

Sugita, M., Cao, X., Watts, G.F.M., Rogers, R.A., Bonifacino, J.S., and Brenner, M.B. (2002). Failure of trafficking and antigen presentation by CD1 in AP-3-deficient cells. Immunity *16*, 697–706.

Swank, R.T., Reddington, M., Howlett, O., and Novak, E.K. (1991). Platelet storage pool deficiency associated with inherited abnormalities of the inner ear in the mouse pigment mutants muted and mocha. Blood *78*, 2036–2044.

Swetha, M.G., Sriram, V., Krishnan, K.S., Oorschot, V.M.J., Brink, Ten, C., Klumperman, J., and Mayor, S. (2011). Lysosomal membrane protein composition, acidic pH and sterol content are regulated via a light-dependent pathway in metazoan cells. Traffic *12*, 1037–1055.

Theos, A.C., Tenza, D., Martina, J.A., Hurbain, I., Peden, A.A., Sviderskaya, E.V., Stewart, A., Robinson, M.S., Bennett, D.C., Cutler, D.F., et al. (2005). Functions of adaptor protein (AP)-3 and AP-1 in tyrosinase sorting from endosomes to melanosomes. Mol Biol Cell *16*, 5356–5372.

Tian, J.-H., Wu, Z.-X., Unzicker, M., Lu, L., Cai, Q., Li, C., Schirra, C., Matti, U., Stevens, D., Deng, C., et al. (2005). The role of Snapin in neurosecretion: snapin knock-out mice exhibit impaired calcium-dependent exocytosis of large dense-core vesicles in chromaffin cells. J Neurosci *25*, 10546–10555.

Togawa, A., Morinaga, N., Ogasawara, M., Moss, J., and Vaughan, M. (1999). Purification and cloning of a brefeldin A-inhibited guanine nucleotide-exchange protein for ADP-ribosylation factors. J Biol Chem *274*, 12308–12315.

Voglmaier, S.M., Kam, K., Yang, H., Fortin, D.L., Hua, Z., Nicoll, R.A., and Edwards, R.H. (2006). Distinct endocytic pathways control the rate and extent of synaptic vesicle protein recycling. Neuron *51*, 71–84.

Vowels, J.J., and Payne, G.S. (1998). A dileucine-like sorting signal directs transport into an AP-3-dependent, clathrin-independent pathway to the yeast vacuole. Embo J *17*, 2482–2493.

Warner, T.S., Sinclair, D.A., Fitzpatrick, K.A., Singh, M., Devlin, R.H., and Honda, B.M. (1998). The light gene of Drosophila melanogaster encodes a homologue of VPS41, a yeast gene involved in cellular-protein trafficking. Genome *41*, 236–243.

Yang, W., Li, C., Ward, D.M., Kaplan, J., and Mansour, S.L. (2000). Defective organellar membrane protein trafficking in Ap3b1-deficient cells. J Cell Sci *113 (Pt 22)*, 4077–4086.

Yu, X., Breitman, M., and Goldberg, J. (2012). A structure-based mechanism for arf1-dependent recruitment of coatomer to membranes. Cell *148*, 530–542.

Zhen, L., Jiang, S., Feng, L., Bright, N.A., Peden, A.A., Seymour, A.B., Novak, E.K., Elliott, R., Gorin, M.B., Robinson, M.S., et al. (1999). Abnormal expression and subcellular distribution of subunit proteins of the AP-3 adaptor complex lead to platelet storage pool deficiency in the pearl mouse. Blood *94*, 146–155.

Zwiewka, M., Feraru, E., Möller, B., Hwang, I., Feraru, M.I., Kleine-Vehn, J., Weijers, D., and Friml, J. (2011). The AP-3 adaptor complex is required for vacuolar function in Arabidopsis. Cell Res. *21*, 1711–1722.

CHAPTER 3:

RNAi SCREEN IDENTIFIES A ROLE FOR ADAPTOR PROTEIN AP-3

IN SORTING TO THE REGULATED SECRETORY PATHWAY[*]

Cédric S. Asensio[1], Daniel W. Sirkis[1,2], and Robert H. Edwards[1,2]

[1]Departments of Physiology and Neurology

[2]Graduate Program in Pharmaceutical Sciences & Pharmacogenomics

University of California, San Francisco

San Francisco, California 94158

Citation:
Asensio, C.S., Sirkis, D.W., and Edwards, R.H. (2010). RNAi screen identifies a role for adaptor protein AP-3 in sorting to the regulated secretory pathway. *J Cell Biol 191*, 1173–1187.

Abstract

The regulated release of proteins including peptide hormones, neural peptides and growth factors depends on their sorting into large dense core vesicles (LDCVs) capable of regulated exocytosis. LDCVs form at the *trans*-Golgi network (TGN), but the mechanism of sorting to this regulated secretory pathway (RSP) and in particular the cytosolic machinery have remained poorly understood. Using as reporter a membrane protein that depends on cytosolic sequences for sorting to LDCVs, and an RNA interference screen in *Drosophila* cells, we now identify a small number of genes, including several subunits of the heterotetrameric adaptor protein AP-3, that are required for sorting to the RSP. In mammalian neuroendocrine cells, loss of AP-3 dysregulates the exocytosis of soluble as well as membrane cargo, and the mechanism involves a primary defect in LDCV formation. Previous work has implicated AP-3 in the endocytic pathway, but we find that AP-3 promotes sorting to the RSP within the biosynthetic pathway, at the level of the TGN. Although LDCVs still form in the absence of AP-3, they contain substantially less synaptotagmin 1, indicating a role for AP-3 in concentration of the proteins required for regulated exocytosis.

Introduction

The function of proteins involved in extracellular signaling depends on their regulated secretion in response to the appropriate stimuli. Regulated secretion contributes to the role of peptide hormones such as insulin, of neural peptides such as opioids and of growth factors such as brain-derived neurotrophic factor (BDNF). The regulated release of proteins thus has a central role in human disease as well as normal physiology, synaptic plasticity, behavior and development.

The regulated secretion of proteins requires their sorting into a specialized secretory pathway capable of regulated exocytosis, the regulated secretory pathway (RSP). In contrast to the constitutive secretory pathway, which confers the immediate release of newly synthesized proteins from essentially all eukaryotic cells, the RSP enables release from specialized cells in response to physiologically appropriate signals. However, we know very little about how proteins sort into the regulated rather than constitutive pathway.

Morphologically, the RSP usually corresponds to large vesicles containing a dense core of aggregated cargo. These large dense core vesicles (LDCVs) bud from the *trans*-Golgi network (TGN) (Eaton et al., 2000; Orci et al., 1987; Tooze and Huttner, 1990), and previous study has suggested that lumenal interactions such as the aggregation of "granulogenic" proteins drive their formation (Kim et al., 2001; Turkewitz, 2004). Previous studies have suggested that sorting to LDCVs occurs by default, with proteins destined for other organelles removed during the subsequent, well-established process of LDCV maturation (Arvan and Castle, 1998; Morvan and Tooze, 2008). However, the direct analysis of budding from the TGN has demonstrated the sorting of regulated from constitutive cargo at this step, before maturation (Tooze and Huttner, 1990). LDCV membrane proteins such as carboxypeptidase E and sortilin may serve as the receptors for soluble cargo (Chen et al., 2005; Cool et al., 1997). In contrast to these lumenal

interactions, we know little about any cytosolic machinery like that which generates transport vesicles from essentially all the other membrane compartments in eukaryotic cells.

Several membrane proteins contain cytosolic sequences that direct them to LDCVs. In the case of the enzyme peptidylglycine α-amidating monooxygenase (PAM) and the endothelial adhesion molecule P-selectin, however, these sequences are not required for sorting to the RSP since lumenal interactions suffice (Blagoveshchenskaya et al., 2002; Harrison-Lavoie et al., 2006). On the other hand, the neuronal vesicular monoamine transporter (VMAT2), which fills neurosecretory vesicles with monoamines, depends on a conserved C-terminal cytoplasmic dileucine-like motif (K*EE*KMA**IL**) for sorting to LDCVs (Erickson et al., 1995; Liu et al., 1994). Mutation of the dileucine–like core disrupts multiple trafficking events including endocytosis, but replacement of the upstream acidic residues (Glu-478 and –479) with alanine (EE/AA mutation) diverts VMAT2 from the regulated to the constitutive secretory pathway, increasing cell surface delivery without affecting endocytosis (Krantz et al., 1997). Glu-478 and –479 thus appear to have a specific role in sorting to the RSP, and the LDCV membrane protein phogrin contains a remarkably similar sequence also required for localization to LDCVs (Torii et al., 2005). Since VMAT2 does not appear at the cell surface before sorting to LDCVs (Li et al., 2005), the motif presumably acts within the biosynthetic rather than endocytic pathway, most likely at the level of the TGN, where LDCVs form. The requirement for a cytoplasmic motif in sorting to the RSP further suggests an interaction with cytosolic sorting machinery. Indeed, we have now used VMAT as a reporter to identify genes involved in biogenesis of the RSP.

Results

The increased plasma membrane expression of EE/AA VMAT2 due to its diversion from regulated to constitutive secretory pathway (Krantz et al., 2000) suggested that cellular defects in sorting to the RSP might similarly increase the surface delivery of wild type VMAT2. We have thus used the cell surface exposure of VMAT to screen for genes involved in biogenesis of the RSP. Although endocytosis might be expected to influence cell surface expression, direct sorting of VMAT2 to the RSP at the level of the TGN, without passage through the plasma membrane (Li et al., 2005), should minimize the chance of identifying genes involved in endocytosis. Screening for increased surface delivery should also reduce the likelihood of identifying genes with nonspecific deleterious effects.

***Drosophila* S2 cells exhibit a regulated secretory pathway**

Drosophila S2 cells are very sensitive to RNAi and have been used to screen for genes involved in a wide range of cellular processes (Bard et al., 2006; Foley and O'Farrell, 2004; Goshima et al., 2007; Guo et al., 2008), but it is not known whether S2 cells express sorting machinery that can recognize the dileucine-like motif in VMAT. On the other hand, even "constitutive" secretory cells such as chinese hamster ovary (CHO) cells have been suggested to express a cryptic pathway for regulated secretion (Chavez et al., 1996). In addition, S2 cells resemble phagocytes (Ramet et al., 2002; Stroschein-Stevenson et al., 2006), and mammalian macrophages exhibit the regulated release of catecholamines (Flierl et al., 2007), indicating that they must express both a VMAT and vesicles capable of regulated exocytosis. To test this possibility in S2 cells, we used *Drosophila* VMAT (dVMAT), which contains a dileucine-like motif (S*DE*KKS**LI**) remarkably similar to the mammalian sequence, with two acidic residues (italics) 4 and 5 positions upstream of the dileucine (bold) (Greer et al., 2005). We replaced the upstream acidic residues (Asp-584 and Glu-585) with alanine (DE/AA mutation), using a lumenal hemagglutinin (HA) epitope tag to assess surface expression (Greer et al., 2005) and a fusion of GFP to the N-terminus of dVMAT

to determine the total amount of protein expressed. S2 cells were incubated for 2 h with HA antibody conjugated to Alexa 647, and flow cytometry used to quantify the fluorescence of individual cells. Despite equivalent total dVMAT expression, we observed very low cell surface delivery of WT dVMAT relative to the DE/AA mutant. A scatter plot shows that DE/AA dVMAT has a much higher ratio of Alexa 647 to GFP fluorescence than WT (Fig. 1A), with an ~7-fold difference in mean surface/total transporter. Kolmogorov-Smirnov (KS) analysis of the cumulative frequency distribution for the ratios from individual cells confirms the highly significant difference between WT and DE/AA dVMAT ($p < 10^{-14}$) (Fig. 1B). Since the analogous mutation in rat VMAT2 has a very similar effect on cell surface expression and selectively disrupts sorting to the RSP (Krantz et al., 1997; Li et al., 2005), we infer that S2 cells must express some of the same sorting machinery.

We then determined whether S2 cells can in fact mediate regulated secretion, examining first their ability to store soluble cargo of the RSP. Using mammalian atrial natriuretic factor (ANF) since this peptide hormone has been shown to undergo regulated exocytosis in *Drosophila* (Shakiryanova et al., 2005), we studied a C-terminal fusion to GFP. To produce a comparable control that should undergo only constitutive secretion, we fused GFP directly to the signal sequence (ss) of ANF. Measurement of fluorescence in the supernatant shows ~5-fold less basal secretion of ANF-GFP than ss-GFP (Fig. 1C), suggesting efficient storage of ANF. To determine whether S2 cells can release ANF in a regulated manner, we stimulated cells expressing ANF-GFP for one hour with lipopolysaccharide (LPS). LPS increases secretion of ANF-GFP by ~2-fold (Fig. 1D), and this effect is blocked by the removal of external Ca^{++} (Fig. 1E). LPS also has no effect on secretion of ss-GFP (Fig. 1D), consistent with the constitutive release of this protein. In addition, since LDCVs differ from other secretory vesicles in their dependence on the calcium-dependent activator protein for secretion (CAPS) (Berwin et al., 1998; Elhamdani et al., 1999; Martin and Walent, 1989; Speese et al., 2007), we used dsRNA to knock down the *Drosophila*

orthologue (dCAPS), and find that this eliminates regulated release of ANF from S2 cells (Fig. 1F). S2 cells thus express a functional RSP. Colocalization of mCherry-dVMAT with ANF-GFP but not ss-GFP further supports the sorting of dVMAT to this pathway (Fig. 2).
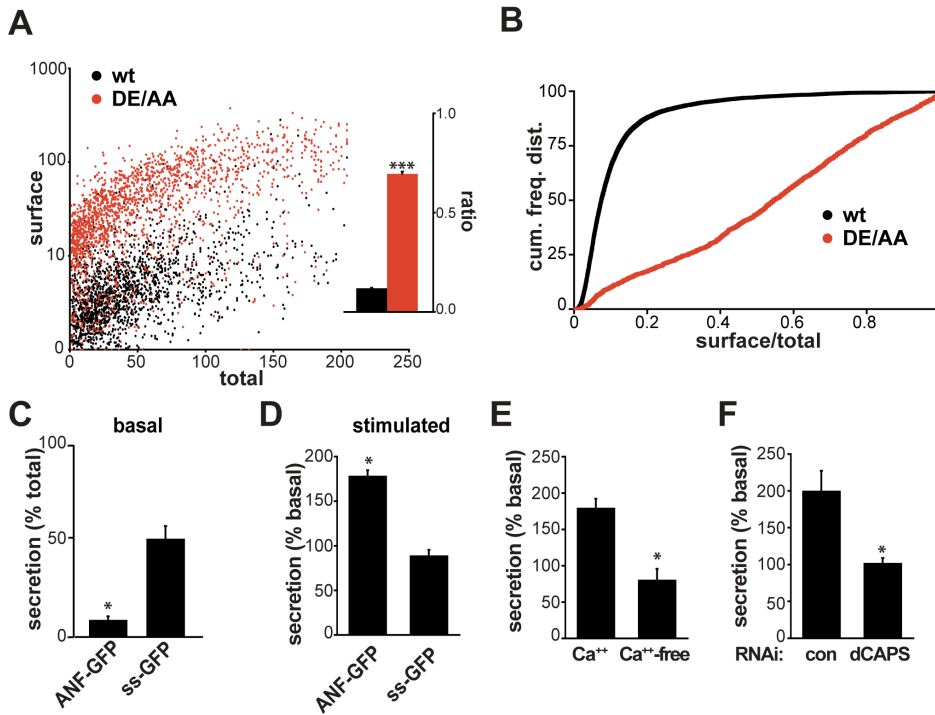
Figure 1. S2 cells express a regulated secretory pathway
(A,B) S2 cells were transiently transfected with wt (black) or DE/AA (red) GFP- and HA-tagged Drosophila VMAT (dVMAT), incubated for two h at room temperature with external HA antibody conjugated to Alexa 647, washed, and the fluorescence of individual cells determined by flow cytometry (A). The bar graph (inset) displays mean ratio of surface/total fluorescence (n>1800 cells). Kolmogorov-Smirnov analysis of the cumulative frequency distributions binned by surface/total dVMAT ratios (B) indicates a significant change in the DE/AA distribution relative to wild type (p < 10^{-14}). (C-F) S2 cells were transiently transfected with atrial natriuretic factor (ANF)-GFP (C-E) or the signal sequence of ANF fused directly to GFP (ss-GFP) (C,D), washed, incubated for 1 hour and the cellular as well as secreted GFP fluorescence measured using a plate reader. Normalized to intracellular fluorescence, the media of cells expressing ANF-GFP shows less fluorescence than cells expressing ss-GFP (C). Treatment with 100 μg/mL LPS induces secretion of ANF-GFP but not ss-GFP (D). Pretreatment with BAPTA-AM in calcium-free buffer (E) or knockdown of Drosophila calcium-dependent activator protein for secretion (dCAPS) with dsRNA (F) block the secretion evoked by LPS. *, p < 0.05 for by two-tailed Student's t-test. The data represent mean values from 3-4 independent experiments, and error bars s.e.m.
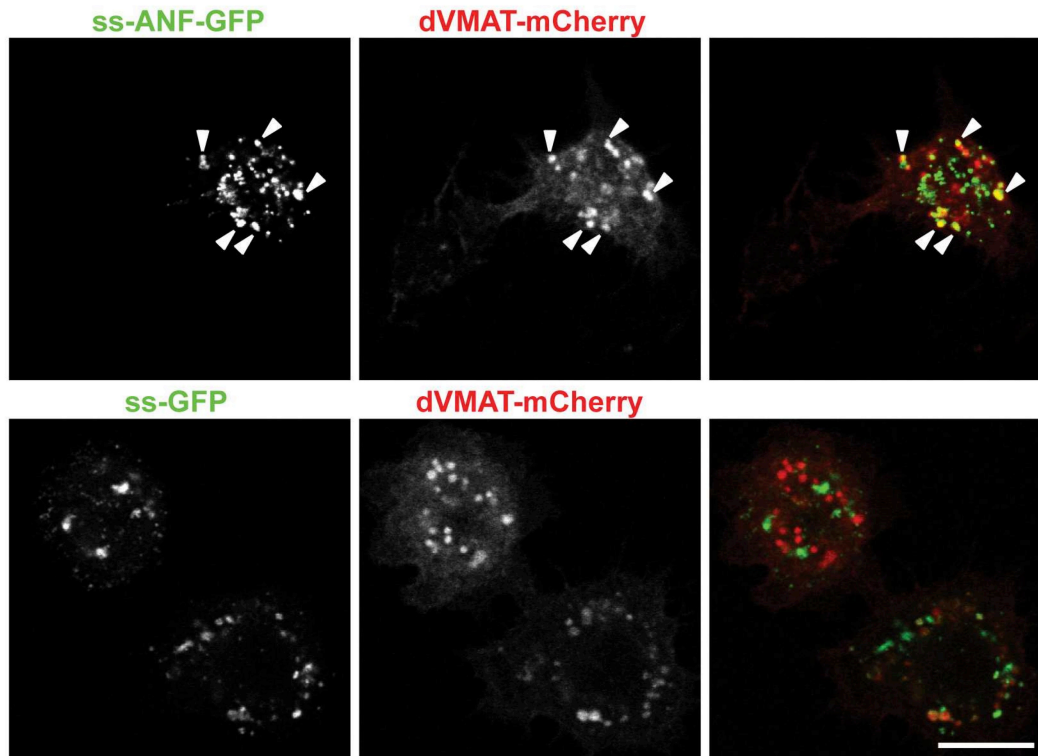
Figure 2. Colocalization of dVMAT with ANF-GFP but not ss-GFP in S2 cells
S2 cells transiently transfected with mCherry-dVMAT and either ANF-GFP (upper panels) or ss-GFP (lower panels) were plated on conA, washed, fixed and visualized by confocal microscopy. dVMAT colocalizes partially with ANF-GFP (arrowheads), but very little if at all with ss-GFP. Scale bar indicates 10 μm.

An RNAi screen in S2 cells identifies genes that regulate cell surface dVMAT expression

To identify cellular machinery involved in biogenesis of the RSP, we performed a genome-wide RNAi screen in S2 cells, using a library of 7216 sequences that target *Drosophila* genes conserved to mammals. S2 cells transfected with GFP-dVMAT-HA were seeded into 96-well plates and treated twice with dsRNA. After treatment for 6 days, the cells were incubated with HA antibody conjugated to Alexa 647, and assayed for antibody uptake and total expression by high-throughput flow cytometry, enabling individual measurements from many cells for each condition (Fig. 3). The ratio of surface/total dVMAT was computed for each cell and a Z-score calculated relative to other wells in the same plate that serve as controls. The entire screen was performed twice, once using transiently transfected S2 cells, and a second time with stable

72

transformants. After pooling the results from both screens with z-score ≥3, we removed genes that reduce the number of cells available for analysis or influence expression of the GFP-tagged reporter (Table 1). Since essentially all of these genes affect transcription or translation, we excluded a small number of additional genes because they also involve transcription or translation.
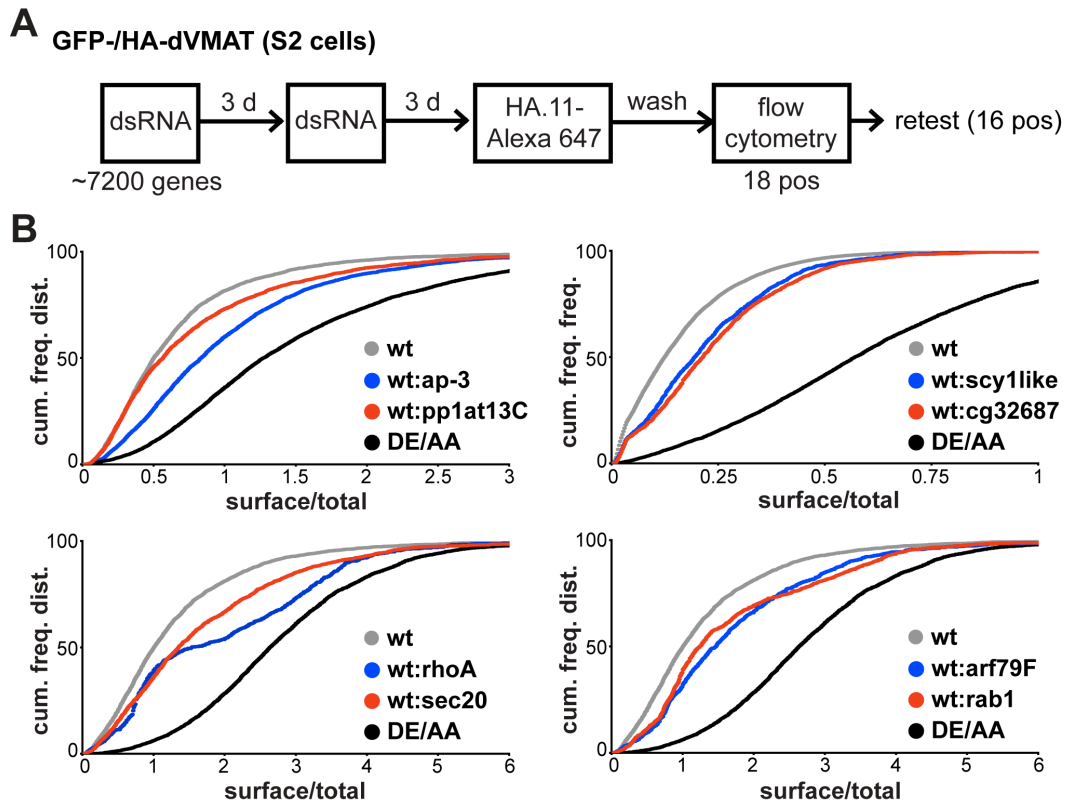
Figure 3. S2 cell screen identifies genes that regulate the surface expression of dVMAT
(A) The flow chart illustrates the procedure used for screening. S2 cells transfected with GFP-/HA-dVMAT were treated twice with double stranded (ds) RNA over a 6-day period in a 96-well plate, incubated with external HA antibody conjugated to Alexa 647 for 2 h, washed, and the fluorescence of both GFP and Alexa 647 measured at the level of individual cells by flow cytometry. Of 7200 genes conserved from *Drosophila* to mammals, 18 positives (Z-score ≥ 3) were identified and retested using non-overlapping dsRNA. Kolmogorov-Smirnov analysis of the cumulative frequency distribution reveals that 16 of 18 genes were again positive (p < 10^{-14} in at least two independent experiments). (B) Cumulative frequency distributions for selected dsRNA in representative retest experiments show the differences from control (wt) and DE/AA dVMAT.

CG	cell # (% avg)	GFP (z-score)	protein
17603	0.1	6.5	transcription initiation factor TFIID
8117	0.4	4.1	transcription elongation factor TFIIS
8151	0.4	7.0	TFIIH basal transcription factor complex subunit 1
1420	0.6	-1.3	pre-mRNA-splicing factor SLU7
8151	2.0	0.2	TFIIH basal transcription factor complex subunit 1
8987	2.3	8.8	DNA polymerase gamma subunit 1
12225	4.2	-1.7	transcription elongation factor SPT6
7238	5.5	0.3	essential protein present in native splicing complexes
11979	5.5	-3.0	DNA-directed RNA polymerase II
3350	5.7	-0.1	transcription factor-like protein 4
5193	6.2	-0.9	transcription initiation factor IIB
4651	7.1	1.4	60S ribosomal protein L13
1433	9.2	-0.3	transcription unit protein
12324	9.5	-2.2	40S ribosomal protein S15Ab
2875	9.6	0.9	nucleolar complex protein 4 homolog
12261	9.7	-0.9	mitochondrial ribosomal protein S22
2503	9.9	-0.8	Paf1, RNA polymerase II associated factor
4647	10.3	0.0	mitochondrial 39S ribosomal protein L49
12275	11.3	-1.4	40S ribosomal protein S10a
6249	11.4	-1.7	3'-5' exoribonuclease CSL4 homolog
5317	11.9	1.6	ribosomal protein L7
3455	12.2	1.7	proteasome subunit p42
8142	12.3	0.0	replication factor C subunit 4
5931	12.5	1.0	U5 small nuclear ribonucleoprotein 200 kDa helicase
7993	15.5	1.5	processing of pre-rRNA and the assembly of the 60S ribosomal subunit
12373	15.7	-0.2	mitochondrial ribosomal protein L18
4760	16.0	-0.6	RNP
5818	16.3	-0.8	mitochondrial ribosomal protein L4
3312	16.5	-0.4	RNA-binding protein 4F
9348	19.0	5.0	TAF6 RNA polymerase II
7728	19.3	0.0	ribosome biogenesis protein BMS1 homolog
8064	19.4	0.3	18S rRNA biogenesis
2063	19.6	2.0	transcriptional regulator protein
3294	19.7	-0.6	U2 small nuclear ribonucleoprotein auxiliary factor 35
1307	20.1	-0.1	peptidyl-tRNA hydrolase 2
33123	21.0	0.4	leucyl-tRNA synthetase
2670	23.5	0.3	transcription initiation factor TFIID subunit 7
4651	23.7	0.7	60S ribosomal protein L13
3180	28.1	0.2	DNA-directed RNA polymerase II
8939	28.2	0.1	ribosomal RNA methyltransferase
9091	29.0	1.9	60S ribosomal protein L37
3308	29.6	0.4	deoxyribonuclease
18174	30.5	-0.9	26S proteasome non-ATPase regulatory subunit 14
7246	33.5	-0.5	U3 small nucleolar RNA-associated protein 6
3817	37.8	-0.7	nucleolar protein, constituent of pre-60S ribosomal
7847	38.7	1.2	transcription factor
7028	38.7	-1.1	PRP4 pre- mRNA-processing factor 4
7006	40.0	-0.7	60S ribosome subunit biogenesis protein NIP7

11879	42.7	1.7	yemanuclein
3193	42.9	2.5	splicesome assembly factor
6539	43.3	-0.1	DEAD/DEAH RNA helicase 1
1420	43.5	1.2	step II splicing factor SLU7
2972	44.0	-3.3	RNA-binding protein NOB1
1957	45.0	-0.6	cleavage and polyadenylation specificity factor
2194	45.2	1.5	dihydropyrimidine dehydrogenase
4528	46.2	4.4	U1 small nuclear ribonucleoprotein A
3695	47.1	-1.5	cofactor required for Sp1 transcriptional activation, subunit 3
2939	47.6	0.1	transcription factor
4573	48.0	-0.3	mitochondrial glutamyl-tRNA synthetase
8950	49.7	-0.3	transcription factor IIIC-gamma subunit
12288	49.9	0.9	required for pre-25S rRNA processing
3808	50.0	0.1	tRNA methyltransferase
9054	58.0	-0.4	ATP-dependent RNA helicase
9193	58.0	0.3	cyclin
7776	63.9	0.8	histone H4/H2A acetyltransferase
1873	67.2	-0.3	elongation factor 1-alpha
9151	72.5	0.1	transcription factor
8915	74.6	-0.5	RNA helicase
3663	76.2	0.6	isochorismatase domain containing 1
13867	78.7	3.1	mediator of RNA polymerase II transcription
1245	83.2	0.3	transcription factor
12752	85.1	0.5	NTF2-related export protein 2
6348	96.1	-0.3	transcription factor
3668	98.5	0.9	fork head transcription factor
11107	108.4	-0.1	pre-mRNA splicing factor ATP-dependent RNA helicase
6493	109.7	9.6	Dicer-2
18783	124.1	0.6	transcription factor
8922	126.6	0.2	40S ribosomal protein S5a
6684	128.8	-0.1	40S ribosomal protein S25
7439	139.7	9.4	Argonaute-2
3497	144.4	-0.3	transcription factor RBP-L
5874	145.1	2.9	negative elongation factor A
17841	146.5	-0.3	purine-binding transcription factor
8900	158.2	0.3	40S ribosomal protein S18
12288	173.9	-0.6	RNA-binding protein 34
1671	247.8	3.0	transducin

Table 1. Genes identified in the S2 cell screen that were excluded from further analysis
These genes, with their known or putative function indicated, were excluded from further analysis due to the low number of cells available for analysis, or effects on expression of the GFP-dVMAT reporter relative to other wells from the same plate. The remainder were excluded because, like those reducing cell number or altering GFP expression, they function in transcription or translation.

We retested the remaining 18 genes with non-overlapping dsRNA sequences to exclude false positives due to off-target effects. In at least two of four independently performed experiments, we confirmed the increase in dVMAT surface expression for 16 of the 18 genes ($p < 0.003$ by Kolmogorov-Smirnov analysis of the cumulative frequency distributions; Fig. 4). Remarkably, the screen identified nine proteins with a primary role in membrane trafficking, four cytoskeletal proteins or enzymes that have been implicated in the regulation of membrane trafficking, and two proteins of unknown function (Table 2). Since the genes identified may influence VMAT surface expression through a variety of mechanisms, including some unrelated to the RSP, we then performed a series of secondary screens.

CG	gene symbol	homologue/domain	Z-score	Class
8416	rho1	rhoC	5.8	I
2023	cg2023	sec20	3.6	I
7057	AP-50	AP-2μ1	3.2	I
7262	cg7262	nucleoporin 93	3.0	I
9156	pp1-13C	PP1cc	3.0	I
3320	rab1	rab1A	3.8	II
8385	arf79F	arf1	3.3	II
32687	cg32687	leucine rich repeat 58	3.0	II
11427	ruby	AP-3ß2	3.8	III
11197	garnet	AP-3∂1	3.7	III
8945	cg8945	carboxypeptidase	3.4	III
14899	cg14899	derlin-2	3.3	III
3201	mlc-c	myosin light chain	3.3	III
4707	cg4707	zinc finger	3.1	III
1973	yata	scy1-like kinase	3.0	III
8027	cg8027	GlcNAc-1-phospho-transferase (a-/b-)	3.0	III

Table 2. Genes identified in the S2 cell screen and confirmed with non-overlapping dsRNA
List of genes identified as positive in the S2 cell screen using GFP-/HA-tagged dVMAT as reporter. The Z-score indicates significance assessed using a within-plate comparison. Class I dsRNAs increase cell surface expression of DE/AA dVMAT, class II reduce surface expression of the mutant, and class III have no effect.

Dependence on the VMAT sorting motif

To determine whether the effect of genes identified in the screen depends on the VMAT dileucine-like motif, we examined their interaction with the DE/AA mutation. Class I genes increase HA antibody uptake by DE/AA as well as WT dVMAT (Fig. 4, top), suggesting that they act independently of the extended dileucine. Mechanisms that might account for the additive effect include an impairment of endocytosis and an increase in constitutive secretion. Indeed, we identified the μ subunit of adaptor protein AP-2 (μ2) presumably because it has an important role in clathrin-dependent endocytosis, and knockdown would be expected to increase cell surface expression of DE/AA dVMAT since the mutant resides at higher levels than WT at the plasma membrane. It is more surprising that knockdown of AP-2 increases HA antibody uptake by WT dVMAT considering the low rate of its delivery to the plasma membrane, but it is important to note that we did not identify other proteins known to be involved in endocytosis. To determine whether the knockdown of other class I genes increases cell surface dVMAT by promoting constitutive secretion, we examined the basal release over one hour of ANF-GFP from unstimulated S2 cells. dsRNA to PP1cc, sec20 and particularly rhoC all significantly increase release of ANF-GFP (Fig. 4, top center), and the role of sec20 in retrograde transport from Golgi to endoplasmic reticulum presumably accounts for the effect of dsRNA to this gene (Lewis et al., 1997).

Knockdown of class II genes (*rab1*, *arf79F* and *cg32687*) reduces HA antibody uptake by DE/AA dVMAT (Fig. 4, middle). Since dsRNA to these sequences increases antibody uptake by WT dVMAT, an opposite effect on the mutant might appear surprising. However, the discrepancy may simply reflect a role for these proteins in constitutive as well as regulated secretion, with targeting of DE/AA dVMAT to the constitutive pathway making it more sensitive than wild type dVMAT to the RNAi. Consistent with this possibility and partial knockdown by the dsRNA, complete block of the secretory pathway with brefeldin A (BFA) significantly

reduces DE/AA dVMAT surface expression without any effect on WT dVMAT (data not shown). In addition, a screen for genes important in constitutive secretion has already identified *rab1* and *arf79F* (homologous to Arf1 in mammals) (Bard et al., 2006), and we find that their knockdown decreases constitutive secretion of ANF-GFP (Fig. 4, middle center). Class II genes may thus have roles in both regulated and constitutive pathways.

Class III genes show no additional effects on HA antibody uptake by DE/AA dVMAT (Fig. 4, bottom), suggesting their dependence on the extended dileucine motif. Indeed, the Scy1-like kinase and N-acetylglucosamine (GlcNAc)-1-phosphotransferase have been implicated in trafficking through the Golgi complex, back to the endoplasmic reticulum and to lysosomes, respectively (Burman et al., 2008; Tiede et al., 2005). However, RNAi to Scy1-like kinase or GlcNAc-1-phosphotransferase does not increase constitutive release of ANF-GFP (Fig. 4 bottom center). In contrast, two other dsRNA in this class (AP-3 and derlin) increase the constitutive release of ANF, consistent with diversion of this soluble protein from the regulated to constitutive pathway.

To determine whether genes identified in the screen actually impair the regulated secretion of soluble cargo as well as the sorting of a polytopic membrane protein, we examined the regulated release of ANF-GFP in response to stimulation with LPS. Most of the genes identified do not affect regulated release, suggesting either independent effects on cell surface expression of VMAT, or differential effects on the sorting of membrane and soluble cargo. However, knock-down of two class I (*nup93* and *pp1-13C*) and two class III genes (*AP-3* and *cg8945*) do abolish regulated release (Fig. 4). The screen has thus identified a small number of genes required for regulated secretion.
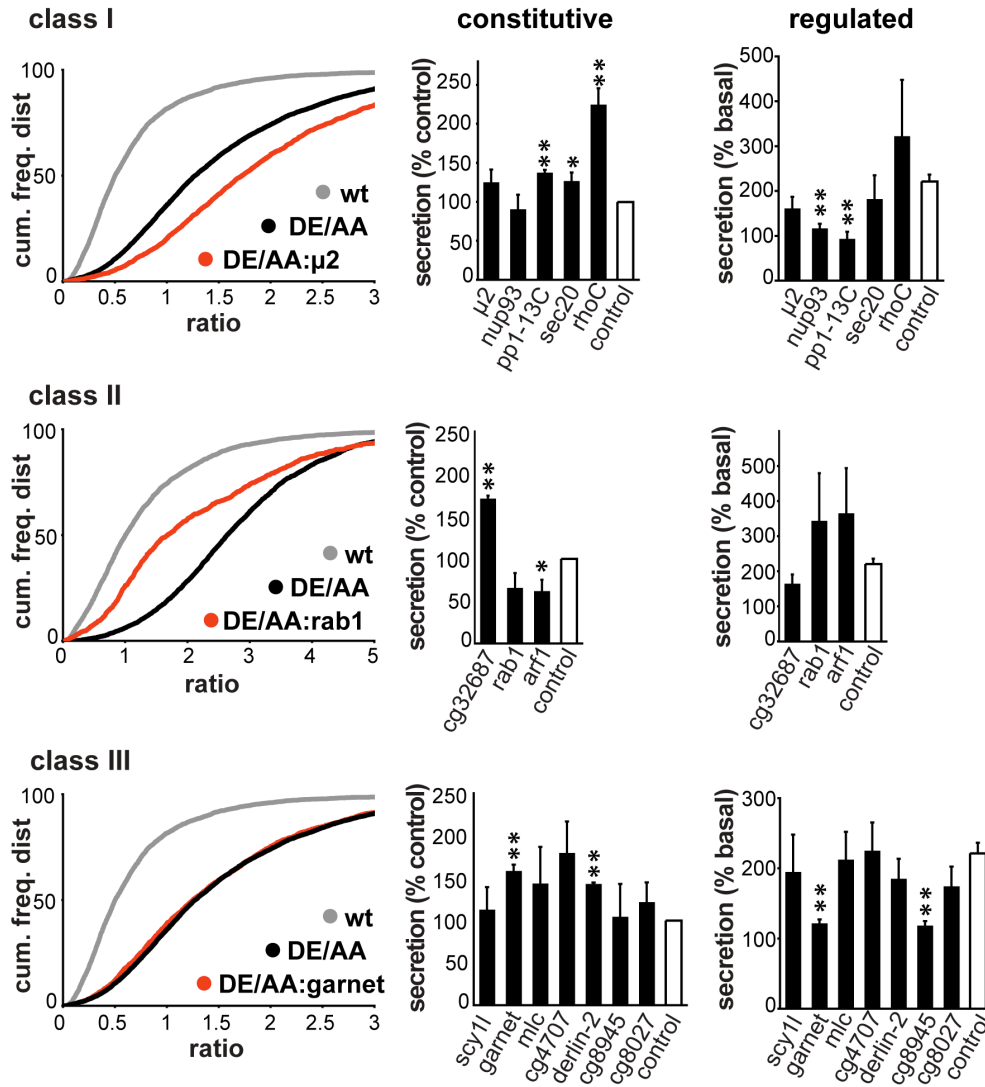
Figure 4. Classification of genes identified in the screen by mechanism and effect on the regulated secretion of soluble cargo

S2 cells transfected with DE/AA GFP-/HA-dVMAT were treated with dsRNA targeting genes identified in the screen, and the uptake of external HA antibody measured as described in Fig. 1. Left panels, representative cumulative frequency distributions are shown for selected genes in each class. Class I genes increase, class II genes decrease and class III genes have no effect on antibody uptake by DE/AA dVMAT. Middle panels, S2 cells expressing ANF-GFP were treated with dsRNA and basal (unstimulated) secretion of GFP fluorescence determined as in Fig. 1D. Secretion was normalized to cellular ANF-GFP and expressed as percent of the fluorescence secreted by control cells. Right panels, S2 cells expressing ANF-GFP were treated with dsRNA and LPS-induced secretion measured as in Fig. 1E. *, $p < 0.05$ and **, $p < 0.01$ relative to control by two-tailed Student's t-test; n=3-5. The data shows mean values, and error bars the s.e.m.

Loss of AP-3 dysregulates secretion from mammalian neuroendocrine cells

Remarkably, two genes identified in the screen (*garnet* and *ruby*) encode subunits of the heterotetrameric adaptor protein-3 (AP-3) complex. The third subunit of AP-3 present in the library (*carmine*) was confirmed positive on specific retesting, and the fourth subunit (*orange*) was not present in the library. AP-3 is known to play a role in the formation of lysosome-related organelles (LROs) such as melanosomes and platelet dense granules, in addition to synaptic vesicles (Newell-Litwa et al., 2007). Similar to LDCVs, LROs are acidic and some can undergo regulated exocytosis. However, AP-3 contributes to formation of these organelles from endosomes whereas LDCVs bud directly from the TGN, within the biosynthetic pathway (Eaton et al., 2000; Tooze and Huttner, 1990).

To assess a role for AP-3 in sorting to the LDCVs of mammalian neuroendocrine cells, we used the rat pheochromocytoma PC12 cell line. Knockdown of the sole AP-3 δ subunit destabilizes the complex (Kantheti et al., 1998), reducing the amount of σ3A by ~80% (Fig. 5A) and very substantially increasing HA antibody uptake by VMAT2 (Fig. 5B). In addition, the loss of AP-3 greatly impairs the stimulation of secretogranin (Sg) II release by depolarization, with little effect on the absolute amount of basal release (Fig. 5C,D). Since AP-3 knockdown reduces the cellular content of SgII (to ~35% of control cells) (Fig 5E), however, constitutive release is in fact increased relative to control, consistent with diversion from regulated to constitutive pathway.

To determine whether the loss of AP-3 has a similar effect on LDCV composition *in vivo*, we measured the granin content of adrenal glands from *mocha* mice, which lack AP-3. Both SgII and chromogranin A show a dramatic reduction in *mocha* mice (to ~5% and ~20% of wild type animals, respectively) (Fig. 5F), consistent with the results from PC12 cells, and excluding an off-target effect of the RNAi. Identified in *Drosophila* S2 cells as important for sorting to the RSP,

AP-3 thus has a similar role in the regulated exocytosis of both membrane and soluble cargo by mammalian neuroendocrine cells.
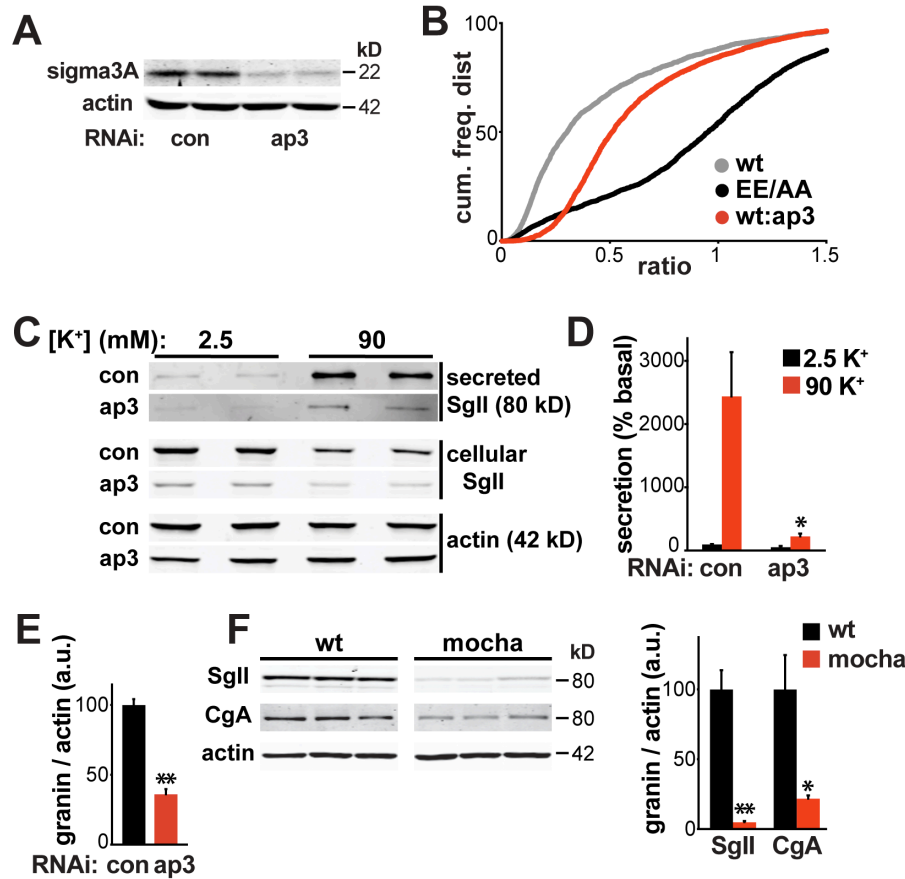
Figure 5. AP-3 RNAi increases VMAT2 surface expression and impairs regulated release of SgII from PC12 cells

(A, B) Western analysis of extracts from PC12 cells transiently transfected with AP-3δ small interfering (si) RNA (50 nM) show an ~80% reduction in adaptor protein (AP)-3 subunit σ3A relative to cells transfected with control siRNA (A). PC12 cells cotransfected with wild type or EE/AA GFP-/HA-VMAT2, with or without AP-3δ siRNA were subjected to flow cytometry as described in Fig. 1 (B). Kolmogorov-Smirnov analysis of the cumulative frequency distributions for wild type VMAT2 + control siRNA (grey), wild type VMAT2 + AP-3δ siRNA (red), and EE/AA VMAT2 + control siRNA (black) indicates a significant change in the AP-3 siRNA distribution relative to wild type (p < 10^{-14}). (C, D) PC12 cells were transiently transfected with AP-3δ or control siRNA, washed and incubated for 30 minutes in Tyrode's solution containing 2.5 mM (basal) or 90 mM (stimulated) K^+. Cellular and secreted secretogranin II (SgII) were measured by quantitative fluorescent immunoblotting (C), with the secreted SgII normalized to basal secretion in the control (D). AP-3δ RNAi greatly reduces the depolarization-induced secretion of SgII, * p < 0.05 relative to stimulated secretion from control by two-tailed Student's t-test, n=4. (E) AP-3δ RNAi reduces the cellular content of SgII relative to actin. *, p < 0.005 relative to control by two-tailed Student's t-test; n=4. (F) The adrenal glands of *mocha* mice lacking AP-3 show a dramatic reduction in the content of SgII and chromogranin A (CgA) relative to the adrenals of control littermates. *, p < 0.05 and **, p < 0.005 relative to wild type by two-tailed Student's t-test; n=3. The data show mean values, and error bars the s.e.m.

Previous work has shown that the loss of AP-3 increases the amount of monoamine released per vesicle and the size of LDCVs, but did not examine the regulation of release (Grabner et al., 2006). To assess the regulated exocytosis of LDCVs, we used direct, optical imaging of a reporter based on the ecliptic pHluorin (Miesenböck et al., 1998), a modified form of GFP that undergoes quenching at the low pH of secretory vesicles and hence increases in fluorescence with exocytosis (Sankaranarayanan et al., 2000). In particular, we fused the pHluorin to a lumenal domain of VMAT2 (Onoa et al., 2010), and monitored individual exocytotic events at the plasma membrane of live, transfected PC12 cells by total internal reflection fluorescence (TIRF) microscopy. Since the low surface expression of VMAT2-pHluorin complicates identification of the transfected cells, we alkalinized the internal compartments briefly with NH_4Cl to reveal the total fluorescence and selected cells with similar expression levels (Fig. 6B). In addition, we briefly lowered the external pH to 5.5, and observed substantially increased quenching of VMAT2-pHluorin after AP-3 knockdown (Fig. 6B), consistent with increased cell surface expression. Cells treated with control siRNA also show very few spontaneous exocytotic events in the absence of stimulation but massive exocytosis in response to depolarization. In contrast, AP-3 RNAi significantly increases baseline, constitutive exocytosis of VMAT2, and greatly reduces the response to stimulation (Fig. 6A,C,D).
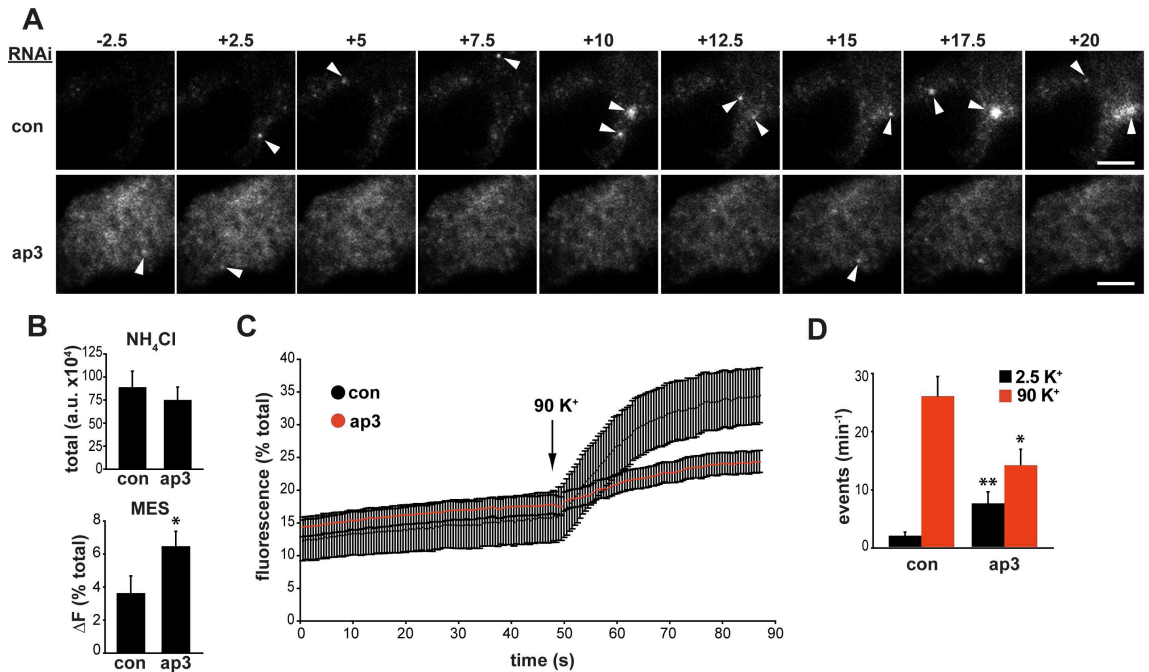
Figure 6. AP-3 RNAi dysregulates the exocytosis of VMAT2

PC12 cells were transfected with AP-3δ or control siRNA (50 nM), co-transfected two days later with the same siRNA and VMAT2 containing a lumenal pHluorin (VMAT2-pHluorin), then imaged live by total internal reflectance fluorescence (TIRF) microscopy after an additional two days. Basal exocytosis of VMAT2-pHluorin was measured in Tyrode's solution containing 2.5 mM K^+, and release stimulated in Tyrode's with 90 mM K^+. (A) Representative images acquired before and after depolarization show increased baseline fluorescence and fewer stimulated events after transfection with AP-3 siRNA. (B) Total VMAT2 fluorescence was revealed by alkalinization in Tyrode's solution containing 50 mM NH_4Cl, pH 7.4 (upper panel), and surface VMAT2-pHluorin revealed by acidification in Tyrode's with 25 mM MES, pH 6.5 (lower panel). AP-3δ RNAi increases the surface fraction of VMAT2 in cells despite expression equivalent to transfection with control siRNA. *, $p < 0.05$ relative to control by two-tailed Student's t-test; n=12 for control and 14 for AP-3 siRNA. (C) Whole cell fluorescence expressed as % total fluorescence (revealed in NH_4Cl) shows a robust response to depolarization with 90 mM K^+ (arrow) in control cells, but a greatly impaired response after AP-3 siRNA. The traces indicate the mean values of 12 individual traces for control and 14 for AP-3 RNAi cells, and error bars indicate the s.e.m. (D) The quantification of individual exocytotic events shows increased basal VMAT2-pHluorin exocytosis with AP-3 RNAi but a reduction in stimulated exocytosis. *, $p < 0.02$ and **, $p < 0.002$ relative to control by two-tailed Student's t-test; n=31 for control and n=19 for AP-3. The bars indicate mean values, and error bars the s.e.m. The scale bars indicate 5 µm.

AP-3 contributes to LDCV biogenesis

How does AP-3 contribute to regulated secretion? The loss of AP-3 might have pleiotropic effects that indirectly influence the regulation of LDCV exocytosis. Alternatively, AP-3 may have a primary role in LDCV production that influences their composition and consequently, their fusion. We therefore characterized the properties of LDCVs produced in the absence of this adaptor. Separating PC12 membranes by equilibrium sedimentation through sucrose, we find

that the knockdown of AP-3 reduces the proportion of SgII migrating in fractions that would, in control cells, contain LDCVs. AP-3 RNAi also shifts SgII to lighter fractions (Fig. 7A). In separate experiments, we took advantage of cotransfected ANF-GFP to assay more (~80) gradient fractions using a fluorescent plate reader and so achieve higher resolution. Like endogenous SgII, ANF-GFP shows a shift toward light fractions with AP-3 RNAi (Fig. 7B). Importantly, the RNAi has no effect on migration of the synaptic vesicle protein synaptophysin (Fig. 7A). AP-3 thus has a specific effect on the properties of LDCVs, suggesting that any defect in fusion results from a change in their composition and hence their formation.

To determine whether AP-3 RNAi affects the number of LDCVs and their morphology, we used electron microscopy. The analysis shows a substantial reduction in the number and density of LDCVs in PC12 cells subjected to knockdown of AP-3 (Fig. 7C), consistent with a role for AP-3 in their production. As suggested by previous work (Grabner et al., 2006), the size of LDCVs also increases significantly with a reduction in AP-3 (Fig. 7D).
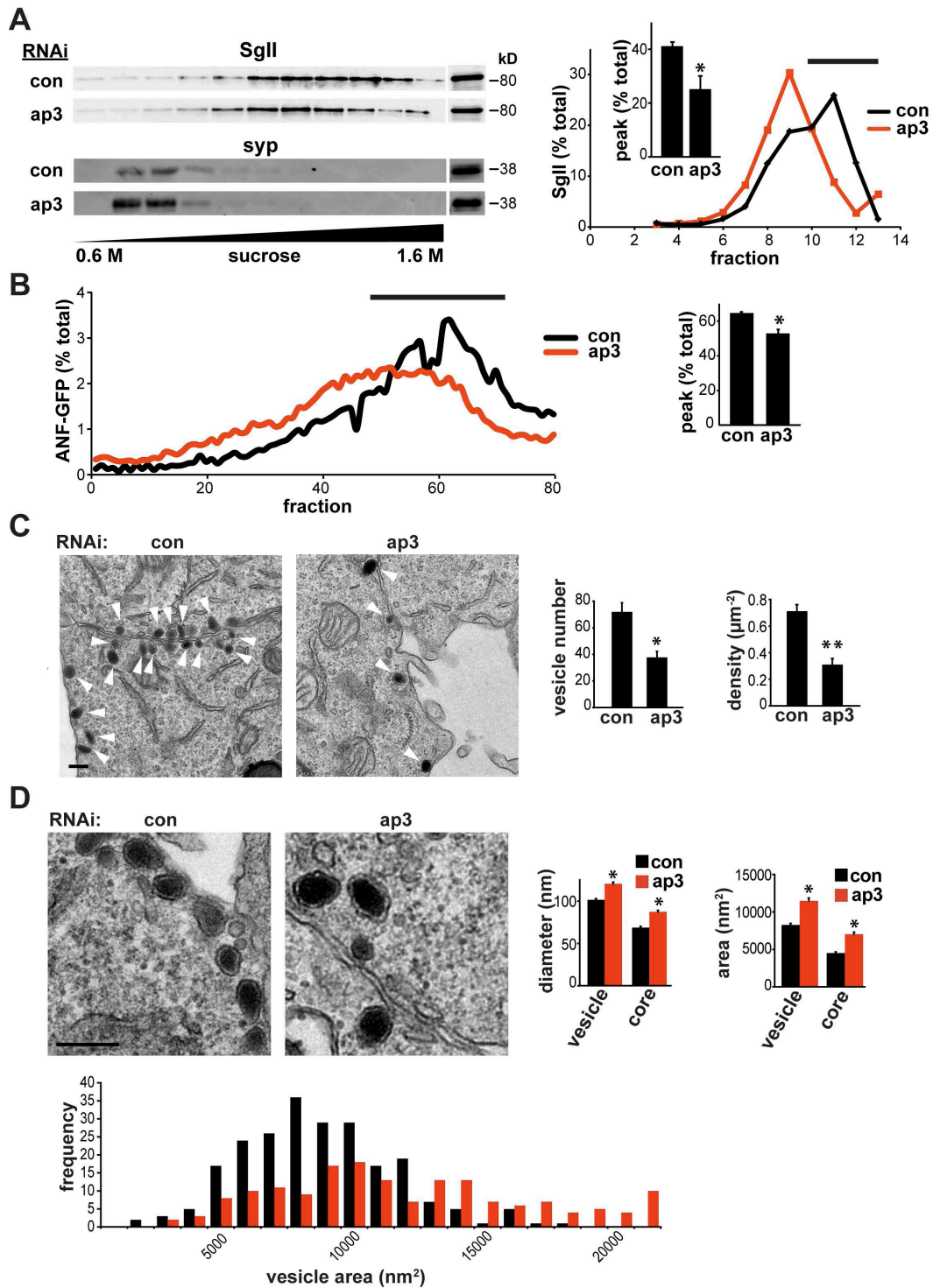
Figure 7. AP-3 RNAi affects the properties of LDCVs

(A,B) PC12 cells were transfected twice with AP-3δ or control siRNA (50 nM), and the postnuclear supernatant (input) obtained 2-3 days after the second transfection separated by equilibrium sedimentation through 0.6-1.6 M sucrose. Fractions were collected from the top of the gradient, and assayed for synaptophysin (syp) and SgII by quantitative fluorescent immunoblotting, with each fraction expressed as percent of total gradient immunoreactivity, and the area under the LDCV peak (indicated by a black line) expressed as a percent of the area under the entire curve (inset). AP-3 RNAi greatly reduces the LDCV

85

peak and shifts the SgII immunoreactivity toward lighter fractions, without affecting the synaptic vesicle protein syp. *, p < 0.05 relative to control by two-tailed Student's t-test; n=3 transfections. (B) PC12 cells were cotransfected with ANF-GFP and either AP-3 or control siRNA, and the postnuclear supernatant sedimented as above. In this case, however, ~80 fractions were collected from the top of the gradient directly into a 96-well plate, and the fluorescence of ANF-GFP measured directly using a plate reader. The graph indicates ANF-GFP fluorescence for each fraction expressed as percent of total gradient fluorescence. The bar graph (right) shows the area under the curve for the LDCV peak (indicated by a black line), expressed as percent of total area. **, p < 0.001 relative to control by two-tailed Student's t-test; n=3 transfections. (C,D) PC12 cells were transfected twice with either control or AP-3 siRNA and processed for electron microscopy 2 days after the second transfection. (C) Low magnification electron micrographs show a large reduction in the number of LDCVs (arrowheads) of cells transfected with AP-3 siRNA (right) relative to controls (left). Bar graphs indicate the number of LDCVs per cell in the section (left) and LDCV density (right). *, p < 0.0005; **, p < 0.000001; n=20 cells/condition. (D) Higher magnification electron micrographs show that AP-3 RNAi increases the size of LDCVs. Bar graphs indicate the diameter (left) and area (right) of both the entire LDCV and the electron-dense core. The LDCV area is presented as a frequency histogram (below). *, p < 0.01; n=205-221 LDCVs/condition. The scale bars indicate 200 nm.

To assess a specific role for AP-3 in LDCV production, we used metabolic labelling with $^{35}SO_4^-$, which occurs specifically within the TGN (Baeuerle and Huttner, 1987), where LDCVs form. Sulfation also labels both SgII and the constitutively secreted heparan sulfate proteoglycan (HSPG) (Tooze and Huttner, 1990). Four hours after labeling, $^{35}SO_4^-$-HSPG essentially disappears from control PC12 cells, consistent with constitutive release, and this does not change with AP-3 RNAi (Fig. 8A). In contrast, $^{35}SO_4^-$-SgII undergoes prolonged storage in control PC12 cells. In cells lacking AP-3, however, $^{35}SO_4^-$-SgII undergoes constitutive secretion. Analysis of the medium confirms the constitutive release of $^{35}SO_4^-$-HSPG that is unaffected by AP-3 RNAi, and the dysregulated secretion of $^{35}SO_4^-$-SgII produced by loss of AP-3 (Fig. 8B). AP-3 thus influences the fate of LDCVs rather than constitutive secretory vesicles, consistent with a specific role in formation of the RSP.

AP-3 might influence either the biogenesis of LDCVs at the TGN or the process of maturation after budding that involves the removal of proteins destined for other organelles (Morvan and Tooze, 2008). The adaptor AP-1 rather than AP-3 has been implicated in LDCV maturation (Dittie et al., 1996), but to assess a distinct role for AP-3 in budding from the TGN, we again

used metabolic labeling with $^{35}SO_4^-$, allowing only 15 minutes of chase to enable a direct analysis of the newly formed vesicles (Tooze and Huttner, 1990). These vesicles were then separated from the TGN donor compartment by velocity centrifugation through sucrose, the top fractions (1-5) pooled and LDCVs further separated from constitutive secretory vesicles by equilibrium sedimentation through sucrose. In PC12 cells treated with control siRNA, the constitutively secreted $^{35}SO_4^-$-HSPG migrates in fractions 8-10, whereas LDCV protein $^{35}SO_4^-$-SgII migrates in fractions 12-13 (Fig. 8C). In contrast, AP-3 RNAi shifts the $^{35}SO_4^-$-SgII signal towards lighter fractions partially overlapping with $^{35}SO_4^-$-HSPG signal. The redistribution of $^{35}SO_4$-SgII shows that AP-3 promotes sorting into LDCVs at the level of the TGN.
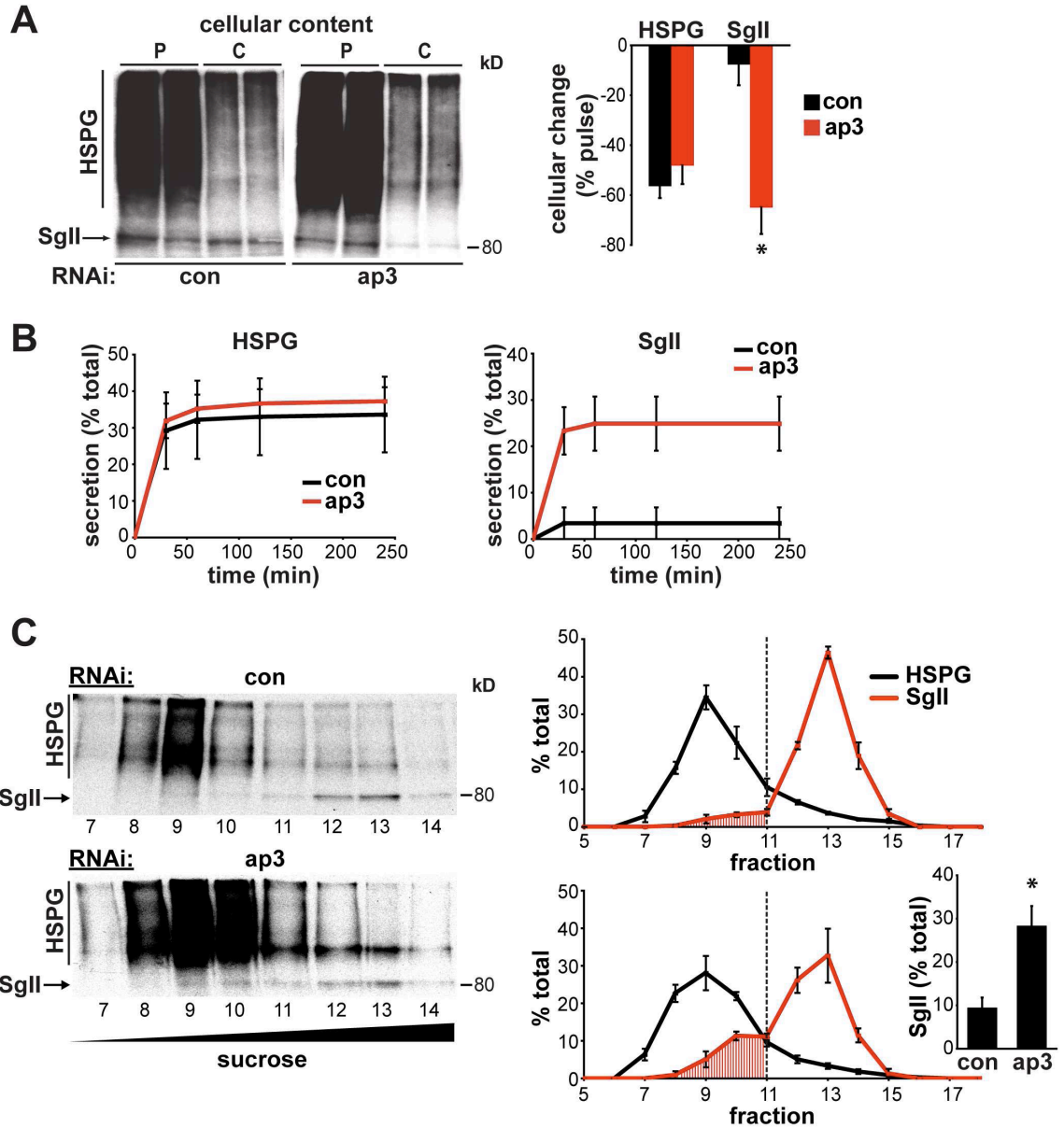
Figure 8. AP-3 RNAi diverts SgII to constitutive secretory vesicles budding from the TGN

(A,B) PC12 cells were transfected twice with AP-3 or control siRNA (50 nM), labeled for 5 min with 0.5-1 mCi/mL $^{35}SO_4$ and either harvested directly (pulse, p) or incubated at 37° C for 4 h (chase, c) in complete medium containing 1.6 mM nonradioactive Na_2SO_4. (A) Separation of duplicate cell extracts by electrophoresis followed by autoradiography shows that, after 4 h, control cells store almost all of the labeled SgII. In contrast, AP-3 RNAi dramatically reduces the storage of SgII, with no effect on the constitutively secreted HSPG. Bars indicate the percent of labeled protein lost from the cell in the chase relative to the pulse. *, p < 0.02 relative to control by two-tailed Student's t-test; n=3. (B) Aliquots of media from the times indicated confirm the constitutive secretion of HSPG unaffected by AP-3 RNAi, and the constitutive release of SgII produced by AP-3 RNAi. (C) PC12 were transfected and labeled with $^{35}SO_4$ as described above, incubated at 37° C for 15 minutes after the pulse, and a postnuclear supernatant separated by velocity sedimentation through a 0.3-1.2 M continuous sucrose gradient, with the TGN-derived vesicles in fractions 1-5 separated further by equilibrium sedimentation on a 0.5-2 M continuous sucrose gradient. Fractions (500 µl) were collected from the top of the gradient and aliquots (50 µl) separated by electrophoresis, followed by fluorography (left). Only fractions with significant amounts of

88

radioactivity are shown, and the labeled HSPG and SgII in each fraction expressed as percent of the total labeled protein on the gradient (right). The amount of SgII in the HSPG peak increases with AP-3 RNAi, and the bar graph indicates the area under the HSPG curve as a percent of the area under the entire SgII curve (inset). *, p < 0.05 relative to control by two-tailed Student's t-test. The data indicate the mean of 3 independent transfections, and error bars the s.e.m.

The shift in LDCV proteins to lighter fractions suggests that, in the absence of AP-3, LDCV cargo may sort instead to constitutive secretory vesicles. Indeed, vesicles with dense cores still bud without AP-3, and the presence of a dense core may account for their intermediate density. To reconcile the mild morphological phenotype of AP-3 RNAi with the severe functional effect on secretion, we examined the distribution of membrane proteins implicated in regulated exocytosis. Equilibrium sedimentation through sucrose shows that the v-SNAREs VAMP2 and 3 migrate over a wide range of fractions, with enrichment in lighter membranes, but the distribution shows no clear change with RNAi for AP-3 (Fig. 9A). In contrast, AP-3 RNAi redistributes the calcium sensor synaptotagmin 1 (Fernandez-Chacon, 2001; Chapman, 2008) from heavy to light membranes (Fig. 9), a dramatic effect that presumably contributes to the gross disturbance in regulated secretion.

Figure 9. AP-3 RNAi affects the membrane composition of LDCVs
PC12 cells were transfected twice with AP-3δ or control siRNA (50 nM), and the postnuclear supernatant obtained 2-3 days after the second transfection separated by equilibrium sedimentation through 0.6-1.6 M sucrose. Fractions were collected from the top of the gradient, and assayed for VAMP2, VAMP3 and synaptotagmin 1 (syt1) by quantitative fluorescent immunoblotting (A). The amounts in each fraction, in light membranes (peak I) and in LDCV fractions (peak II) are expressed as percent total gradient immunoreactivity (B). AP-3 RNAi greatly reduces the LDCV peak of syt1, VAMP2 and VAMP3 and shifts the syt1 immunoreactivity toward lighter fractions. *, $p < 0.05$ relative to control by two-tailed Student's t-test; n=3 transfections.

Discussion

An RNAi screen identifies genes required for sorting to the regulated secretory pathway

Using a sensitive reporter, RNAi in *Drosophila* S2 cells and high-throughput flow cytometry, we identified a remarkably small number of genes required for sorting to the regulated secretory pathway. Most of these have a known role in membrane trafficking, supporting the specificity of the screening assay. However, the sequences identified might influence cell surface expression of VMAT through mechanisms unrelated to the RSP, and the μ subunit of adaptor AP-2 falls into this category since this protein is required for clathrin-dependent endocytosis. Indeed, only four genes impair regulated secretion.

Since the screen had the potential to identify genes required for multiple aspects of LDCV biogenesis, including some unrelated to the cytosolic dileucine-like motif in VMAT, we classified them further in terms of their interaction with this motif, and in particular, the upstream acidic residues. Consistent with a role independent of the dileucine-like motif, the knockdown of two class I genes (*nup93* and *pp1-13c*) increases cell surface expression of DE/AA as well as wild type dVMAT. Although a subunit of the nuclear pore complex, nup93 exhibits structural similarity to coat proteins, and one subunit of the COPII coat indeed belongs to a subcomplex of the nuclear pore (Brohawn et al., 2008; Devos et al., 2004). Considering its localization to the nuclear envelope, nup93 may thus have a role in sorting to the RSP at the level of the endoplasmic reticulum, where sorting may begin (Martinez-Menarguez et al., 1999). Knockdown of the catalytic subunit in protein phosphatase I (PP1) also impairs regulated secretion, and a number of kinases have been implicated in sorting at the TGN. In addition to lipid kinases, which synthesize the phosphatidylinositol-4-phosphate required for recruitment of multiple proteins to the Golgi complex (De Matteis and Luini, 2008), protein kinase D contributes to constitutive secretion (Liljedahl et al., 2001). PP1 may promote sorting to the RSP by antagonizing the

function of these kinases, thereby regulating the production of LDCVs as well as constitutive secretory vesicles.

Among class III genes, we identified a carboxypeptidase that influences regulated exocytosis. Interestingly, previous work has suggested that the membrane-associated protease carboxypeptidase E (CPE) promotes sorting to the RSP of multiple peptides including pro-opiomelanocortin and insulin (Cawley et al., 2004; Cool et al., 1997). Although CPE contributes to peptide processing, the carboxypeptidase identified in this screen is required for the trafficking of VMAT, a polytopic membrane protein that does not undergo proteolytic processing, as well as for the regulated secretion of ANF. In addition, the gene identified here shows stronger similarity to the CPB than CPE family, suggesting a distinct role.

AP-3 is required for sorting to the regulated pathway

The screen also identified multiple subunits of the adaptor protein AP-3. The knockdown of these subunits produces some of the strongest effects on surface expression of dVMAT, and the most profound on ANF, with increased constitutive as well as reduced regulated secretion. Further, we find that AP-3 RNAi increases VMAT2 surface expression in PC12 cells, and markedly impairs the regulated secretion of SgII from this mammalian cell line.

Like other class III genes, the DE/AA mutation occludes the effect of AP-3 RNAi, suggesting that they act in the same pathway. Consistent with this, previous work has suggested that the interaction of a dileucine motif with AP-3 requires acidic residues 4 and 5 residues upstream (Janvier et al., 2003), at the same positions found in dVMAT, mammalian VMAT2 and phogrin. Moreover, recent work on the closely related adaptor AP-2 suggests a structural basis for the more stringent requirement of AP-3 for upstream acidic residues (Kelly et al., 2008). Although it can be difficult to assess the relevance of adaptor-cargo interactions identified *in vitro*, the work

now provides functional evidence that AP-3 interacts directly with the extended dileucine motif in VMAT2 to mediate its sorting into the RSP.

The results show that the loss of AP-3 disrupts the regulated exocytosis of LDCVs. AP-3 RNAi almost eliminates the regulated release of SgII from PC12 cells, with only a minimal effect on the amount secreted constitutively. Since AP-3 knockdown reduces the cellular content of SgII, however, it increases the proportion that undergoes constitutive release. Importantly, the loss of AP-3 greatly reduces the storage of granin proteins in *mocha* mice as well as PC12 cells, establishing the physiological relevance of the findings *in vitro* and excluding potential off-target effects of the RNAi. In addition, the analysis of VMAT2 exocytosis by direct optical imaging demonstrates both an increase in constitutive release and a dramatic reduction in regulated release produced by the loss of AP-3.

AP-3 has previously been suggested to influence the morphology of LDCVs. The *mocha* mutation increases the size of chromaffin granules by direct electrochemical measurement of quantal monoamine release and by electron microscopy (Grabner et al., 2006). We also observe enlarged LDCVs after AP-3 knockdown in PC12 cells. However, Grabner et al. (2006) examined release only after the direct application of calcium to permeabilized cells, and so did not specifically address the regulation of release. The results presented here thus provide the first evidence that AP-3 is required for regulated secretion.

AP-3 influences LDCV formation

To understand how the loss of AP-3 disrupts regulated exocytosis, we examined the effect on LDCVs. In addition to the increased diameter, we observe a major reduction (~50%) in number of LDCVs. Soluble LDCV cargo (endogenous SgII and transfected ANF-GFP) also shifts toward lighter fractions by equilibrium sedimentation. These effects strongly suggest that AP-3 contributes to LDCV formation or maturation, rather than simply their regulated exocytosis.

We took advantage of labeling with $^{35}SO_4^-$ to determine how AP-3 influences the fate of secretory vesicles formed at the TGN. In contrast to control cells which release negligible amounts of SgII even after 4 h of chase, AP-3 RNAi results in the release of SgII within 30 minutes after budding from the TGN, with no effect on the constitutively released HSPG. Since LDCV maturation continues long after budding from the TGN, the rapid release of SgII suggests a role for AP-3 that precedes maturation, such as sorting within the TGN. Consistent with than earlier locus for AP-3 action, LDCV maturation is not apparently required for the regulation of exocytosis (Tooze et al., 1991).

To address a role for AP-3 in sorting at the TGN, we examined the formation of secretory vesicles 15 minutes after labeling with $^{35}SO_4^-$. At this time, vesicles containing $^{35}SO_4^-$-SgII and – HSPG have budded from the TGN, and equilibrium sedimentation can be used to separate light constitutive secretory vesicles (containing HSPG) from heavier immature LDCVs (containing SgII). Using this assay, we find that the loss of AP-3 redistributes SgII into lighter fractions. Although the mis-sorting is again not complete, it is similar to that observed at steady-state for SgII and for EE/AA rat VMAT2 (Krantz et al., 2000). These results indicate that AP-3 has a role in sorting to LDCVs at the level of the TGN.

AP-3 has generally been considered to function within the endocytic rather than biosynthetic pathway. AP-3 mediates sorting to lysosomes and LROs such as melanosomes and secretory lysosomes (Dell'Angelica, 2009; Newell-Litwa et al., 2007), and these membranes, in contrast to LDCVs, form within the endocytic pathway. Loss of AP-3 also affects the behavior of lytic granules, the LROs of cytotoxic T cells, but does not influence the sorting of soluble cargo into lytic granules, and this has again been attributed to a defect in the endocytic pathway (Clark et al., 2003). Consistent with this role, AP-3 localizes primarily to endosomes (Peden et al., 2004). However, lower levels also localize to other sites including the Golgi complex (Dell'Angelica et al., 1997; Peden et al., 2004). In addition, AP-3 contains neural as well as ubiquitous subunits, and the neural isoform may localize even more strongly to the Golgi complex. It is nonetheless possible that AP-3 on endosomes promotes sorting to the RSP by recycling to the TGN components required for LDCV formation, but AP-3 promotes recycling to lysosomes and LROs, not the Golgi complex (Dell'Angelica, 2009). Although unanticipated from previous work, the requirement for AP-3 in sorting to the RSP now argues for a functional role in the biosynthetic pathway, at the TGN.

Supporting a role in the biosynthetic pathway, AP-3 functions at the TGN in yeast (Cowles et al., 1997; Stepp et al., 1997). In contrast to the main lysosomal targeting pathway that delivers hydrolases such as carboxypeptidase Y to the vacuole through an endosomal intermediate, AP-3 contributes to an alternative pathway that targets alkaline phosphatase directly to the vacuole. However, this pathway has been considered specific to yeast. The evidence of a role for AP-3 in sorting to the RSP now suggests that a component of the alternative lysosome targeting pathway participates directly in the formation of regulated secretory vesicles from the TGN of metazoans. Since the alternative lysosome targeting pathway lacks an endosomal intermediate, it may have been particularly well suited to minimize the loss of soluble cargo and acquire the capacity for regulated release of proteins that mediate extracellular signaling.

Despite the effects of AP-3 loss on LDCV number, morphology and density, vesicles with a dense core still form, both in PC12 cells after RNAi and in *mocha* mice. What then accounts for the disproportionately severe functional effect on regulated exocytosis? The budding assay suggests that proteins normally segregated to the RSP intermix with those destined for constitutive secretion, and this may account for the intermediate density as well as increased size. Supporting this possibility, we find that the loss of AP-3 redistributes synaptotagmin 1 to fractions even lighter than those containing soluble LDCV cargo. As a major calcium sensor for regulated exocytosis of LDCVs (Schonn, 2008; Voets, 2001), the change in synaptotagmin distribution presumably contributes to the loss of regulated release. In addition, previous work on the trafficking of synaptotagmin 1 has also identified a conserved C-terminal dileucine motif with upstream acidic residues (*EE*VDA**ML**) that may account for the dependence on AP-3 (Blagoveshchenskaya, 1999; Jarousse, 2001). However, the effect of AP-3 deficiency seems more profound than that produced by loss of synaptotagmin 1 (Schonn, 2008; Voets, 2001), strongly suggesting that AP-3 also influences the distribution of other proteins that influence the mode of exocytosis.

Materials and Methods

Molecular biology

EGFP and mCherry were fused to the N-terminus of HA-dVMAT (a gift of D. Krantz, UCLA) to produce GFP-/HA-dVMAT or mCherry-/HA-dVMAT, respectively. The DE/AA mutation was introduced by overlap extension PCR. ANF-GFP was generously provided by E. Levitan (University of Pittsburgh), and ss-GFP constructed by amplifying the signal sequence of ANF and fusing it directly to GFP. For expression in *Drosophila* S2 cells, all cDNAs were subcloned into pAc5.1 (Invitrogen, CA). For expression in PC12 cells, all cDNAs were subcloned into the chicken actin-based vector pCAAGS.

Cell culture

Drosophila S2 cells were maintained in Schneider medium (Invitrogen, CA) supplemented with 10% heat-inactivated fetal bovine serum at 27° C in a humidified incubator. Transfection of S2 cells was performed using either Nucleofection (Amaxa) for transient expression or Fugene HD reagent (Roche) for stable expression, both according to the manufacturer's instructions. For stable expression, S2 cells were cotransfected with GFP-/HA-dVMAT and pCoHygro (Invitrogen) in a 10:1 molar ratio, and selected in 300 μg/mL hygromycin for 4 weeks. PC12 cells were maintained in DME-H21 medium supplemented with 10% horse serum and 5% calf serum (Cosmic) at 37° C. Transfection of PC12 cells was performed using Lipofectamine 2000 (Invitrogen) according to the manufacturer's instructions.

Antibodies and immunofluorescence

The HA.ll mouse monoclonal antibody was obtained from Covance, the M2-FLAG mouse monoclonal antibody from Sigma-Aldrich, the SgII rabbit polyclonal antibody from Meridian Life Science, the σ3A mouse monoclonal antibody from BD Transduction Laboratories, the actin mouse monoclonal antibody from Millipore, the Zenon Alexa 647 labeling kit from Invitrogen, and the synaptophysin (p38) monoclonal antibody from Sigma-Aldrich.

Screen and analysis

S2 cells transfected with GFP-dVMAT-HA were treated in 96-well plates with dsRNA prepared from the University of California, San Francisco (UCSF) DmRNAi library version 1 (7216 genes) (Goshima et al., 2007). After growth for 72 h, the cells were again treated with the same dsRNA, incubated an additional 72 h, and surface HA expression determined by adding external HA.11 antibody bound to Zenon Alexa 647 (1:1000) for 2 h in standard medium, removing the unbound antibody with two washes, and subjecting the cells to high-throughput flow cytometry (lsrII, BD Biosciences, CA) for both GFP and Alexa 647 fluorescence. The ratio of Alexa 647 to GFP fluorescence was calculated for individual cells and the mean ratio calculated from all cells in the well.

Assuming that treatment with most dsRNA does not affect surface dVMAT expression, the mean Alexa647/GFP fluorescence ratio from all wells of a plate should resemble the ratio from cells without dsRNA, and thus serve as a within-plate negative control. Z-scores were determined by subtracting the overall mean Alexa 647/GFP ratio (derived from the entire plate) from the ratios for individual wells, normalizing to the standard deviation determined from the mean ratios of all wells in the plate. This analysis limits statistical artifacts caused by inter-plate variability and has been used widely for high-throughput, cell-based screens (Malo et al., 2006), with a script written for the statistical software "R" to automate the analysis (Team, 2008). To minimize false

positives, a stringent Z-score > 3.0 (p value < 0.0014) was used to identify dsRNA sequences positive in the screen. The screen was also performed twice, once using transiently transfected S2 cells, and once with stable transformants. The positives from both screens were then combined, and those with few remaining cells or altered GFP expression removed from further consideration, leaving 18 sequences (0.25% of the original library) available for further study.

To exclude off-target effects, we retested the 18 positives with non-overlapping dsRNA sequences from the same gene. In each experiment, the cumulative frequency distribution of fluorescence ratios from individual cells was plotted, compared to control RNAi, and statistical significance analyzed by Kolmogorov-Smirnov. We applied the stringent Bonferroni correction for 19 samples (18 positives + control), and considered as positive a p-value < 0.0025 in at least two independent experiments. A typical data set consisted of 50-500 cells per dsRNA treatment in the screen, and 1000-5000 cells in the retest. Of 18 positives from the original screen, 16 showed a consistent increase in dVMAT cell surface expression on retest and were thus considered true positives.

Secretion assays

S2 cells transfected with ANF-GFP were washed with phosphate-buffered saline (PBS), resuspended in Tyrode's medium (in mM: 119 NaCl, 2.5 KCl, 2 $CaCl_2$, 2 $MgCl_2$, 30 glucose, 25 HEPES [pH 7.4]), split equally into two tubes, incubated in the presence or absence of 100 μg/mL LPS (Sigma-Aldrich) for 1 h at 27° C, sedimented, and the fluorescence from 200 μl aliquots of the supernatant measured in triplicate using a plate reader (Tecan, Switzerland), with stimulated secretion expressed as a percent of the respective unstimulated condition.

siRNAs to rat AP-3δ1 (5'-UUCUUGGUCAUGAUCCAUGTG-3' antisense and 5'-CAUGGAUCAUGACCAAGAATT-3' sense) were transfected twice (at 50 nM) three days apart,

the PC12 cells washed 2-3 days later and incubated in Tyrode's buffer containing 2.5 mM K$^+$ (basal) or 90 mM K$^+$ (stimulated) for 30 minutes at 37° C. The supernatant was then collected, cell lysates prepared as previously described (Li et al., 2005), and the samples analyzed by quantitative, fluorescent immunoblotting.

Adrenal gland granin content

mocha mice (Jackson Labs) were backcrossed to C57BL/6 to remove *grizzled* and *Pde6b*^{rd1} alleles, and the adrenal glands homogenized in 150 mM NaCl, 50 mM Tris-HCl, pH 8.0, 1% NP-40, 0.5% sodium deoxycholate and protease inhibitors (Roche) including 1 mM EGTA and 1 mM PMSF. After sedimentation at 14,000*g* to remove nuclei and cell debris, 20 μg protein was separated by electrophoresis through polyacrylamide, transferred to nitrocellulose, and the membranes immunoblotted for SgII and CgA, with actin as loading control and the appropriate secondary antibodies conjugated to IRDye800 (Rockland). The immunoreactivity was quantified by imaging with a LICOR system (Odyssey) and ImageJ (NIH), and results normalized to actin.

TIRF microscopy

For TIRF microscopy, PC12 cells plated onto glass chambers (LabTek) coated with poly-L-lysine (Sigma-Aldrich) were transfected with siRNAs (50 nM) to rat AP-3δ, and two days later co-transfected with siRNAs and VMAT2-pHluorin. After an additional 3 days, images were collected for 100 ms at 2 Hz and room temperature using a TIRF microscope (Nikon TE2000E inverted microscope) with 100x objective (Oil Plan Apo NA 1.49) and a Photometrics QuantEM EMCCD camera. To reveal surface and total VMAT2 fluorescence, cells were incubated sequentially with Tyrode's solution containing 25 mM MES, pH 6.5 and then 50 mM NH$_4$Cl, pH 7.4. To examine basal and regulated release, cells were incubated in Tyrode's solution containing, respectively, 2.5 mM or 90 mM K$^+$ for one minute each. Movies were acquired in NIS-Elements

Advanced Research, exported as AVI files and image sequences were analyzed using ImageJ software (NIH).

Density gradient fractionation

Equilibrium sedimentation through sucrose was performed as previously described (Waites et al., 2001). Briefly, a postnuclear supernatant was prepared from PC12 cells by homogenization with a ball bearing device (8 μm clearance), loaded onto a 0.6 M-1.6 M continuous sucrose gradient, and sedimented at 30,000 rpm in an SW41 rotor for 14-16 h at 4° C. Fractions (~200 μl each) were collected from the top directly into a 96-well plate (Costar) and ANF-GFP fluorescence read using a plate reader (Tecan, Switzerland). For SgII and p38, pools of 4 fractions were analyzed by quantitative, fluorescent immunoblotting.

Electron microscopy

PC12 cells were plated onto aclar film discs (Pella) coated with poly-L-lysine, transfected twice with siRNA (50 nM), washed with calcium/magnesium-free (cmf)-PBS 2 days after the second transfection and fixed with 2.5% glutaraldehyde in cmf-PBS. The discs were washed three times with 0.1 M sodium cacodylate buffer (pH 7.2) and postfixed for 30 min on ice with 1% osmium tetroxide in cacodylate buffer containing 1.6% potassium ferricyanide. The discs were then washed three times with cacodylate buffer, three times with water, incubated with 0.5% uranyl acetate for 30 min (in the dark), and washed again with water. The samples were dehydrated in a graded series of ethanols while progressively lowering the temperature from 4° C to -40° C, then embedded in Epon resin. After peeling off the aclar, sections were cut and then viewed in a FEI Tecnai 12 electron microscope (Phillips) at 120 kV, capturing images with a digital camera at 6800 magnification, and analyzing them with ImageJ. Morphologically identifiable LDCVs were counted for each cell sectioned, and the cytoplasmic area determined by subtracting the area of the nucleus from the whole cell. Density was calculated as the number of LDCVs per cell section

divided by the cytoplasmic area. LDCV and core diameters were determined as the shortest distance between points on opposite sides.

Budding assay

Vesicle budding from the TGN was examined as previously described (Tooze and Huttner, 1990). Briefly, PC12 cells were depleted of endogenous SO_4 for 25 min, labeled for 5 min with 0.5-1 mCi/mL $^{35}SO_4$ and chased for 15 min in complete medium containing 1.6 mM nonradioactive Na_2SO_4. The cells were homogenized with a ball bearing device, debris sedimented, the resulting postnuclear supernatant loaded onto a 0.3 M-1.2 M continuous sucrose gradient, and newly formed vesicle separated from the TGN by velocity centrifugation for 19 min at 4° C in an SW41 rotor at 25,000 rpm. Fractions (1 mL) were collected from the top of the gradient, pooled fractions 1-5 loaded onto an 0.5-2 M continuous sucrose gradient sedimented to equilibrium in an SW41 rotor at 25,000 rpm and 4° C for 16 h. Fractions (500 µl) were collected from the top of the gradient and aliquots (50 µl) separated by electrophoresis through polyacrylamide followed by fluorography and quantitation of the resulting images by densitometry.

References

Arvan, P., and D. Castle. 1998. Sorting and storage during secretory granule biogenesis: looking backward and looking forward. *Biochem J*. 332 (Pt 3):593-610.

Baeuerle, P.A., and W.B. Huttner. 1987. Tyrosine sulfation is a trans-Golgi-specific protein modification. *J Cell Biol*. 105:2655-64.

Bard, F., L. Casano, A. Mallabiabarrena, E. Wallace, K. Saito, H. Kitayama, G. Guizzunti, Y. Hu, F. Wendler, R. Dasgupta, N. Perrimon, and V. Malhotra. 2006. Functional genomics reveals genes involved in protein secretion and Golgi organization. *Nature*. 439:604-7.

Berwin, B., E. Floor, and T.F. Martin. 1998. CAPS (mammalian UNC-31) protein localizes to membranes involved in dense-core vesicle exocytosis. *Neuron*. 21:137-45.

Blagoveshchenskaya, A.D., M.J. Hannah, S. Allen, and D.F. Cutler. 2002. Selective and signal-dependent recruitment of membrane proteins to secretory granules formed by heterologously expressed von Willebrand factor. *Mol Biol Cell*. 13:1582-93.

Brohawn, S.G., N.C. Leksa, E.D. Spear, K.R. Rajashankar, and T.U. Schwartz. 2008. Structural evidence for common ancestry of the nuclear pore complex and vesicle coats. *Science*. 322:1369-73.

Burman, J.L., L. Bourbonniere, J. Philie, T. Stroh, S.Y. Dejgaard, J.F. Presley, and P.S. McPherson. 2008. Scyl1, mutated in a recessive form of spinocerebellar neurodegeneration, regulates COPI-mediated retrograde traffic. *J Biol Chem*. 283:22774-86.

Cawley, N.X., J. Zhou, J.M. Hill, D. Abebe, S. Romboz, T. Yanik, R.M. Rodriguiz, W.C. Wetsel, and Y.P. Loh. 2004. The carboxypeptidase E knockout mouse exhibits endocrinological and behavioral deficits. *Endocrinology*. 145:5807-19.

Chavez, R.A., S.G. Miller, and H.P. Moore. 1996. A biosynthetic regulated secretory pathway in constitutive secretory cells. *J Cell Biol*. 133:1177-91.

Chen, Z.Y., A. Ieraci, H. Teng, H. Dall, C.X. Meng, D.G. Herrera, A. Nykjaer, B.L. Hempstead, and F.S. Lee. 2005. Sortilin controls intracellular sorting of brain-derived neurotrophic factor to the regulated secretory pathway. *J Neurosci*. 25:6156-66.

Clark, R.H., J.C. Stinchcombe, A. Day, E. Blott, S. Booth, G. Bossi, T. Hamblin, E.G. Davies, and G.M. Griffiths. 2003. Adaptor protein 3-dependent microtubule-mediated movement of lytic granules to the immunological synapse. *Nat Immunol*. 4:1111-20.

Cool, D.R., E. Normant, F. Shen, H.C. Chen, L. Pannell, Y. Zhang, and Y.P. Loh. 1997. Carboxypeptidase E is a regulated secretory pathway sorting receptor: genetic obliteration leads to endocrine disorders in Cpe(fat) mice. *Cell*. 88:73-83.

Cowles, C.R., G. Odorizzi, G.S. Payne, and S.D. Emr. 1997. The AP-3 adaptor complex is essential for cargo-selective transport to the yeast vacuole. *Cell*. 91:109-18.

De Matteis, M.A., and A. Luini. 2008. Exiting the Golgi complex. *Nat Rev Mol Cell Biol*. 9:273-84.

Dell'Angelica, E.C. 2009. AP-3-dependent trafficking and disease: the first decade. *Curr Opin Cell Biol*. 21:552-9.

Dell'Angelica, E.C., H. Ohno, C.E. Ooi, E. Rabinovich, K.W. Roche, and J.S. Bonifacino. 1997. AP-3: an adaptor-like protein complex with ubiquitous expression. *EMBO J*. 16:917-28.

Devos, D., S. Dokudovskaya, F. Alber, R. Williams, B.T. Chait, A. Sali, and M.P. Rout. 2004. Components of coated vesicles and nuclear pore complexes share a common molecular architecture. *PLoS Biol*. 2:e380.

Dittie, A.S., N. Hajibagheri, and S.A. Tooze. 1996. The AP-1 adaptor complex binds to immature secretory granules from PC12 cells, and is regulated by ADP-ribosylation factor. *J Cell Biol*. 132:523-36.

Eaton, B.A., M. Haugwitz, D. Lau, and H.P. Moore. 2000. Biogenesis of regulated exocytotic carriers in neuroendocrine cells. *J Neurosci*. 20:7334-44.

Elhamdani, A., T.F. Martin, J.A. Kowalchyk, and C.R. Artalejo. 1999. Ca(2+)-dependent activator protein for secretion is critical for the fusion of dense-core vesicles with the membrane in calf adrenal chromaffin cells. *J Neurosci*. 19:7375-83.

Erickson, J.D., L.E. Eiden, M.K. Schafer, and E. Weihe. 1995. Reserpine- and tetrabenazine-sensitive transport of (3)H-histamine by the neuronal isoform of the vesicular monoamine transporter. *J Mol Neurosci*. 6:277-87.

Flierl, M.A., D. Rittirsch, B.A. Nadeau, A.J. Chen, J.V. Sarma, F.S. Zetoune, S.R. McGuire, R.P. List, D.E. Day, L.M. Hoesel, H. Gao, N. Van Rooijen, M.S. Huber-Lang, R.R. Neubig, and P.A. Ward. 2007. Phagocyte-derived catecholamines enhance acute inflammatory injury. *Nature*. 449:721-5.

Foley, E., and P.H. O'Farrell. 2004. Functional dissection of an innate immune response by a genome-wide RNAi screen. *PLoS Biol*. 2:E203.

Goshima, G., R. Wollman, S.S. Goodwin, N. Zhang, J.M. Scholey, R.D. Vale, and N. Stuurman. 2007. Genes required for mitotic spindle assembly in Drosophila S2 cells. *Science*. 316:417-21.

Grabner, C.P., S.D. Price, A. Lysakowski, A.L. Cahill, and A.P. Fox. 2006. Regulation of large dense-core vesicle volume and neurotransmitter content mediated by adaptor protein 3. *Proc Natl Acad Sci U S A*. 103:10035-40.

Greer, C.L., A. Grygoruk, D.E. Patton, B. Ley, R. Romero-Calderon, H.Y. Chang, R. Houshyar, R.J. Bainton, A. Diantonio, and D.E. Krantz. 2005. A splice variant of the Drosophila vesicular monoamine transporter contains a conserved trafficking domain and functions in the storage of dopamine, serotonin, and octopamine. *J Neurobiol*. 64:239-58.

Guo, Y., T.C. Walther, M. Rao, N. Stuurman, G. Goshima, K. Terayama, J.S. Wong, R.D. Vale, P. Walter, and R.V. Farese. 2008. Functional genomic screen reveals genes involved in lipid-droplet formation and utilization. *Nature*. 453:657-61.

Harrison-Lavoie, K.J., G. Michaux, L. Hewlett, J. Kaur, M.J. Hannah, W.W. Lui-Roberts, K.E. Norman, and D.F. Cutler. 2006. P-selectin and CD63 use different mechanisms for delivery to Weibel-Palade bodies. *Traffic*. 7:647-62.

Janvier, K., Y. Kato, M. Boehm, J.R. Rose, J.A. Martina, B.Y. Kim, S. Venkatesan, and J.S. Bonifacino. 2003. Recognition of dileucine-based sorting signals from HIV-1 Nef and LIMP-II by the AP-1 gamma-sigma1 and AP-3 delta-sigma3 hemicomplexes. *J Cell Biol*. 163:1281-90.

Kantheti, P., X. Qiao, M.E. Diaz, A.A. Peden, G.E. Meyer, S.L. Carskadon, D. Kapfhamer, D. Sufalko, M.S. Robinson, J.L. Noebels, and M. Burmeister. 1998. Mutation in AP-3 delta in the mocha mouse links endosomal transport to storage deficiency in platelets, microsomes and synaptic vesicles. *Neuron*. 21:111-122.

Kelly, B.T., A.J. McCoy, K. Spate, S.E. Miller, P.R. Evans, S. Honing, and D.J. Owen. 2008. A structural explanation for the binding of endocytic dileucine motifs by the AP2 complex. *Nature*. 456:976-79.

Kim, T., J.H. Tao-Cheng, L.E. Eiden, and Y.P. Loh. 2001. Chromogranin A, an "on/off" switch controlling dense-core secretory granule biogenesis. *Cell*. 106:499-509.

Krantz, D.E., D. Peter, Y. Liu, and R.H. Edwards. 1997. Phosphorylation of a vesicular monoamine transporter by casein kinase II. *J Biol Chem*. 272:6752-9.

Krantz, D.E., C. Waites, V. Oorschot, Y. Liu, R.I. Wilson, P.K. Tan, J. Klumperman, and R.H. Edwards. 2000. A phosphorylation site in the vesicular acetylcholine transporter regulates sorting to secretory vesicles. *J. Cell Biol.* 149:379-395.

Lewis, M.J., J.C. Rayner, and H.R. Pelham. 1997. A novel SNARE complex implicated in vesicle fusion with the endoplasmic reticulum. *EMBO J*. 16:3017-24.

Li, H., C.L. Waites, R.G. Staal, Y. Dobryy, J. Park, D.L. Sulzer, and R.H. Edwards. 2005. Sorting of vesicular monoamine transporter 2 to the regulated secretory pathway confers the somatodendritic exocytosis of monoamines. *Neuron*. 48:619-33.

Liljedahl, M., Y. Maeda, A. Colanzi, I. Ayala, J. Van Lint, and V. Malhotra. 2001. Protein kinase D regulates the fission of cell surface destined transport carriers from the trans-Golgi network. *Cell*. 104:409-20.

Liu, Y., E.S. Schweitzer, M.J. Nirenberg, V.M. Pickel, C.J. Evans, and R.H. Edwards. 1994. Preferential localization of a vesicular monoamine transporter to dense core vesicles in PC12 cells. *J Cell Biol*. 127:1419-33.

Malo, N., J.A. Hanley, S. Cerquozzi, J. Pelletier, and R. Nadon. 2006. Statistical practice in high-throughput screening data analysis. *Nat Biotechnol*. 24:167-75.

Martin, T.F., and J.H. Walent. 1989. A new method for cell permeabilization reveals a cytosolic protein requirement for Ca2+ -activated secretion in GH3 pituitary cells. *J Biol Chem*. 264:10299-308.

Martinez-Menarguez, J.A., H.J. Geuze, J.W. Slot, and J. Klumperman. 1999. Vesicular tubular clusters between the ER and Golgi mediate concentration of soluble secretory proteins by exclusion from COPI-coated vesicles. *Cell*. 98:81-90.

Miesenböck, G., D.A. De Angelis, and J.E. Rothman. 1998. Visualizing secretion and synaptic transmission with pH-sensitive green fluorescent proteins. *Nature*. 394:192-5.

Morvan, J., and S.A. Tooze. 2008. Discovery and progress in our understanding of the regulated secretory pathway in neuroendocrine cells. *Histochem Cell Biol*. 129:243-52.

Newell-Litwa, K., E. Seong, M. Burmeister, and V. Faundez. 2007. Neuronal and non-neuronal functions of the AP-3 sorting machinery. *J Cell Sci*. 120:531-41.

Onoa, B., H. Li, J.A. Gagnon-Bartsch, L.A. Elias, and R.H. Edwards. 2010. Vesicular monoamine and glutamate transporters select distinct synaptic vesicle recycling pathways. *J Neurosci*. 30:7917-27.

Orci, L., M. Ravazzola, M. Amherdt, A. Perrelet, S.K. Powell, D.L. Quinn, and H.P. Moore. 1987. The trans-most cisternae of the Golgi complex: a compartment for sorting of secretory and plasma membrane proteins. *Cell*. 51:1039-51.

Peden, A.A., V. Oorschot, B.A. Hesser, C.D. Austin, R.H. Scheller, and J. Klumperman. 2004. Localization of the AP-3 adaptor complex defines a novel endosomal exit site for lysosomal membrane proteins. *J Cell Biol*. 164:1065-76.

Ramet, M., P. Manfruelli, A. Pearson, B. Mathey-Prevot, and R.A. Ezekowitz. 2002. Functional genomic analysis of phagocytosis and identification of a Drosophila receptor for E. coli. *Nature*. 416:644-8.

Sankaranarayanan, S., D. De Angelis, J.E. Rothman, and T.A. Ryan. 2000. The use of pHluorins for optical measurements of presynaptic activity. *Biophys J*. 79:2199-208.

Shakiryanova, D., A. Tully, R.S. Hewes, D.L. Deitcher, and E.S. Levitan. 2005. Activity-dependent liberation of synaptic neuropeptide vesicles. *Nat Neurosci*. 8:173-8.

Speese, S., M. Petrie, K. Schuske, M. Ailion, K. Ann, K. Iwasaki, E.M. Jorgensen, and T.F. Martin. 2007. UNC-31 (CAPS) is required for dense-core vesicle but not synaptic vesicle exocytosis in Caenorhabditis elegans. *J Neurosci*. 27:6150-62.

Stepp, J.D., K. Huang, and S.K. Lemmon. 1997. The yeast adaptor protein complex, AP-3, is essential for the efficient delivery of alkaline phosphatase by the alternate pathway to the vacuole. *J Cell Biol*. 139:1761-74.

Stroschein-Stevenson, S.L., E. Foley, P.H. O'Farrell, and A.D. Johnson. 2006. Identification of Drosophila gene products required for phagocytosis of Candida albicans. *PLoS Biol*. 4:e4.

Team, R.D.C. 2008. R: A language and environment for statistical computing. r foundation for statistical computing, vienna.

Tiede, S., S. Storch, T. Lubke, B. Henrissat, R. Bargal, A. Raas-Rothschild, and T. Braulke. 2005. Mucolipidosis II is caused by mutations in GNPTA encoding the alpha/beta GlcNAc-1-phosphotransferase. *Nat Med*. 11:1109-12.

Tooze, S.A., T. Flatmark, J. Tooze, and W.B. Huttner. 1991. Characterization of the immature secretory granule, an intermediate in granule biogenesis. *J Cell Biol*. 115:1491-503.

Tooze, S.A., and W.B. Huttner. 1990. Cell-free protein sorting to the regulated and constitutive secretory pathways. *Cell*. 60:837-47.

Torii, S., N. Saito, A. Kawano, S. Zhao, T. Izumi, and T. Takeuchi. 2005. Cytoplasmic transport signal is involved in phogrin targeting and localization to secretory granules. *Traffic*. 6:1213-24.

Turkewitz, A.P. 2004. Out with a bang! Tetrahymena as a model system to study secretory granule biogenesis. *Traffic*. 5:63-8.

Waites, C.L., A. Mehta, P.K. Tan, G. Thomas, R.H. Edwards, and D.E. Krantz. 2001. An acidic motif retains vesicular monoamine transporter 2 on large dense core vesicles. *J Cell Biol*. 152:1159-68.

CHAPTER 4:

WIDESPREAD DYSREGULATION OF PEPTIDE HORMONE RELEASE IN MICE LACKING ADAPTOR PROTEIN AP-3[*]

Daniel W. Sirkis[1,2], Cédric S. Asensio[2], and Robert H. Edwards[1,2]

[1]Graduate Program in Pharmaceutical Sciences and Pharmacogenomics

[2]Departments of Physiology and Neurology

University of California, San Francisco

San Francisco, California 94158

---

[*]This chapter comprises a manuscript submitted for publication to *Proceedings of the National Academy of Sciences USA* in October 2012, and which is currently under review. As the first author of this paper, I:
- conducted all experiments described herein;
- performed glucose tolerance tests and collected blood for insulin measurements with Cédric Asensio;
- frequently discussed methods and data interpretation with both Cédric Asensio and Robert Edwards;
- wrote the manuscript with Robert Edwards

Abstract

The regulated secretion of peptide hormones, neural peptides and many growth factors depends on their sorting into large dense core vesicles (LDCVs) capable of regulated exocytosis. LDCVs form at the *trans*-Golgi network, but the mechanisms that sort proteins to this regulated secretory pathway and indeed the cytosolic machinery that produces LDCVs remain poorly understood. Recently, we used RNAi to identify a role for heterotetrameric adaptor protein AP-3 in regulated secretion and LDCV formation. Indeed, *mocha* mice lacking AP-3 have a severe neurological and behavioral phenotype, but this has been attributed to a role for AP-3 in the endolysosomal pathway, and the contribution of dysregulated protein release has not been investigated. We now find that adrenal chromaffin cells from *mocha* animals show increased constitutive exocytosis of both soluble and membrane LDCV cargo, reducing the extent of stimulation. We also observe increased basal release of both insulin and glucagon from AP-3-deficient pancreatic islet cells, suggesting a global disturbance in the release of peptide hormones. AP-3 exists as both ubiquitous and neuronal isoforms, but we find that loss of both is required to impair LDCV production. In addition, we show that loss of the related adaptor protein AP-1 has no effect on regulated secretion but greatly exacerbates the effect of AP-3 RNAi, indicating distinct roles for the two adaptors in formation of the regulated secretory pathway.

Introduction

In contrast to most proteins which undergo immediate and unregulated secretion after biosynthesis, proteins destined for regulated release require sorting into LDCVs, but the mechanisms responsible for sorting to LDCVs and indeed LDCV formation remain poorly understood. LDCVs bud from the *trans*-Golgi network (TGN) (Orci et al., 1987; Sossin et al., 1990; Tooze and Huttner, 1990), and previous work has suggested that lumenal interactions such as the aggregation of granulogenic proteins drive their formation (Kim et al., 2001; Turkewitz, 2004). Indeed, sorting to LDCVs has been suggested to occur by default, with proteins destined for other organelles removed during the well-established process of LDCV maturation (Klumperman et al., 1998; Morvan and Tooze, 2008). However, direct analysis of budding from the TGN has demonstrated the sorting of regulated from constitutive cargo at this early step, before maturation (Tooze and Huttner, 1990). In addition, LDCV membrane proteins such as carboxypeptidase E and sortilin have been proposed to serve as the receptors for soluble cargo (Cool et al., 1997; Chen et al., 2005). In contrast to these lumenal and membrane interactions, the cytosolic machinery involved in sorting to LDCVs and LDCV formation has remained poorly understood.

Several membrane proteins contain cytosolic sequences that direct them to LDCVs. For example, the neuronal vesicular monoamine transporter VMAT2, which fills neurosecretory vesicles with monoamine transmitter, depends on a conserved, C-terminal, cytoplasmic dileucine-like motif for sorting to LDCVs (Liu et al., 1994; Krantz et al., 2000; Li et al., 2005), and the LDCV membrane protein IA-2β (phogrin) relies on a remarkably similar sequence (Torii et al., 2005). Since the requirement for a cytoplasmic motif suggested an interaction with cytosolic sorting machinery, we recently used VMAT as a reporter to screen by RNAi in *Drosophila* S2 cells for proteins involved in biogenesis of the regulated secretory pathway, identifying multiple subunits of the heterotetrameric adaptor protein AP-3 (Asensio et al., 2010). Loss of AP-3 results in mis-sorting of VMAT in both S2 and mammalian neuroendocrine PC12 cells, dysregulated

secretion, a reduction in the number and alteration in the morphology of LDCVs. An assay for budding from the TGN also revealed a disturbance in the sorting of LDCV cargo (Asensio et al., 2010). Although most work in mammalian cells has focused on the role of AP-3 within the endolysosomal pathway, in trafficking from early endosomes to the lysosome (Peden et al., 2004; Dell Angelica, 2009), these findings support an alternative role for AP-3 in the biosynthetic pathway suggested by work in *S. cerevisiae* (Cowles et al., 1997; Nickerson et al., 2009). Loss of AP-3 also impairs sorting of the calcium sensor synaptotagmin 1 (syt1) to LDCVs, suggesting that AP-3 concentrates the proteins required for regulated secretion. In addition, loss of AP-3 reduces the storage of granin proteins that form the dense core, both in PC12 cells and in *mocha* mice lacking AP-3. However, the relative importance of AP-3 in regulated secretion and formation of the regulated pathway *in vivo* has remained unknown. AP-3 also occurs in both neuronal and ubiquitous forms, with alternative isoforms for several of the subunits, and we do not know which is responsible for LDCV formation.

Results

To determine whether the loss of AP-3 *in vivo* affects regulated secretion, we cultured adrenal chromaffin cells from control and AP-3-deficient *mocha* mice, measuring the release of endogenous secretogranin II (SgII) in response to the nicotinic agonist DMPP (Chung et al., 1999). Western blotting of the medium indicated that DMPP stimulates SgII secretion from control cells, but SgII was undetectable in the medium of *mocha* cells (Fig. S1). However, the substantial reduction in cellular SgII content of *mocha* adrenal glands (Asensio et al., 2010) and of cultured *mocha* adrenal chromaffin cells (Fig. S1) made it difficult to determine whether the cells simply do not contain and release enough SgII to detect, or actually exhibit a defect in regulated release.
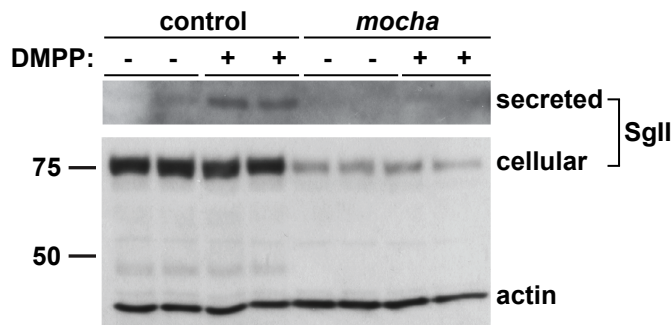
Figure S1. ***mocha* chromaffin cells display marked reductions in secreted and cellular SgII**
Chromaffin cells were stimulated with 20 μM DMPP in Tyrode's solution, or left unstimulated in Tyrode's alone. After a 15 min incubation at 37°C, supernatants were collected and mixed with SDS-PAGE sample buffer, and cells lysed by the addition of sample buffer. Secreted and cellular SgII were detected by immunoblotting. DMPP clearly induces secretion of SgII from control cells, but not from *mocha* cells. Analysis of cellular SgII shows a marked reduction in *mocha* cells. Cellular actin was used as a loading control.

To assess regulated exocytosis by chromaffin granules, we used total internal reflection fluorescence (TIRF) microscopy to image neuropeptide and LDCV membrane protein reporters fused to the supercliptic pHluorin (Miesenböck et al., 1998; Sankaranarayanan et al., 2000). The pHluorin is a modified form of green fluorescent protein (GFP) with increased sensitivity to

protons that is quenched at the low internal pH of LDCVs and therefore increases in fluorescence with exposure to the higher external pH on exocytosis. Since neuropeptide Y (NPY)-pHluorin has been shown to undergo regulated exocytosis (Kögel et al., 2010), we used lentiviral transduction to express this fusion protein and monitored individual exocytotic events at the plasma membrane of living chromaffin cells. In the absence of stimulation, control cells showed very few spontaneous fusion events over 90 s of imaging, but AP-3-deficient *mocha* cells exhibited substantially more (Fig. 1 *A* and *B*). Both control and *mocha* cells showed a clear increase in exocytosis in response to stimulation by DMPP, but the extent of stimulation relative to baseline reveals an ~70% reduction in *mocha* cells compared to controls (Fig. 1*B*). To extend these findings to an LDCV membrane protein, we transduced chromaffin cells with a virus encoding VMAT2-pHluorin, with the lumenal location of pHluorin enabling detection of release events (Anantharam et al., 2010; Onoa et al., 2010). Similar to NPY-pHluorin, VMAT2-pHluorin also showed a clear increase in basal, unstimulated exocytosis in *mocha* relative to control cells, and this again resulted in an ~75% reduction in stimulated release (Fig. 1*C*). The loss of AP-3 thus dysregulates the release of LDCVs as monitored using either soluble or membrane cargo.
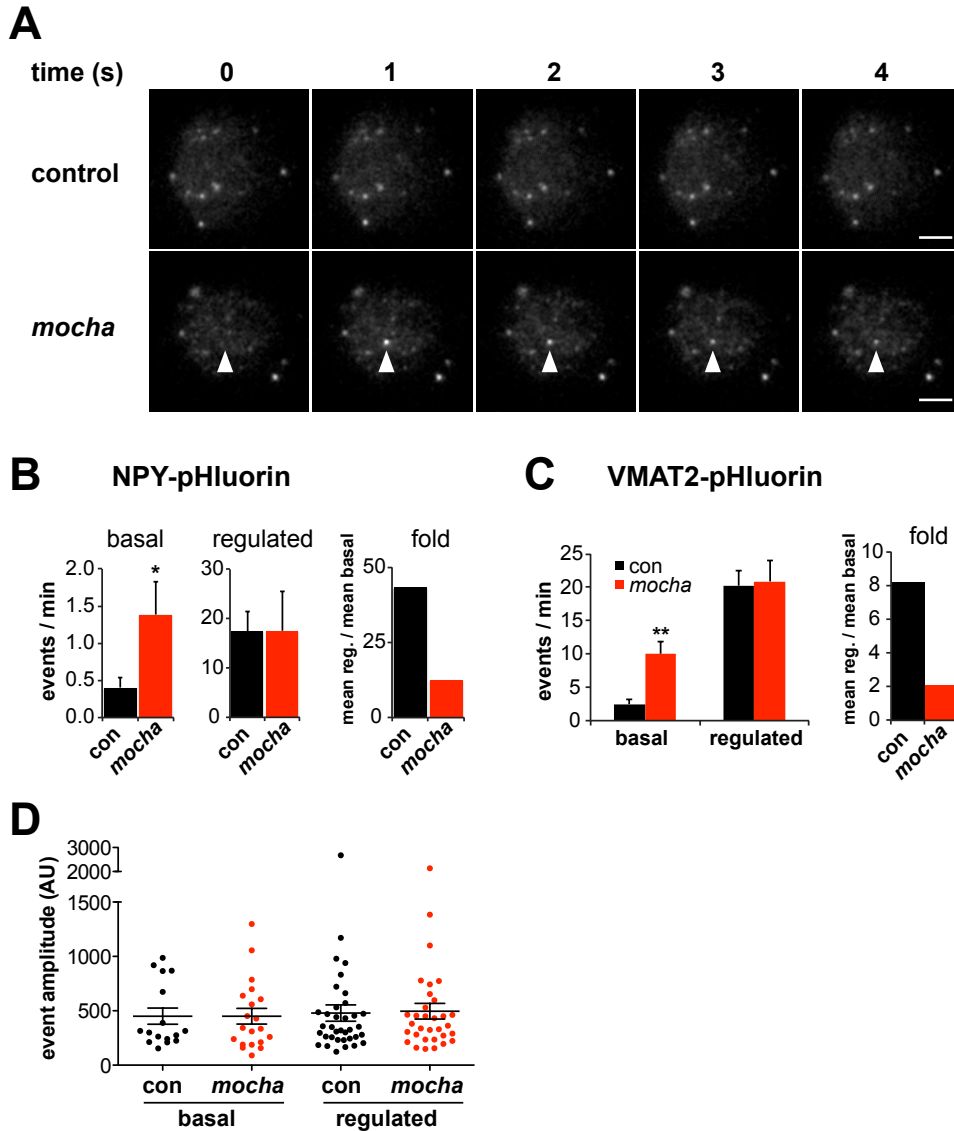
Figure 1. *mocha* chromaffin cells display dysregulated release of NPY and VMAT2

Chromaffin cells were transduced with lentivirus encoding either NPY- or VMAT2-pHluorin, then imaged live 4-7 days later by TIRF microscopy. Basal exocytosis was measured in Tyrode's solution, and release stimulated in Tyrode's containing 5 μM DMPP. (*A*) Representative images acquired during the unstimulated phase show a typical basal exocytotic event in a *mocha* cell. Scale bars indicate 5 μm. (*B*) Quantification of individual exocytotic events shows increased basal NPY-pHluorin exocytosis in *mocha* cells, and a similar number of events relative to control cells after stimulation. *p<0.04 relative to control; for basal, n=38 for control and n=38 for *mocha*; for stimulated, n=22 for control and n=22 for *mocha* Normalizing mean regulated events to mean basal events shows that *mocha* cells have an ~70% reduction in secretion fold change in response to stimulation relative to control cells. (*C*) Quantification of exocytotic events as above shows increased basal VMAT2-pHluorin exocytosis in *mocha* cells. **p<0.0003 relative to control; n=18 for control and n=16 for *mocha*. Analysis of the secretion fold change shows that *mocha* cells have an ~75% reduction relative to control. (*D*) Analysis of the amplitude of exocytotic events monitored using NPY-pHluorin reveals that basal and regulated events of both control and *mocha* cells are comparable in size. The bars indicate mean values, and error bars the s.e.m.

The role of AP-3 in defining LDCV membrane protein composition has suggested that loss of the adaptor results in mixing of constitutive and regulated secretory pathways (Asensio et al., 2010). The resulting constitutive secretion (measured biochemically in the case of endogenous SgII (Asensio et al., 2010)) could thus result from either the spontaneous release of constitutive secretory vesicles which contain mis-sorted LDCV cargo but no dense core, or the dysregulated release of LDCVs. To distinguish between these possibilities, we have again taken advantage of TIRF microscopy. Release from constitutive vesicles without a dense core should yield events with reduced amplitude relative to controls, whereas dysregulated LDCV fusion should yield events with a size similar to controls. Analyzing individual exocytotic events, we observed that the basal as well as stimulated events observed in *mocha* cells have an amplitude similar to those observed in controls (Fig. 1*D*). The heightened basal secretion observed in *mocha* cells thus apparently results from dysregulated exocytosis of LDCVs rather than constitutive secretory vesicles without a dense core.

The increased basal exocytosis of NPY and VMAT2 from *mocha* chromaffin cells is consistent with earlier experiments using RNAi in pheochromocytoma PC12 cells (Asensio et al., 2010), but does the loss of AP-3 also dysregulate release from other neuroendocrine tissues? Pancreatic β cells store insulin in LDCVs morphologically and biochemically similar to chromaffin granules (Arvan and Halban, 2004; Suckale and Solimena, 2010). To assess the regulated release of insulin *in vivo*, we measured baseline serum insulin levels while fasting and stimulated levels 15-20 minutes after intraperitoneal injection of glucose (Fig. 2*A*). Before glucose administration, we observed a slight reduction in the serum insulin levels of *mocha* mice relative to controls, but this did not reach significance. After glucose administration, the control animals showed a clear increase in serum insulin but the *mocha* mice did not (Fig. 2*A*), suggesting a failure of regulated release.

To assess the consequences of dysregulated insulin release for carbohydrate metabolism, we also measured blood glucose. Surprisingly, we observed no clear difference in fasting blood

glucose levels between control and *mocha* mice (Fig. S2*A*). After glucose administration, *mocha* animals show an increase in blood glucose but less than controls (Fig. S2*A*), a surprising effect in light of the lower serum insulin levels which would have been expected to impair glucose tolerance (Fig. 2*A*). The effects of the *mocha* mutation on blood glucose levels thus do not correlate with the effects on insulin. However, blood glucose levels reflect the combined action of multiple circulating hormones, many of which may be affected by the loss of AP-3. Indeed, the dysregulated release of other peptide hormones may indirectly affect the release of insulin.

To examine insulin release independent of systemic effects, we isolated pancreatic islets and acutely incubated them in medium containing either low or high concentrations of glucose. Figure 2*B* shows that in contrast to the clear stimulation of insulin release by high concentrations of glucose in control islet cells, *mocha* cells exhibit increased basal release with little if any stimulation by high glucose. As opposed to the reduced content of SgII in *mocha* chromaffin cells, cellular insulin levels showed no difference between *mocha* and control islets (Fig. 2*C*), indicating that the change in basal secretion was not secondary to altered expression of the hormone. In the case of insulin, the *mocha* mutation thus dramatically and selectively impairs regulated secretion.
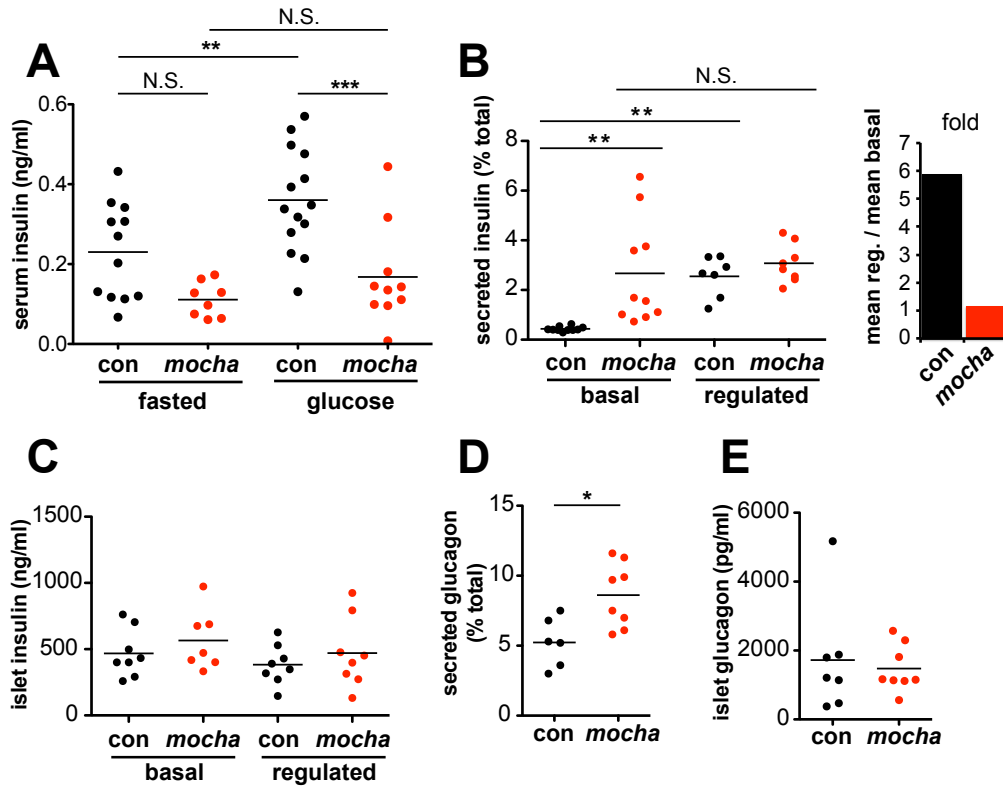
Figure 2. *mocha* mice show dysregulated secretion of insulin and glucagon
(*A*) Serum insulin levels were determined after an overnight fast (baseline) and 15-20 min after i.p. injection of glucose (2 mg/g body weight). In contrast to the controls, *mocha* insulin levels do not significantly increase after glucose injection. The data derive from two independent experiments; n=14 control and n=10 *mocha* mice. **$p<0.01$; ***$p<0.001$ by Newman-Keuls post-hoc test. Pancreatic islets were isolated acutely and bathed in either 2.8 mM (basal) or 28 mM (regulated) glucose for 1 h at 37°C. (*B*) *mocha* islets display markedly increased basal insulin secretion compared to controls. In contrast, control and *mocha* islets secrete comparable amounts of insulin in response to high glucose. For control islets, this represents an ~6-fold increase in secretion in response to glucose elevation. For *mocha* islets, insulin secretion is not significantly increased in response to glucose elevation. **$p<0.01$ by Dunnett's post-hoc test, n=7-10 (*C*) After collecting secreted insulin, the islets were pelleted and lysed by sonication to extract cellular insulin. Cellular insulin levels are similar between all groups. (*D*) Basal glucagon secretion measured in 28 mM glucose is significantly increased by the *mocha* mutation. (*E*) Cellular glucagon levels do not differ between *mocha* and control mice. *$p<0.02$, n=6-8 The bars represent mean values.

Since the effects of the *mocha* mutation on release of other peptide hormones may complicate the observations *in vivo*, we also examined glucagon, a peptide released from pancreatic a cells that opposes the action of insulin: glucagon raises blood glucose levels in response to starvation. Although we observed no effect of the *mocha* mutation on fasting serum

glucagon (Fig. S2*B*), baseline glucagon secretion was increased in acutely isolated islets (Fig. 2*D*). In addition, the glucagon content of *mocha* islet cells did not differ from controls (Fig. 2*E*), and the morphology of the islets *in situ* appears unchanged (Fig. S2*C*). Thus, *mocha* mice show dysregulated release of two peptide hormones with opposing actions, suggesting a global effect on peptide hormone release that makes it difficult to predict the net consequences for glucose homeostasis *in vivo*.
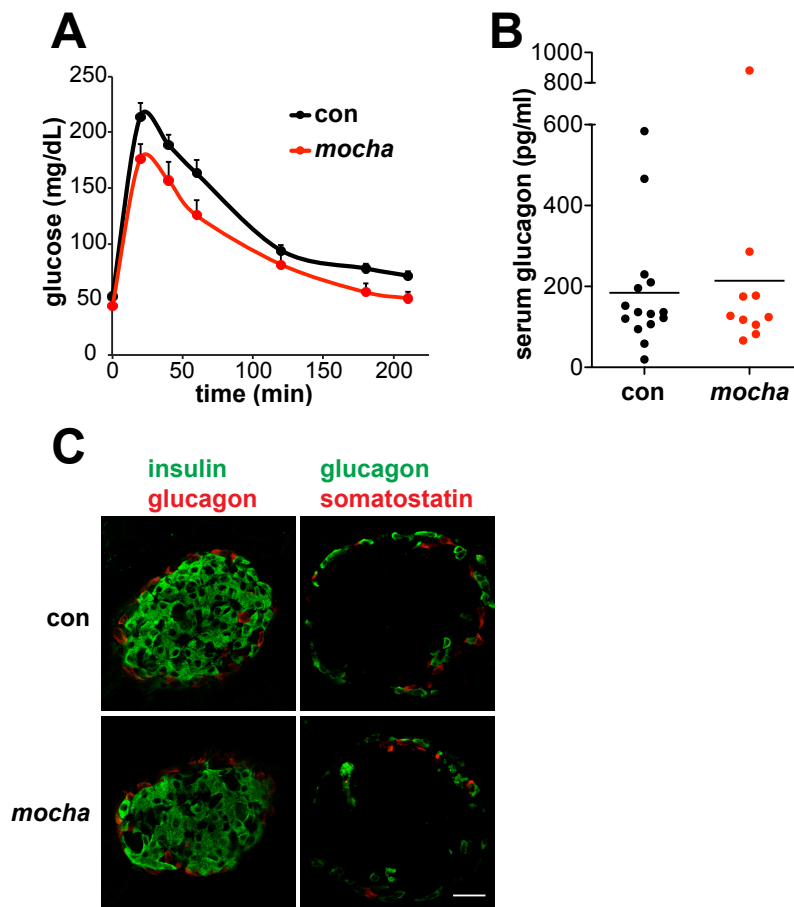
Figure S2. Glucose tolerance, serum glucagon and islet morphology in *mocha* mice
(*A*) Control and *mocha* mice were fasted overnight and challenged with glucose (2 mg/g body weight) delivered i.p. *mocha* mice show slightly improved glucose tolerance relative to controls. $p < 0.02$ for the area under the glucose-time curve; n=8 control and n=5 *mocha* mice. (*B*) Control and *mocha* mice display comparable serum glucagon levels after an overnight fast. n=15 control and n=10 *mocha* mice (*C*) *mocha* mice exhibit normal pancreatic islet morphology as determined by double staining for insulin/glucagon and glucagon/somatostatin. Scale bar indicates 30 μm.

117

The heterotetrameric AP-3 complex is known to exist in two isoforms, one expressed by all tissues, and another expressed more specifically by neurons and endocrine tissue including the adrenal gland and pancreatic islets (Grabner et al., 2006; Newell-Litwa et al., 2007; Suckow et al., 2010). In metazoan cells, the ubiquitous isoform contributes to trafficking from early endosomes to the lysosome through a pathway that does not involve multivesicular bodies (Peden et al., 2004; Dell Angelica, 2009). In contrast, the neural isoform has been implicated in the formation of synaptic vesicles from an endosomal intermediate (Faundez et al., 1998; Seong et al., 2005), suggesting that this isoform may also contribute to the formation of LDCVs. To test this possibility, we used *pearl* mice lacking the ubiquitous isoform of the β3 subunit (β3A) and β3B knockouts lacking the neural isoform of β3. Since the δ subunit of AP-3 exists as only a single isoform, and the loss of one subunit usually destabilizes the complex (Kantheti et al., 1998; Peden et al., 2002), we first stained cells in culture for δ to assess the effect of the mutations on the complex as a whole. We were surprised to observe no effect of losing either β3 isoform on the levels of immunoreactive δ in chromaffin cells (Fig. 3*A*), particularly considering the abundance of the ubiquitous β3A subunit in most tissues. However, we did observe reduced expression of δ by β3A-deficient, non-chromaffin cells in the culture (Fig. 3*B*), presumably because they do not express the neural isoform and therefore cannot exhibit redundancy. Consistent with the relative abundance of adrenal cortical cells (Bielohuby et al., 2007) and of the ubiquitous AP-3 isoform, western analysis of adrenal homogenates showed low levels of AP-3 δ in β3A-deficient *pearl* animals (Fig. 3*C*) but normal levels in β3B knock-outs (Fig. 3*D*).

To determine whether the loss of β3A or β3B influences the formation of LDCVs, we then examined the effects on SgII. We were surprised to observe that in contrast to *mocha* cells which showed the reduction previously reported (Asensio et al., 2010), both β3 mutants had normal levels of SgII by immunofluorescence (Fig. 3*A*). By western analysis of adrenal extracts, both β3A-deficient *pearl* and β3B knockouts also contained normal levels of immunoreactive SgII (Fig. 3 *C* and *D*). However, loss of both isoforms in the adrenal gland of double mutant

mice showed a reduction in SgII comparable to that observed in *mocha* mice (Fig. 3*E*). With regard to the formation of LDCVs, the two isoforms thus exhibit redundancy.
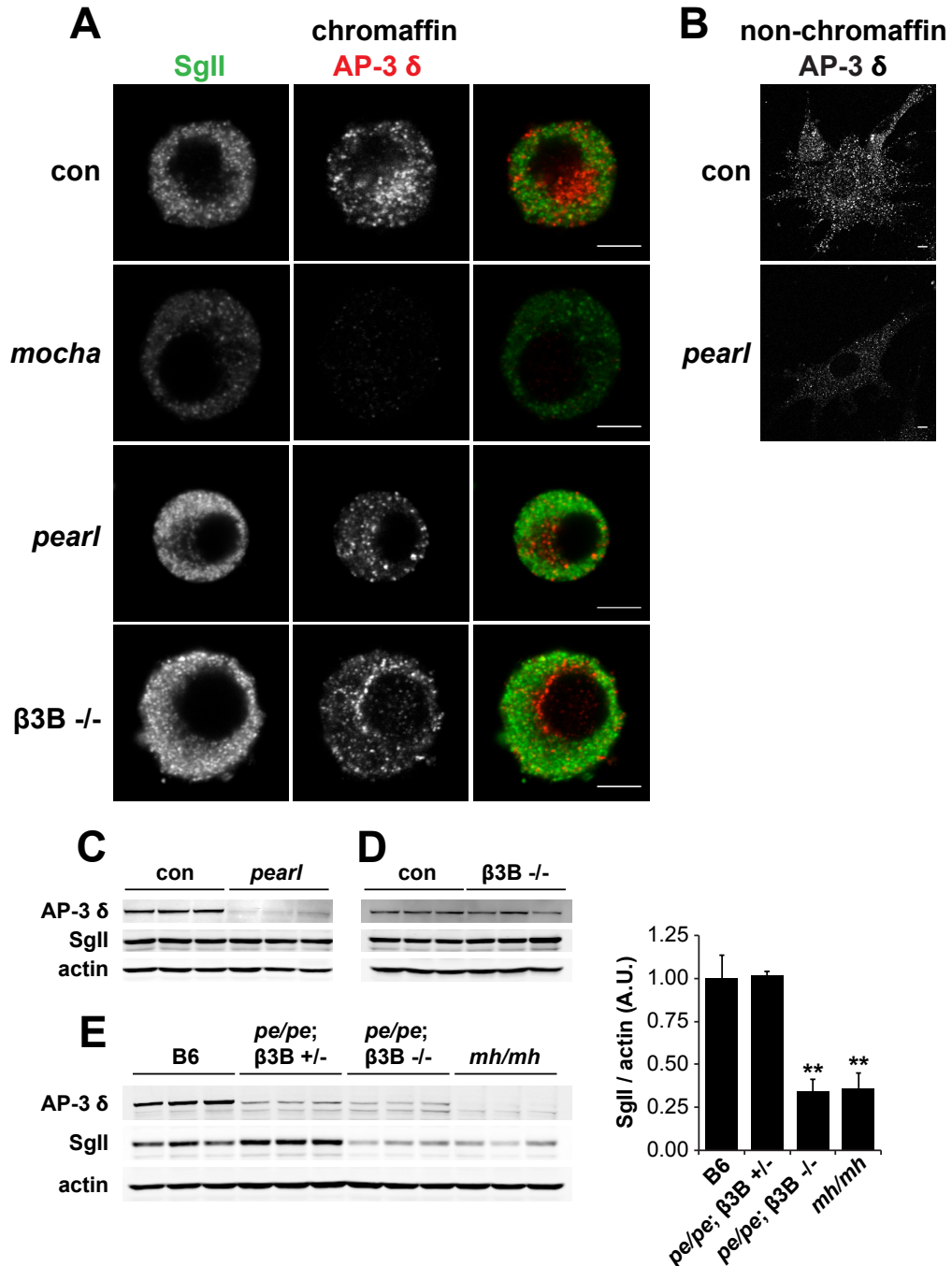
Figure 3. Concomitant loss of both β3A and β3B is required to reduce adrenal SgII
(*A*) Effect of individual AP-3 subunit mutations on SgII and AP-3 δ levels by immunofluorescence. Adrenal chromaffin cells from *mocha* (δ), *pearl* (β3A), β3B -/-, and control mice were stained with a rabbit polyclonal antibody to SgII and a mouse monoclonal antibody to AP-3 δ, followed by an anti-rabbit antibody conjugated to Alexa Fluor 488 and an anti-mouse antibody conjugated to Alexa Fluor 594.

Representative confocal micrographs show the expected reduction in SgII and absence of AP-3 δ staining in *mocha* chromaffin cells, but unchanged SgII and AP-3 δ in both *pearl* and β3B -/- cells. (*B*) Non-chromaffin, fibroblast-like *pearl* cells present in the culture show a clear reduction in AP-3 δ. Scale bars indicate 5 μm. (*C*) The adrenal glands of *pearl* mice show a clear reduction in overall AP-3 levels, but unchanged SgII. (*D*) Adrenal glands of β3B -/- mice show no change in overall AP-3 or SgII levels. (*E*) Adrenal glands of double mutant *pe/pe*; β3B -/- mice show a clear reduction in SgII levels relative to age-matched C57BL/6 controls and *pe/pe*; β3B +/- controls. *mocha* adrenals show a reduction in SgII similar to that in *pe/pe*; β3B -/- mice. **$p<0.001$ relative to control by Dunnett's post-hoc test; n = 3. The data show mean values, and error bars indicate s.e.m.

The reduced expression of SgII in mice lacking AP-3 might reflect increased basal secretion or an entirely distinct process. LDCV contents have indeed been shown to undergo transcriptional regulation through a variety of mechanisms (Ohneda et al., 2000; Suckale and Solimena, 2010). We therefore measured adrenal SgII and chromogranin A (CgA) transcripts from control and *mocha* adrenals by quantitative reverse transcription (qRT)-PCR. Both SgII and CgA mRNA were substantially reduced (by ~50%) in *mocha* mice, although not to the same extent as the protein (Asensio et al., 2010) (Fig. 4*A*). PC12 cells showed a similar reduction in SgII mRNA after AP-3 RNAi (Fig. 4*B*).

Since AP-3 influences trafficking within the endolysosomal pathway, loss of the adaptor may also influence SgII levels through increased degradation in the lysosome. To test this possibility, we inhibited lysosomal proteases after AP-3 knockdown in PC12 cells, but did not observe any increase in the levels of SgII (Fig. 4*C*). On the other hand, the level of lysosomal hydrolase precursor procathepsin D dramatically increased in response to the inhibition of lysosomal degradation, indicating the effectiveness of the inhibitors (Fig. 4*C*). The reduction in cellular SgII observed with loss of AP-3 thus reflects reduced expression as well as increased constitutive release, but not increased degradation.
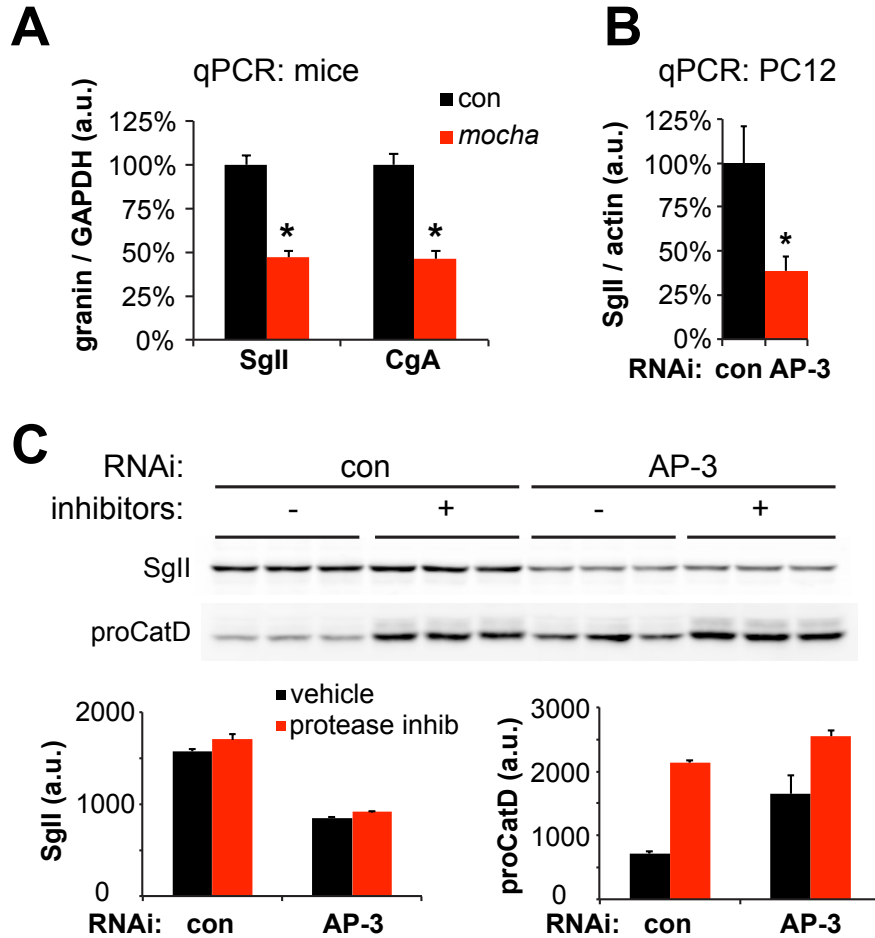
Figure 4. Loss of AP-3 reduces granin mRNA but does not increase its degradation
(*A*) Quantitative RT-PCR (qPCR) analysis of adrenal gland transcripts from *mocha* mice shows an ~50% reduction in SgII and CgA expression relative to the adrenals of littermate controls. *, $p<1\times10^{-4}$ (n=6-7 adrenals per genotype). (*B*) qPCR analysis of PC12 cells transfected with AP-3 δ siRNA shows an ~60% reduction in SgII expression relative to cells transfected with control siRNA. *, $p<0.02$ (n=5-6 transfections). (*C*) Incubation of PC12 cells with lysosomal protease inhibitors for ~24 h has no effect on cellular SgII levels in cells transfected with either AP-3 δ or control siRNA. In contrast, the protease inhibitors markedly elevate the levels of the lysosomal hydrolase precursor procathepsin D. The data show mean values, and error bars indicate s.e.m.

AP-3 resembles AP-1 in terms of sequence, the ability to recognize similar trafficking motifs and subcellular location at endosomes and the Golgi apparatus (Janvier et al., 2003; Theos et al., 2005; Mattera et al., 2011). In addition, AP-1 associates with immature LDCVs and promotes their maturation through the clathrin-dependent removal of proteins destined for other organelles (Dittie et al., 1996; Klumperman et al., 1998). To determine whether silencing of AP-

1 recapitulates the phenotype of AP-3 knockdown, we targeted AP-1 β-adaptin since this is the only mammalian AP-1 subunit without a known paralog and hence with reduced potential for redundancy. Cotransfecting AP-1 siRNA with HA-tagged AP-1 β cDNA into PC12 cells, quantitative western analysis showed knockdown efficiency >95% (Fig. 5*A*). However, the loss of AP-1 had no effect on regulated secretion of endogenous SgII (Fig. 5*B*). As expected, AP-3 RNAi significantly impaired the stimulation of release, but AP-1 knockdown robustly potentiated the effect of AP-3 RNAi on regulated secretion (Fig. 5*B*). Thus, AP-1 is not essential for regulated release from neuroendocrine cells, but becomes important in the absence of AP-3, and therefore appears to promote LDCV formation through a distinct mechanism.
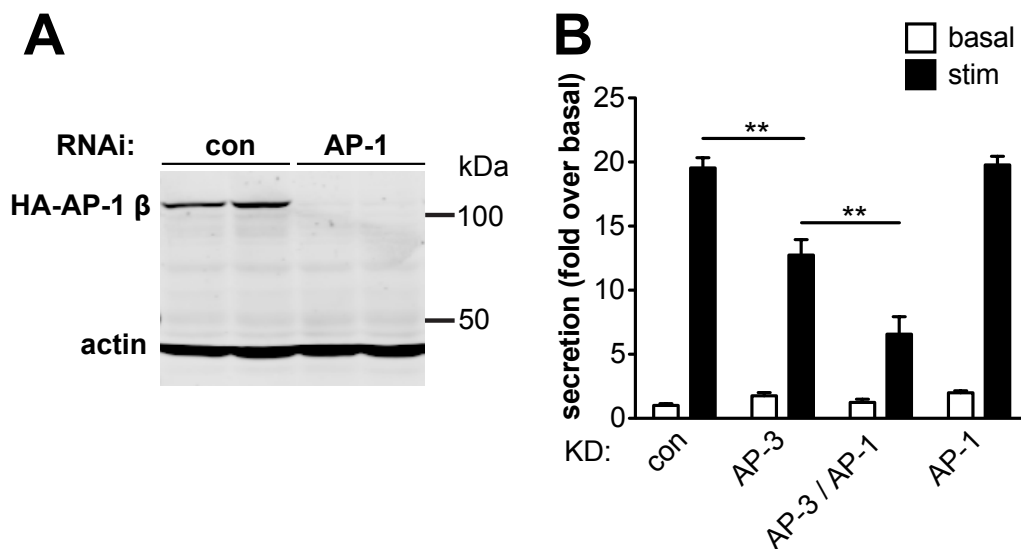
Figure 5. AP-1 knockdown potentiates the effect of AP-3 knockdown on regulated secretion
(*A*) Cells were transiently transfected with an HA-AP-1 β construct, plus control or AP-1 β siRNA. Knockdown was assessed by quantitative fluorescent immunoblot for HA, with actin serving as a loading control. (*B*) PC12 cells were transiently transfected with control, AP-1 β, AP-3 δ or both siRNAs, washed, and incubated for 30 min in Tyrode's solution containing 2.5 mM (basal) or 50 mM (stimulated) K^+. Secreted SgII was measured by quantitative fluorescent immunoblotting and normalized to basal secretion in the control. AP-1 β RNAi alone does not affect the depolarization-induced secretion of SgII. In contrast, AP-3 δ RNAi reduces regulated secretion, and combined AP-1 β / AP-3 δ RNAi potentiates the reduction in regulated secretion. *, $P < 0.01$ (Newman-Keuls post-hoc test; n = 4 transfections). The data show mean values, and error bars indicate s.e.m.

Discussion

The results show that *mocha* mice have a major defect in the regulated secretion of peptide hormones. Although *mocha* animals exhibit seizures, hyperactivity, poor fertility and premature lethality (Lane and Deol, 1974; Noebels and Sidman, 1989), this has generally been attributed to a role for AP-3 in the endolysosomal pathway and the formation of lysosome-related organelles (LROs) including synaptic vesicles (Faundez et al., 1998; Dell Angelica, 2009). However, the dysregulated exocytosis of adrenal chromaffin granules and both insulin- and glucagon-containing granules from pancreatic islet cells now supports a role for AP-3 in the biosynthetic pathway and specifically, LDCV formation. Indeed, previous work in *mocha* mice has shown enlarged chromaffin granules by amperometry and electron microscopy (Grabner et al., 2006). The exact phenotype appears to vary among different neuroendocrine tissues, with increased basal secretion in both adrenal chromaffin and pancreatic islet cells but a virtually complete loss of stimulation only in β cells. In addition, PC12 cells lacking AP-3 show both increased constitutive and reduced stimulated release (Asensio et al., 2010). Despite these differences, the impairment is substantial and the involvement of multiple tissues suggests effects on the release of neural peptides and growth factors as well as peptide hormones. The results thus indicate a major contribution of this cellular defect to the severe physiological and behavioral phenotype of *mocha* mice as well as an important role for AP-3 in the biosynthetic pathway.

In previous work, we found that the loss of AP-3 reduces the amount of SgII stored in PC12 cells and the adrenal gland (Asensio et al., 2010). This reflects the increased baseline exocytosis of LDCVs, but we now find down-regulation of multiple granin mRNAs as well, indicating unanticipated transcriptional effects of AP-3 deficiency. Although AP-3 has a role in the endolysosomal pathway, we also find that the reduced granin content does not reflect increased degradation. The role for AP-3 in regulated secretion thus appears distinct from its well-established role in trafficking to the lysosome.

The analysis of isoform-specific knockouts indicates redundancy between the ubiquitous and neural isoforms of AP-3 with regard to LDCV formation. Using SgII as a reporter for a defect in the regulated secretory pathway, we find that only the loss of both β3A and β3B causes a reduction in adrenal SgII levels. However, the loss of these isoform-specific subunits has opposite effects on other trafficking phenomena. In neurons, loss of β3B mimics the effect of the full *mocha* mutation, with reduced presynaptic expression of proteins such as the zinc transporter ZnT3 and the chloride carrier ClC-3 (Kantheti et al., 1998; Salazar et al., 2004; Seong et al., 2005). Loss of β3A, on the other hand, increases presynaptic expression of these proteins (Seong et al., 2005). The redundancy of neural and ubiquitous AP-3 forms in LDCV formation thus contrasts with the opposite roles of the two isoforms in delivery of specific proteins to the nerve terminal.

Despite the complete loss of AP-3 and increased basal secretion, adrenal chromaffin cells from *mocha* mice still show some stimulated release, raising the possibility that another system also contributes to LDCV formation. Investigating the role of related adaptor AP-1, we find that loss of AP-1 alone has no effect on regulated secretion by PC12 cells. However, the loss of AP-1 considerably exacerbates the phenotype of AP-3 RNAi, indicating an additive and therefore distinct role for the two adaptors. Interestingly, previous work has implicated AP-1 in the formation of secretory granules by other cell types, such as glue granules produced by the *Drosophila* exocrine salivary gland, and the Weibel-Palade bodies produced by mammalian endothelial cells (Lui-Roberts et al., 2005; Burgess et al., 2011). The results presented here thus suggest a difference between the mechanisms that generate regulated secretory vesicles, with LDCV production by endocrine cells primarily dependent on AP-3 and secretory granule production by exocrine and other tissues more dependent on AP-1. Nonetheless, the non-redundant role of the two adaptors in neuroendocrine cells indicates that they both contribute to regulated secretion, but through different mechanisms. Considering the known role of AP-1 in

LDCV maturation, it is possible that the removal of proteins destined for other organelles

becomes more important after the loss of AP-3.

Materials and Methods

Antibodies

The rabbit SgII antibody was obtained from Meridian Life Science, the mouse actin monoclonal antibody from Millipore, the mouse delta SA4 monoclonal antibody from the Developmental Studies Hybridoma Bank, the goat cathepsin D antibody from Santa Cruz, and the mouse HA.11 monoclonal antibody from Covance.

siRNAs

Silencer Select rat Ap3d1 (antisense, 5'-UUCUUGGUCAUGAUCCAUGTG-3'), Ap1b1 (antisense, 5'-AGCGAAAUCUGUCAUGACCTG-3') and corresponding non-targeting control siRNAs were from Ambion.

Molecular biology

The sequences of NPY-pHluorin (a generous gift of R. Holz, U. Michigan) and VMAT2-pHluorin were amplified by PCR to add 5' BamHI and 3' EcoRI sites, then subcloned into the FUGW lentiviral expression vector, replacing the EGFP coding sequence. AP-1 β adaptin was amplified by PCR from PC12 cDNA with 5' NotI and 3' SalI sites, then ligated along with an N-terminal HA epitope tag into a CMV-driven expression vector derived from pEGFP-C3 (again replacing EGFP). All constructs were verified by sequencing.

Cell culture and lentivirus production

PC12 cells were maintained in DMEH-21 medium supplemented with 10% horse serum (HS) and 5% cosmic calf serum (CCS; HyClone) in 5% CO_2 at 37°C. siRNA transfection was performed using Lipofectamine 2000 (Invitrogen) according to the manufacturer's instructions. HEK293T cells were maintained in DMEH-21 medium with 10% fetal bovine serum (FBS) in 5% CO_2 at 37°C. Lentivirus was produced by transfecting HEK293T cells with FUGW, psPAX2 and pVSVG and Fugene HD (Roche) according to the manufacturer's instructions (Lois et al., 2002).

Chromaffin cell isolation and culture

Mouse adrenal chromaffin cells were isolated and cultured as previously described (Kolski-Andreaco et al., 2007). Briefly, adrenal glands were dissected and placed in cold Ca^{++}-, Mg^{++}-free (CMF) Hank's balanced salt solution (HBSS). The surrounding fat and cortex were removed and the medullae transferred to tubes containing 300 U/ml Collagenase I (Worthington) in CMF-HBSS. Medullae were dissociated by shaking for 40 min at 37°C. Collagenase solution was then replaced by CMF-HBSS containing 200 µg/ml DNAse I (Sigma) and 1% heat-inactivated FBS (Gibco), the tissue triturated first with a P200 pipette tip, then with a 23 gauge needle. The cells were pelleted at 300g for 8 min at room temperature and resuspended in pre-warmed culture medium. Cells were maintained in DMEH-21 medium supplemented with 10% FBS and antibiotics. For lentiviral transduction, freshly isolated chromaffin cells were plated in viral supernatant, and fresh medium was added the following morning.

Total internal reflectance fluorescence (TIRF) microscopy

For TIRF microscopy, control or *mocha* chromaffin cells were plated onto glass chambers coated with poly-L-lysine, immediately transduced with lentivirus encoding either NPY- or VMAT2-pHluorin and imaged live 4-7 days later. Images were typically collected for 40-50 ms at 10 Hz and room temperature using an inverted TIRF microscope (TE2000E; Nikon) with 100x Plan Apo 1.49 NA oil objective, a 1.5x tube lens and an electron-multiplying charge-coupled device camera (QuantEM; Photometrics). Basal exocytosis was measured in Tyrode's solution containing (in mM, 119 NaCl, 25 HEPES-NaOH, pH 7.4, 30 glucose, 2.5 KCl, 2 $CaCl_2$, 2 $MgCl_2$) over 90 s, and release stimulated for 60 s in Tyrode's containing 5 μM 1,1-Dimethyl-4-phenylpiperazinium (DMPP; Sigma). Individual exocytotic events were quantified manually using NIS-Elements software (Nikon). The amplitude of individual exocytotic events was measured by placing 2×2 pixel ROIs manually over the center of events, and the mean ROI intensity prior to an event subtracted from the maximum event intensity.

Glucose tolerance tests and serum insulin measurements

Glucose tolerance was assessed and serum insulin levels measured using 5-15 week-old *mocha* mice and age-matched controls. Mice were fasted overnight (~16 h), weighed the following morning, and blood samples collected for baseline glucose and insulin levels. Mice were then injected intraperitoneally with glucose at 2 mg/g body weight and blood samples collected from the tail vein at the time points indicated. Blood glucose levels were measured using the FreeStyle glucometer (Abbott). To measure serum insulin, the blood was allowed to clot, sedimented at 2000g and 4° C for 20 min, and insulin levels determined using the Ultra Sensitive Mouse Insulin ELISA kit (Crystal Chem).

Pancreatic islet isolation and insulin secretion

Islets were isolated as previously described from 9-16 week-old *mocha* mice and age-matched controls (Szot et al., 2007). Briefly, islets were purified on a Ficoll gradient and allowed to recover for 1 h at 37°C. Five islets were aliquoted into tubes containing HEPES-buffered RPMI medium supplemented with either 2.8 mM glucose (basal) or 28 mM glucose (regulated) and incubated for 1 h at 37°C. The islets were then sedimented and the supernatants collected to measure insulin secretion. The pellets were resuspended and sonicated in 2 mM acetic acid, 0.25% RIA-grade BSA to extract intracellular insulin. Finally, the nuclei were lysed by additional sonication in 67 mM ammonium hydroxide, 0.2% Triton X-100. Secreted and cellular insulin were quantified by ELISA (Mercodia) according to the manufacturer's instructions, and islet DNA quantified to confirm that the amount of islets per tube was similar between conditions. Glucagon was measured by ELISA (R&D Systems).

Immunofluorescence

Chromaffin cells were fixed by adding an equal volume of 4% formaldehyde in CMF-PBS to the culture medium and incubating for 20 min at room temperature. Cells were blocked and permeabilized in CMF-PBS containing 2% BSA, 1% fish skin gelatin and 0.02% saponin. Primary antibodies were diluted in blocking solution at 1:500 (SgII) and 1:100 (delta SA4). The secondary goat anti-rabbit antibodies conjugated to Alexa 488 and goat anti-mouse antibodies conjugated to Alexa 594 (Molecular Probes) were diluted in blocking solution at 1:1000. Images were acquired using a Zeiss LSM 510 confocal microscope and 100x oil objective.

Adrenal gland granin content

pearl and *mocha* mice were obtained from the Jackson Laboratory, and *mocha* animals were backcrossed to C57BL/6 to remove *grizzled* and *Pde6b*[rd1] alleles. *Ap3b2* KO mice were obtained from V, Faundez (Emory) and S. Voglmaier (UCSF). Double mutant *pe/pe*; *Ap3b2* -/- mice were

generated by crossing *pe/pe*; *Ap3b2* +/- males to *pe/+*; *Ap3b2* +/- females. Adrenal glands from 3-6 week-old mice were homogenized in 150 mM NaCl, 50 mM Tris-HCl, pH 8.0, 1% NP-40, 0.5% sodium deoxycholate, and Complete protease inhibitors (Roche) with 1 mM EGTA and 1 mM PMSF. After sedimentation at 14,000 g to remove nuclei and cell debris, 20-40 μg protein was separated by electrophoresis through polyacrylamide, transferred to nitrocellulose, and the membranes immunoblotted for AP-3δ and SgII, with actin as loading control and the appropriate secondary antibodies conjugated to IRDye800 (Rockland Immunochemicals). The immunoreactivity was quantified by imaging with an Odyssey system (LI-COR Biosciences) and ImageJ (National Institutes of Health), and the signals normalized to actin. For western analysis of the SgII secreted from chromaffin cells, Tyrode's solution was collected, sedimented at 300*g* for 3 min at 4°C, and the supernatant mixed with SDS-PAGE sample buffer before electrophoresis through polyacrylamide. Chromaffin cells were directly lysed by the addition of sample buffer. In this case, SgII and actin were detected using ECL plus (GE Healthcare).

qPCR

Total RNA was isolated from PC12 cells and mouse adrenal glands using TRIzol reagent (Invitrogen) according to the manufacturer's instructions. To improve the yield of adrenal RNA, ultrapure glycogen (Invitrogen) was added to the TRIzol as carrier. In addition, adrenal RNA was treated with RNAse-free DNAse I (NEB) to remove contaminating genomic DNA. cDNA was synthesized using oligo(dT) or gene-specific primers and a Transcriptor First Strand cDNA Synthesis kit (Roche). qPCR was performed with SYBR Green (Applied Biosystems) on a Stratagene Mx4000 machine. The following primers were used: rat SgII fwd: 5'-ACAATATAAGACAGAGGAAAATTTT-3', rev: 5'-TGGATAAGAAGCAGAACTG-3'; rat β-actin fwd: 5'-CCGTGAAAAGATGACCCAGATC-3', rev: 5'-CAGGGACAACACAGCCTG-3'; mouse CgA fwd: 5'-CCAACCGCAGAGCAGAG-3', rev: 5'-AGCTGGTGGGCCACCTT-3'; mouse SgII fwd: 5'-AAGTGCTGGAGTACCTCAACC-3',

rev: 5'-TTACATGTTTTCCATGGCCCG-3'; mouse GAPDH fwd:

5'-ATGGTGAAGGTCGGTGTGAAC-3', rev: 5'-TCCACTTTGCCACTGCAAATG-3'.

Lysosomal inhibition

Two days after the second siRNA transfection, PC12 cells were incubated for ~24 h in complete medium supplemented with vehicle or a cocktail of lysosomal protease inhibitors (Sigma) including (in μM) 10 antipain, 10 leupeptin and 5 pepstatin A. Cells were washed on ice with cold PBS and lysed by the addition of 50 mM Tris-HCl, pH 8.0, 150 mM NaCl, 1% Triton X-100, and Complete protease inhibitors (Roche) plus 10 mM EDTA and 1 mM PMSF. Samples were analyzed by quantitative fluorescent immunoblotting.

Secretion assays

Cells were transfected with siRNA (100 nM) on days 1 and 3 after plating, washed 2 days later and incubated in Tyrode's solution containing 2.5 mM K^+ (basal) or 50 mM K^+ (stimulated) for 30 min at 37°C. The supernatants were collected, cell lysates prepared as described above, and the samples analyzed by quantitative fluorescent immunoblotting, with secreted SgII normalized to total cellular protein (Bradford assay).

Statistical analysis

Statistical analysis was performed using the Student's two-tailed t-test unless otherwise indicated.

All procedures involving animals were approved by the UCSF Institutional Animal Care and Use Committee.

Acknowledgements

References

Anantharam, A., Onoa, B., Edwards, R.H., Holz, R.W., and Axelrod, D. (2010). Localized topological changes of the plasma membrane upon exocytosis visualized by polarized TIRFM. J Cell Biol *188*, 415–428.

Arvan, P., and Halban, P.A. (2004). Sorting ourselves out: seeking consensus on trafficking in the beta-cell. Traffic *5*, 53–61.

Asensio, C.S., Sirkis, D.W., and Edwards, R.H. (2010). RNAi screen identifies a role for adaptor protein AP-3 in sorting to the regulated secretory pathway. J Cell Biol *191*, 1173–1187.

Bielohuby, M., Herbach, N., Wanke, R., Maser-Gluth, C., Beuschlein, F., Wolf, E., and Hoeflich, A. (2007). Growth analysis of the mouse adrenal gland from weaning to adulthood: time- and gender-dependent alterations of cell size and number in the cortical compartment. Am. J. Physiol. Endocrinol. Metab. *293*, E139–E146.

Burgess, J., Jauregui, M., Tan, J., Rollins, J., Lallet, S., Leventis, P.A., Boulianne, G.L., Chang, H.C., Le Borgne, R., Krämer, H., et al. (2011). AP-1 and clathrin are essential for secretory granule biogenesis in Drosophila. Mol Biol Cell *22*, 2094–2105.

Chen, Z.-Y., Ieraci, A., Teng, H., Dall, H., Meng, C.-X., Herrera, D.G., Nykjaer, A., Hempstead, B.L., and Lee, F.S. (2005). Sortilin controls intracellular sorting of brain-derived neurotrophic factor to the regulated secretory pathway. J Neurosci *25*, 6156–6166.

Chung, S.H., Joberty, G., Gelino, E.A., Macara, I.G., and Holz, R.W. (1999). Comparison of the effects on secretion in chromaffin and PC12 cells of Rab3 family members and mutants. Evidence that inhibitory effects are independent of direct interaction with Rabphilin3. J Biol Chem *274*, 18113–18120.

Cool, D.R., Normant, E., Shen, F., Chen, H.C., Pannell, L., Zhang, Y., and Loh, Y.P. (1997). Carboxypeptidase E is a regulated secretory pathway sorting receptor: genetic obliteration leads to endocrine disorders in Cpe(fat) mice. Cell *88*, 73–83.

Cowles, C.R., Odorizzi, G., Payne, G.S., and Emr, S.D. (1997). The AP-3 adaptor complex is essential for cargo-selective transport to the yeast vacuole. Cell *91*, 109–118.

Dell Angelica, E.C. (2009). AP-3-dependent trafficking and disease: the first decade. Curr Opin Cell Biol *21*, 552–559.

Dittie, A.S., Hajibagheri, N., and Tooze, S.A. (1996). The AP-1 adaptor complex binds to immature secretory granules from PC12 cells, and is regulated by ADP-ribosylation factor. J Cell Biol *132*, 523–536.

Faundez, V., Horng, J.T., and Kelly, R.B. (1998). A function for the AP3 coat complex in synaptic vesicle formation from endosomes. Cell *93*, 423–432.

Grabner, C.P., Price, S.D., Lysakowski, A., Cahill, A.L., and Fox, A.P. (2006). Regulation of large dense-core vesicle volume and neurotransmitter content mediated by adaptor protein 3. Proc Natl Acad Sci USA *103*, 10035–10040.

Janvier, K., Kato, Y., Boehm, M., Rose, J.R., Martina, J.A., Kim, B.-Y., Venkatesan, S., and Bonifacino, J.S. (2003). Recognition of dileucine-based sorting signals from HIV-1 Nef and LIMP-II by the AP-1 gamma-sigma1 and AP-3 delta-sigma3 hemicomplexes. J Cell Biol *163*, 1281–1290.

Kantheti, P., Qiao, X., Diaz, M.E., Peden, A.A., Meyer, G.E., Carskadon, S.L., Kapfhamer, D., Sufalko, D., Robinson, M.S., Noebels, J.L., et al. (1998). Mutation in AP-3 delta in the mocha mouse links endosomal

transport to storage deficiency in platelets, melanosomes, and synaptic vesicles. Neuron *21*, 111–122.

Kim, T., Tao-Cheng, J.H., Eiden, L.E., and Loh, Y.P. (2001). Chromogranin A, an "on/off" switch controlling dense-core secretory granule biogenesis. Cell *106*, 499–509.

Klumperman, J., Kuliawat, R., Griffith, J.M., Geuze, H.J., and Arvan, P. (1998). Mannose 6-phosphate receptors are sorted from immature secretory granules via adaptor protein AP-1, clathrin, and syntaxin 6-positive vesicles. J Cell Biol *141*, 359–371.

Kolski-Andreaco, A., Cai, H., Currle, D.S., Chandy, K.G., and Chow, R.H. (2007). Mouse adrenal chromaffin cell isolation. J Vis Exp 129.

Kögel, T., Rudolf, R., Hodneland, E., Hellwig, A., Kuznetsov, S.A., Seiler, F., Söllner, T.H., Barroso, J., and Gerdes, H.-H. (2010). Distinct roles of myosin Va in membrane remodeling and exocytosis of secretory granules. Traffic *11*, 637–650.

Krantz, D.E., Waites, C.L., Oorschot, V., Liu, Y., Wilson, R.I., Tan, P.K., Klumperman, J., and Edwards, R.H. (2000). A phosphorylation site regulates sorting of the vesicular acetylcholine transporter to dense core vesicles. J Cell Biol *149*, 379–396.

Lane, P.W., and Deol, M.S. (1974). Mocha, a new coat color and behavior mutation on chromosome 10 of the mouse. J Hered *65*, 362–364.

Li, H., Waites, C.L., Staal, R.G., Dobryy, Y., Park, J., Sulzer, D.L., and Edwards, R.H. (2005). Sorting of vesicular monoamine transporter 2 to the regulated secretory pathway confers the somatodendritic exocytosis of monoamines. Neuron *48*, 619–633.

Liu, Y., Schweitzer, E.S., Nirenberg, M.J., Pickel, V.M., Evans, C.J., and Edwards, R.H. (1994). Preferential localization of a vesicular monoamine transporter to dense core vesicles in PC12 cells. J Cell Biol *127*, 1419–1433.

Lois, C., Hong, E.J., Pease, S., Brown, E.J., and Baltimore, D. (2002). Germline transmission and tissue-specific expression of transgenes delivered by lentiviral vectors. Science *295*, 868–872.

Lui-Roberts, W.W.Y., Collinson, L.M., Hewlett, L.J., Michaux, G., and Cutler, D.F. (2005). An AP-1/clathrin coat plays a novel and essential role in forming the Weibel-Palade bodies of endothelial cells. J Cell Biol *170*, 627–636.

Mattera, R., Boehm, M., Chaudhuri, R., Prabhu, Y., and Bonifacino, J.S. (2011). Conservation and diversification of dileucine signal recognition by adaptor protein (AP) complex variants. J Biol Chem *286*, 2022–2030.

Miesenböck, G., De Angelis, D.A., and Rothman, J.E. (1998). Visualizing secretion and synaptic transmission with pH-sensitive green fluorescent proteins. Nature *394*, 192–195.

Morvan, J., and Tooze, S.A. (2008). Discovery and progress in our understanding of the regulated secretory pathway in neuroendocrine cells. Histochem Cell Biol *129*, 243–252.

Newell-Litwa, K., Seong, E., Burmeister, M., and Faundez, V. (2007). Neuronal and non-neuronal functions of the AP-3 sorting machinery. J Cell Sci *120*, 531–541.

Nickerson, D.P., Brett, C.L., and Merz, A.J. (2009). Vps-C complexes: gatekeepers of endolysosomal traffic. Curr Opin Cell Biol *21*, 543–551.

Noebels, J.L., and Sidman, R.L. (1989). Persistent hypersynchronization of neocortical neurons in the

mocha mutant of mouse. J Neurogenet *6*, 53–56.

Ohneda, K., Ee, H., and German, M. (2000). Regulation of insulin gene transcription. Semin. Cell Dev. Biol. *11*, 227–233.

Onoa, B., Li, H., Gagnon-Bartsch, J.A., Elias, L.A.B., and Edwards, R.H. (2010). Vesicular monoamine and glutamate transporters select distinct synaptic vesicle recycling pathways. J Neurosci *30*, 7917–7927.

Orci, L., Ravazzola, M., Amherdt, M., Perrelet, A., Powell, S.K., Quinn, D.L., and Moore, H.P. (1987). The trans-most cisternae of the Golgi complex: a compartment for sorting of secretory and plasma membrane proteins. Cell *51*, 1039–1051.

Peden, A.A., Oorschot, V., Hesser, B.A., Austin, C.D., Scheller, R.H., and Klumperman, J. (2004). Localization of the AP-3 adaptor complex defines a novel endosomal exit site for lysosomal membrane proteins. J Cell Biol *164*, 1065–1076.

Peden, A.A., Rudge, R.E., Lui, W.W.Y., and Robinson, M.S. (2002). Assembly and function of AP-3 complexes in cells expressing mutant subunits. J Cell Biol *156*, 327–336.

Salazar, G., Love, R., Styers, M.L., Werner, E., Peden, A., Rodriguez, S., Gearing, M., Wainer, B.H., and Faundez, V. (2004). AP-3-dependent mechanisms control the targeting of a chloride channel (ClC-3) in neuronal and non-neuronal cells. J Biol Chem *279*, 25430–25439.

Sankaranarayanan, S., De Angelis, D., Rothman, J.E., and Ryan, T.A. (2000). The use of pHluorins for optical measurements of presynaptic activity. Biophys J *79*, 2199–2208.

Seong, E., Wainer, B.H., Hughes, E.D., Saunders, T.L., Burmeister, M., and Faundez, V. (2005). Genetic analysis of the neuronal and ubiquitous AP-3 adaptor complexes reveals divergent functions in brain. Mol Biol Cell *16*, 128–140.

Sossin, W.S., Fisher, J.M., and Scheller, R.H. (1990). Sorting within the regulated secretory pathway occurs in the trans-Golgi network. J Cell Biol *110*, 1–12.

Suckale, J., and Solimena, M. (2010). The insulin secretory granule as a signaling hub. Trends Endocrinol. Metab. *21*, 599–609.

Suckow, A.T., Craige, B., Faundez, V., Cain, W.J., and Chessler, S.D. (2010). An AP-3-dependent mechanism drives synaptic-like microvesicle biogenesis in pancreatic islet beta-cells. Am. J. Physiol. Endocrinol. Metab. *299*, E23–E32.

Szot, G.L., Koudria, P., and Bluestone, J.A. (2007). Murine pancreatic islet isolation. J Vis Exp 255.

Theos, A.C., Tenza, D., Martina, J.A., Hurbain, I., Peden, A.A., Sviderskaya, E.V., Stewart, A., Robinson, M.S., Bennett, D.C., Cutler, D.F., et al. (2005). Functions of adaptor protein (AP)-3 and AP-1 in tyrosinase sorting from endosomes to melanosomes. Mol Biol Cell *16*, 5356–5372.

Tooze, S.A., and Huttner, W.B. (1990). Cell-free protein sorting to the regulated and constitutive secretory pathways. Cell *60*, 837–847.

Torii, S., Saito, N., Kawano, A., Zhao, S., Izumi, T., and Takeuchi, T. (2005). Cytoplasmic transport signal is involved in phogrin targeting and localization to secretory granules. Traffic *6*, 1213–1224.

Turkewitz, A.P. (2004). Out with a bang! Tetrahymena as a model system to study secretory granule biogenesis. Traffic *5*, 63–68.

CHAPTER 5:

QUANTITATIVE PROTEOMICS IMPLICATES AP-3-MEDIATED EXCLUSION OF t-SNAREs IN THE REGULATION OF SECRETION[*]

Daniel W. Sirkis[1,2], Cédric S. Asensio[2], Jeffrey R. Johnson[3,4,5],
Nevan J. Krogan[3,4,5], and Robert H. Edwards[1,2]

[1]Graduate Program in Pharmaceutical Sciences and Pharmacogenomics

[2]Departments of Physiology and Neurology

[3]Department of Cellular and Molecular Pharmacology

[4]California Institute for Quantitative Biosciences, QB3

[5]J. David Gladstone Institutes

University of California, San Francisco

San Francisco, California 94158

---

[*]This chapter comprises work I have undertaken in collaboration with the Krogan lab at UCSF. Recent findings enabled by quantitative proteomics indicate that heightened levels of the t-SNARE, syntaxin-1A, on large dense-core vesicles (LDCVs) may be responsible for the impaired regulated secretion we observe upon loss of AP-3. Although these experiments are currently ongoing, the body of work described in this chapter will be submitted for publication in the future. For this manuscript in preparation, I:

- carried out the stable isotope labeling by amino acids in cell culture (SILAC)
- isolated the LDCVs used in the proteomic analysis
- worked in collaboration with Jeffrey Johnson on the proteomic analysis
- conducted follow-up experiments on synaptotagmin, IA-2 and syntaxin-1A
- discussed methods, experimental design and interpretation of data with Cédric Asensio and Robert Edwards
- wrote the manuscript

Abstract

The regulated secretion of many peptide hormones, neural peptides and growth factors depends on their sorting into large dense-core vesicles (LDCVs) capable of undergoing regulated exocytosis. LDCVs form at the *trans*-Golgi network, but the mechanism of protein sorting to the regulated secretory pathway (RSP) and in particular the cytosolic machinery involved have remained poorly understood. We recently identified the heterotetrameric adaptor protein AP-3 in a large-scale RNA interference screen for factors required for sorting to the RSP. Using neuroendocrine PC12 cells, we found that loss of AP-3 dysregulated secretion of soluble and membrane LDCV cargo, and the mechanism appeared to involve a defect in LDCV formation. We also observed that loss of AP-3 impaired sorting of the calcium sensor synaptotagmin 1 (syt1) to LDCVs, and thus hypothesized that AP-3 concentrates the membrane proteins required for regulated exocytosis. To identify the global set of LDCV proteins altered by loss of AP-3, we carried out quantitative proteomics on isolated LDCVs. Proteomic analysis confirms previously established reductions in secretogranin II (SgII) and syt1 after AP-3 knockdown, and identifies many additional soluble and membrane proteins whose abundance is altered. We find that over-expression of the islet cell autoantigen protein, IA-2, which is depleted from LDCVs after AP-3 knockdown, is sufficient to partially rescue SgII secretion after AP-3 silencing, but this effect appears to be secondary to an increase in cellular SgII levels. In addition, we find that the levels of two plasma membrane t-SNAREs, syntaxin-1A (stx1A) and SNAP25, increase on LDCVs after AP-3 depletion, and over-expression of stx1A but not SNAP25 is sufficient to robustly impair regulated secretion. Taken together, our findings define a host of novel AP-3-regulated LDCV proteins and support the notion that AP-3 contributes to RSP biogenesis by preventing inappropriate inclusion of t-SNAREs within nascent LDCVs.

Introduction

The action of neural peptides, peptide hormones and growth factors depends on their secretion in response to specific physiological stimuli. Peptide hormones such as insulin and glucagon, for example, are crucial for maintaining normal glycemia. In addition, neural peptides such as substance P and the opioids play critical roles in the perception of pain as well as the reward pathway subverted by drugs of addiction (De Felipe et al., 1998; Murtra et al., 2000; Fields, 2004). Regulated secretion thus plays a central role in normal physiology, behavior and disease.

The secretion of peptide hormones and other proteins in response to a stimulus depends on their sorting into the RSP of neurons, endocrine and exocrine cells. Proteins destined for the regulated pathway must be excluded from the constitutive secretory pathway which enables the immediate and unregulated secretion of newly synthesized proteins from essentially all eukaryotic cells. We currently understand little about how proteins sort specifically into the regulated rather than constitutive secretory pathway.

The work of the RSP is carried out by organelles known as secretory granules or LDCVs. LDCVs bud from the *trans*-Golgi network (TGN) (Orci et al., 1987; Sossin et al., 1990; Tooze and Huttner, 1990), and previous work has suggested that lumenal interactions such as the aggregation of 'granulogenic' proteins drive their formation (Kim et al., 2001). Findings such as these have led some to suggest that sorting to LDCVs occurs by default, with proteins destined for other organelles removed during the subsequent process of LDCV maturation (Klumperman et al., 1998; Morvan and Tooze, 2008). However, the direct analysis of budding from the TGN has demonstrated the sorting of regulated from constitutive cargo at this early step, before maturation (Tooze and Huttner, 1990). In addition, LDCV membrane proteins such as carboxypeptidase E and sortilin have been proposed to serve as the receptors for soluble cargo (Cool et al., 1997; Chen et al., 2005). In contrast to these lumenal interactions, our knowledge about the cytosolic machinery involved in sorting to LDCVs remains limited, although our lab

has recently established a role for the heterotetrameric adaptor protein AP-3 in sorting proteins to the RSP (Asensio et al., 2010).

Several membrane proteins contain cytosolic sequences that direct them to LDCVs. For example, the neuronal vesicular monoamine transporter, VMAT2, which fills neurosecretory vesicles with monoamine, depends on a conserved C-terminal cytoplasmic dileucine-like motif for sorting to LDCVs (Liu et al., 1994; Krantz et al., 2000; Li et al., 2005). The requirement for a cytoplasmic motif in sorting to the RSP suggested an interaction with cytosolic sorting machinery. Indeed, we recently used VMAT as a reporter to screen for proteins involved in biogenesis of the RSP, and identified multiple subunits of the heterotetrameric adaptor protein AP-3 (Asensio et al., 2010). Loss of AP-3 resulted in mis-sorting of VMAT in both *Drosophila* S2 cells and mammalian neuroendocrine PC12 cells, as well as impaired regulated secretion, with fewer and morphologically abnormal LDCVs. In addition, we found that loss of AP-3 impaired sorting of the calcium sensor syt1 to LDCVs, suggesting that AP-3 may concentrate the proteins required for regulated secretion (Asensio et al., 2010). However, an alternative hypothesis is that AP-3 ensures the fidelity of the RSP by excluding inappropriate entry of particular membrane proteins. To test these possibilities, we conducted quantitative proteomics to determine the full spectrum of changes to LDCV proteins that occur upon loss of AP-3. Here we show that AP-3 knockdown results in reductions in a number of functionally important LDCV membrane proteins, but also significantly increases the levels of multiple plasma membrane t-SNAREs not typically found on LDCVs. Importantly, we find that over-expression of one such protein, stx1A, is sufficient to robustly impair regulated secretion, thus recapitulating the effect of AP-3 knockdown.

Results

Quantitative proteomics reveals AP-3-dependent LDCV cargo

      To obtain a precise understanding of the molecular changes that occur to LDCVs upon loss of AP-3, we conducted quantitative proteomics. In particular, we carried out stable isotope labeling by amino acids in cell culture (SILAC)-based proteomics on LDCVs purified from neuroendocrine PC12 cells. We used a previously established method for isolating LDCVs which involves sequential velocity and equilibrium sedimentation through sucrose gradients (Tooze and Huttner, 1990). Using SgII as a marker, we pooled LDCV-containing fractions from the initial, velocity gradient and loaded the combined material onto a second gradient. LDCVs were then sedimented to equilibrium, and SgII used once again to follow the migration of LDCVs into the gradient (Fig. 1 A). To confirm that the isolation protocol worked, the presumptive LDCV-containing fractions were fixed, and the material was pelleted and processed for thin-section EM according to (Tooze and Huttner, 1990). EM analysis confirmed the presence of the expected round, electron-dense vesicles with diameter of ~100 nm (Fig. 1 B).
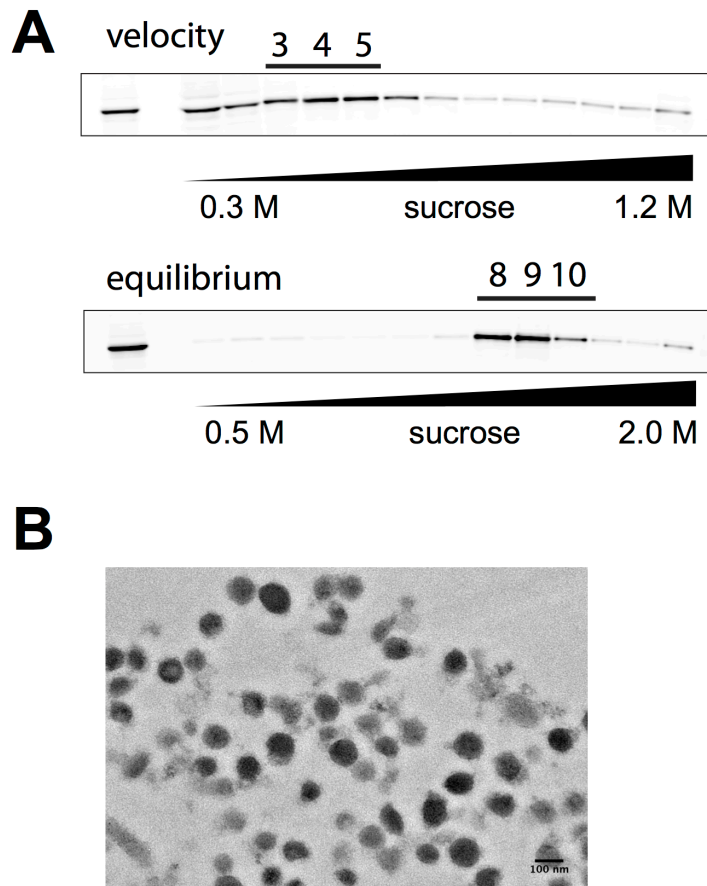
Figure 1. Isolation of LDCVs for proteomic analysis
(A) A PC12 cell PNS was formed and separated by velocity gradient sedimentation through 0.3–1.2 M sucrose. Fractions containing the peak of the SgII immunoreactivity were determined by quantitative fluorescent immunoblotting, pooled and added to the top of a 0.5–2.0 M sucrose gradient, then centrifuged to equilibrium. Fractions containing the peak of the SgII immunoreactivity from the second gradient were pooled, and the material fixed for EM analysis. (B) Thin-section electron micrograph shows the typical round, electron-dense appearance of LDCVs. Scale bar indicates 100 nm.

For the SILAC analysis, cells were grown in either light (control siRNA) or heavy (AP-3 siRNA) amino acids for several passages, and preliminary mass spectrometric analysis indicated ~99.8% incorporation of heavy amino acids (data not shown). After two siRNA transfections, *light* and *heavy* cells were harvested, mixed together, and a combined post-nuclear supernatant (PNS) formed. Equilibrium gradient fractions containing the majority of the SgII immunoreactivity were pooled, the protein precipitated, and samples processed for mass

141

spectrometric analysis. Western analysis of the isolated LDCV fractions indicated that they were largely depleted of markers for early and late endosomes, lysosomes, the Golgi, synaptic-like microvesicles, cytoskeleton and cytosol (Fig. 2 A). We carried out two independent SILAC experiments and identified a total of 31 proteins that were significantly decreased on the LDCVs after AP-3 knockdown ($z \geq 2$ in both experiments), and a total of 14 proteins significantly increased ($z \leq -2$ in both experiments) (Fig. 2 B). Importantly, two of the most significantly decreased proteins were SgII and syt1, both of which we have previously established as being mis-sorted from LDCVs after AP-3 silencing (Asensio et al., 2010). This provides a critical validation of our SILAC approach.

Decreased proteins

A number of well-established, functionally important LDCV membrane proteins were significantly decreased after AP-3 knockdown, including syt1, peptidyl-glycine α-amidating monooxygenase (PAM), and the islet cell autoantigen proteins IA-2 and IA-2β (phogrin) (Fig. 2 C and Table 1). Several other transmembrane proteins identified, such as SV2A and Golgi apparatus protein 1, are better known for their roles on other organelles, but both have been detected previously on LDCVs (Lowe et al., 1988; Xu and Bajjalieh, 2001; Wegrzyn et al., 2007). In addition, a large number of secreted, granin-family proteins were decreased, including secretogranins II, III, V (7B2), VII (VGF) and VIII (proSAAS). Importantly, the related and highly abundant LDCV proteins, chromogranins A and B, were both unchanged by AP-3 knockdown, indicating that loss of AP-3 does not nonspecifically lead to reduction of all LDCV proteins. Also potentially of interest is a reduction in carboxypeptidase E (CPE), a protein which has been proposed to act as a sorting receptor for LDCVs (Cool et al., 1997). In addition, two cytosolic, membrane-associated proteins, synaptotagmin-like protein 4 (granuphilin) and Rab7A were significantly decreased as well. While the former is a well known LDCV-associated protein involved in docking (Gomi et al., 2005; Wang et al., 2011b), the latter is usually thought of as a

late endosome-associated trafficking protein, but it has also been detected in previous LDCV proteomics studies (Wegrzyn et al., 2007). Finally, two proteins which are best known as members of the tetrameric cohesin complex, structural maintenance of chromosomes (SMC) 1A and SMC3 (bamacan), were consistently decreased on LDCVs after knockdown. Notably, both of these proteins appear to have alternative functions in postmitotic cells, with SMC1A being shown to regulate neuronal axon and dendrite morphology (Schuldiner et al., 2008), and SMC3 having an additional role as a secreted, extracellular matrix protein (Wu and Couchman, 1997).

Increased proteins

Of the increased proteins, several are involved in membrane fusion. In particular, the plasma membrane t-SNAREs stx1A[*] and SNAP25, as well as the syntaxin-associated protein, Munc18-1, were increased on LDCVs upon AP-3 depletion (Fig. 2 C and Table 1). Interestingly, the transmembrane protein carboxypeptidase D, which localizes predominantly to the TGN (Varlamov and Fricker, 1998; Varlamov et al., 1999), was also increased, suggesting possible "leakage" into the RSP after AP-3 knockdown. In addition, two rate-limiting enzymes involved in monoamine biosynthesis, GTP cyclohydrolase 1 (which produces tetrahydrobiopterin) and tyrosine hydroxylase (which produces L-DOPA), were significantly increased, suggesting a possible compensatory response by the cell after sensing impairment of the RSP. Finally, a number of cytoskeletal components and associated proteins were also significantly increased, including β-III tubulin, keratin 18, plectin, and moesin.

---

[*]Stx1A was detected in only one of two independent proteomic analyses of LDCVs. However, it was significantly increased in the experiment in which it was detected, and two of its binding partners, SNAP25 and Munc18-1, were significantly increased in both analyses.
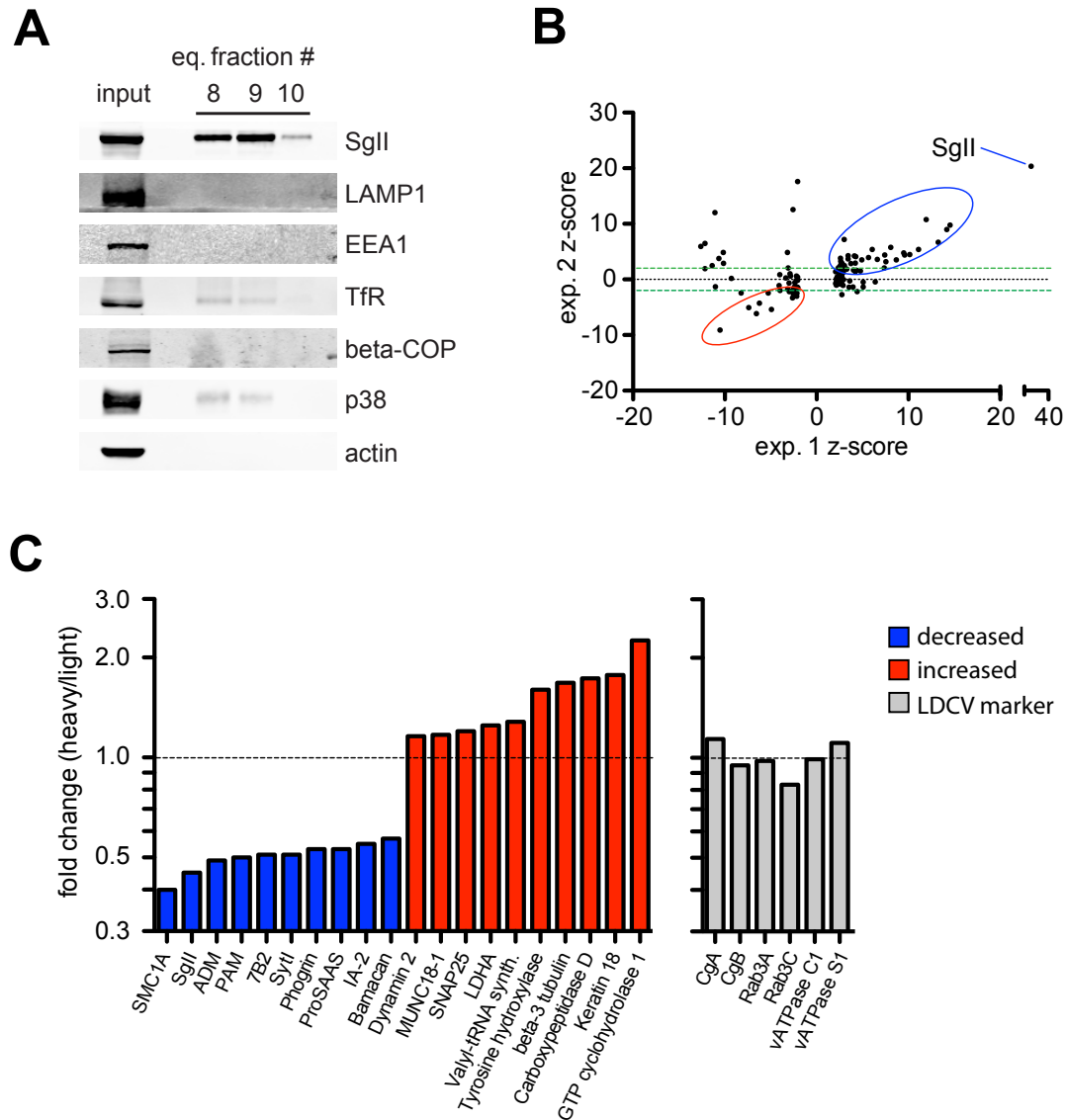
Figure 2. Quantitative proteomics of LDCVs after AP-3 knockdown
Light and heavy amino acid-labeled cells were mixed and their combined PNS separated by velocity gradient sedimentation through 0.3–1.2 M sucrose. Three fractions containing the peak of the SgII immunoreactivity (determined by quantitative fluorescent immunoblotting) were pooled, added to the top of a 0.5–2.0 M sucrose gradient, and centrifuged to equilibrium. Three fractions containing the peak of the SgII immunoreactivity from the second gradient were pooled, and proteins precipitated for mass spectrometric analysis. (A) Aliquots from the peak SgII-containing fractions of the equilibrium gradient were assayed by quantitative fluorescent immunoblotting for markers of other organelles. These fractions are largely depleted of markers for late endosomes and lysosomes (LAMP1), early endosomes (EEA1 and TfR), Golgi (β-COP), SLMVs (p38), cytoskeleton and cytosol (actin). (B) Proteins with z-scores of ≥ 2 or ≤ -2 in the first experimental replicate are shown plotted against their corresponding z-score from the second experimental replicate. Of the 585 proteins detected in both experimental replicates, 31 (5.3%) were significantly decreased with $z \geq 2$ in both experiments (blue oval), and 14 (2.4%) were significantly increased with $z \leq -2$ in both experiments (red oval). (C) The top-ten decreased and increased proteins in terms of heavy/light ratio after AP-3 knockdown are shown. In addition, the ratios of six well-characterized LDCV marker proteins unchanged by the knockdown are displayed. Bars indicate the median peptide ratio.

Decreased proteins

rank	Uniprot accession	Description	heavy/light exp. 1	heavy/light exp. 2	z-score exp. 1	z-score exp. 2
1	Q9Z1M9	Structural maintenance of chromosomes protein 1A	0.51	0.29	4.2	2.9
2	P10362	Secretogranin-2	0.42	0.49	32.8	20.3
3	P43145	ADM	0.35	0.63	3.7	2.9
4	P14925	Peptidyl-glycine alpha-amidating monooxygenase	0.44	0.56	14.2	9.0
5	P27682	Neuroendocrine protein 7B2	0.48	0.54	5.6	3.9
6	P21707	Synaptotagmin-1	0.52	0.50	11.9	10.8
7	Q63475	Receptor-type tyrosine-protein phosphatase N2	0.51	0.56	14.5	9.8
8	Q9QXU9	ProSAAS	0.52	0.55	6.1	5.4
9	Q63259	Receptor-type tyrosine-protein phosphatase-like N	0.52	0.59	13.2	6.7
10	P97690	Structural maintenance of chromosomes protein 3	0.48	0.66	2.6	3.8
11	P35572	Insulin-like growth factor-binding protein 6	0.49	0.66	7.5	3.2
12	P13084	Nucleophosmin	0.67	0.49	3.0	7.2
13	P15087	Carboxypeptidase E	0.53	0.65	11.1	5.4
14	Q8VHQ7	Synaptotagmin-like protein 4	0.58	0.65	8.7	3.5
15	P17246	Transforming growth factor beta-1	0.66	0.63	4.9	3.5
16	Q62638	Golgi apparatus protein 1	0.76	0.55	4.3	4.1
17	Q63083	Nucleobindin-1	0.63	0.69	8.1	5.8
18	P20961	Plasminogen activator inhibitor 1	0.59	0.73	7.4	2.1
19	P19637	Tissue-type plasminogen activator	0.60	0.75	10.2	4.5
20	Q66H50	Fatty acyl-CoA reductase 1	0.72	0.66	3.4	3.7
21	O54858	Carboxypeptidase Z	0.67	0.72	7.4	4.4
22	P07872	Peroxisomal acyl-coenzyme A oxidase 1	0.66	0.73	9.6	4.4
23	Q3MIB4	Lon protease homolog 2, peroxisomal	0.66	0.74	2.6	2.6
24	Q02563	Synaptic vesicle glycoprotein 2A	0.79	0.62	4.1	4.2
25	P09527	Ras-related protein Rab-7a	0.80	0.65	3.4	4.3
26	P47868	Secretogranin-3	0.70	0.76	6.6	3.6
27	P20156	Neurosecretory protein VGF	0.70	0.79	9.5	4.8
28	Q8VHK0	Acyl-coenzyme A thioesterase 8	0.79	0.72	3.0	2.5
29	P11915	Non-specific lipid-transfer protein	0.82	0.79	2.4	2.1
30	P16970	ATP-binding cassette sub-family D member 3	0.84	0.78	2.6	3.3
31	P97852	Peroxisomal multifunctional enzyme type 2	0.89	0.84	2.8	2.9

Increased proteins

rank	Uniprot accession	Description	heavy/light exp. 1	heavy/light exp. 2	z-score exp. 1	z-score exp. 2
1	P22288	GTP cyclohydrolase 1	2.27	2.24	-5.3	-2.4
2	Q5BJY9	Keratin, type I cytoskeletal 18	1.75	1.78	-7.4	-5.1
3	Q9JHW1	Carboxypeptidase D	1.64	1.82	-10.5	-9.1
4	Q4QRB4	Tubulin beta-3 chain	1.81	1.55	-8.2	-2.5
5	P04177	Tyrosine 3-monooxygenase	1.61	1.59	-6.6	-6.2
6	Q04462	Valyl-tRNA synthetase	1.28	1.28	-6.2	-4.3
7	P04642	L-lactate dehydrogenase A chain	1.20	1.30	-4.9	-5.4
8	P60881	Synaptosomal-associated protein 25	1.15	1.25	-2.2	-3.0
9	P61765	Syntaxin-binding protein 1	1.16	1.17	-3.0	-2.2
10	P39052	Dynamin-2	1.15	1.17	-2.6	-2.2
11	Q68FR6	Elongation factor 1-gamma	1.11	1.15	-2.5	-2.6
12	O35763	Moesin	1.12	1.13	-2.1	-2.5
13	P11980	Pyruvate kinase isozymes M1/M2	1.09	1.13	-2.3	-2.6
14	P30427	Plectin	1.06	1.12	-2.6	-3.3

Table 1. LDCV proteins significantly changed upon AP-3 knockdown
These proteins were significantly increased or decreased in each of two independent SILAC experiments. They are ranked according to their magnitude of change, and displayed with their Uniprot accession number. Their median heavy/light peptide ratios and z-scores are shown for both experimental replicates.

Quantitative proteomics of whole-cell lysates after AP-3 knockdown

To assess whether the alterations in vesicle composition after AP-3 knockdown were a result of altered protein trafficking or simply changes in expression, we also carried out SILAC-based proteomics on whole-cell lysates. To our surprise, we found that many, though not all, of the most significantly affected LDCV proteins were changed in the same direction in the whole-cell lysates (Fig. 3). This finding was expected for the soluble granin-related proteins, since these proteins are likely to be decreased due to heightened constitutive secretion (and thus exit from the cell); it was more surprising that membrane proteins such as syt1, IA-2 and IA-2β were also reduced. Importantly, though, the magnitude of change for these proteins is smaller in the whole-cell lysates than the LDCVs. This suggests that the overall change in cellular levels cannot fully account for the change in LDCV levels. Further, since we know from previous work that syt1 exhibits a bona fide sorting defect upon AP-3 knockdown (Asensio et al., 2010), this indicates that the overall cellular reduction observed for some proteins a not necessarily evidence *against* a trafficking defect. Finally, it is interesting to note that the cellular levels of two of the top-scoring

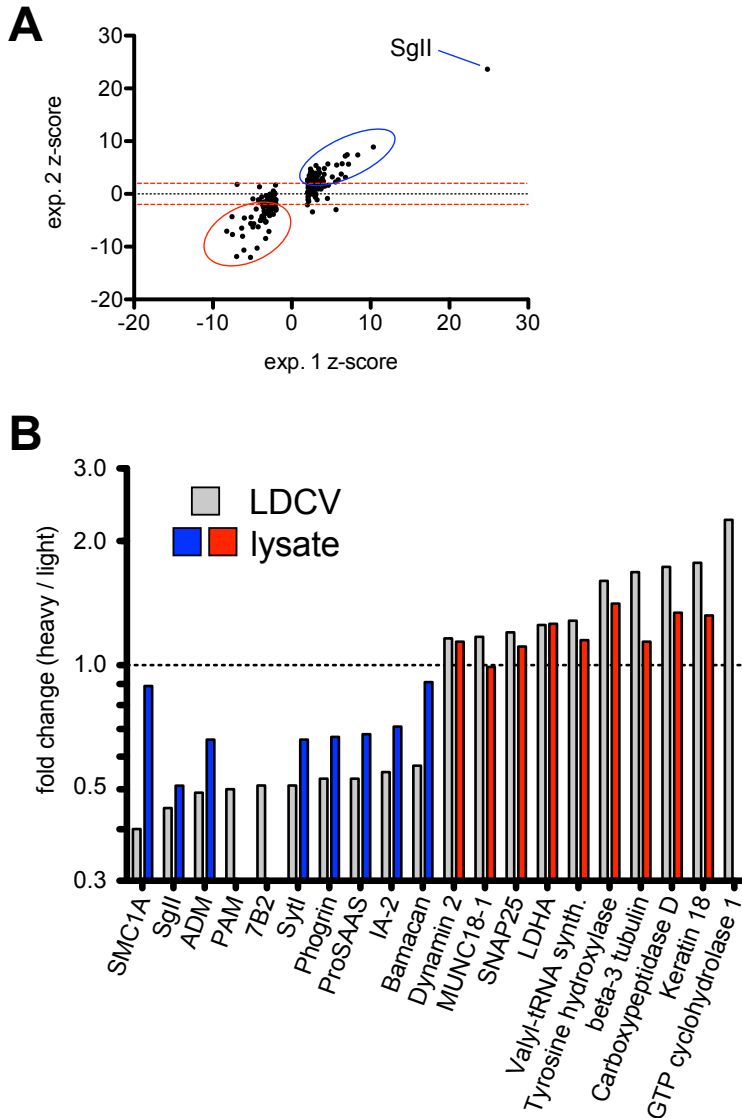proteins in the LDCV analysis, SMC1A and SMC3, which interact with each other, were nearly unchanged (Fig. 3).

Figure 3. Quantitative proteomics of PC12 whole-cell lysates after AP-3 knockdown
Light and heavy amino acid-labeled cells were combined after knockdown, pelleted and lysed for mass spectrometric analysis. (A) Proteins with z-scores of ≥ 2 or ≤ -2 in the first experimental replicate are shown plotted against their corresponding z-scores from the second experimental replicate. Of the 1,190 proteins detected in both experimental replicates, 61 (5.1%) were significantly decreased with $z \geq 2$ in both experiments (blue oval), and 48 (4.0%) were significantly increased with $z \leq -2$ in both experiments (red oval). (B) The top-ten decreased and increased proteins in terms of heavy/light ratio from the LDCV dataset are shown with their corresponding ratios from whole-cell lysate dataset. The chart shows that the levels of most of these proteins are changed in the same direction in both the LDCV and lysate datasets, although the changes are generally of smaller magnitude in the latter. Bars indicate the median peptide ratio. Some proteins, such as PAM, 7B2 and GTP Cyclohydrolase 1 were not detected in the whole-cell lysate dataset.

IA-2 and synaptotagmin 1 modulate the effect of AP-3 KD on regulated secretion

In an effort to identify the proteins responsible for AP-3's effect on the regulation of secretion, we focused on several candidates from the proteomics. Syt1 is a major calcium sensor for regulated release of synaptic vesicles and LDCVs, although in both PC12 and chromaffin cells other syt isoforms appear to function redundantly (Fernández-Chacón et al., 2001; Lynch and Martin, 2007; Schonn et al., 2008). Since syt1 was significantly reduced on LDCVs after AP-3 knockdown, we hypothesized that over-expression of syt1 after AP-3 knockdown might be sufficient to rescue regulated exocytosis, by means of "leakage" of the over-expressed syt1 into the RSP. However, regulated secretion of SgII was not significantly affected (Fig. 4 B), even though we achieved expression ~2.5-fold over endogenous levels (data not shown). In a related experiment, we asked whether simultaneous knockdown of AP-3 and syt1 could exacerbate the secretory defect normally observed with AP-3 knockdown alone. Consistent with previously published findings (Lynch and Martin, 2007), knockdown of syt1 alone had no effect on regulated secretion, but double knockdown of AP-3 and syt1 did slightly exacerbate the defect in regulated secretion (Fig. 4 D). This finding suggests that LDCVs become sensitized to reductions in syt1 upon loss of AP-3, presumably due to the AP-3-associated changes in LDCV protein composition. Taken together, these results indicate that syt1 is not solely responsible for AP-3's effect on regulated secretion.

We also carried out a similar set of experiments on IA-2, a membrane protein that localizes exclusively to LDCVs in multiple cell types, but whose function remains relatively unclear (Rabin et al., 1994; Solimena et al., 1996; Torii, 2009; Nakajima et al., 2011). Mice deficient in both IA-2 and IA-2β have reduced stimulus-evoked insulin secretion, although this appears to stem from the fact that they have reduced intracellular insulin storage rather than from a secretory defect per se (Henquin et al., 2008; Cai et al., 2011). In particular, combined loss of IA-2 and IA-2β is associated with a reduction in the number of insulin granules, and this appears

to be due in part to a reduction in LDCV half-life (Cai et al., 2011). Owing to these interesting molecular properties, we asked whether IA-2 over-expression could alleviate the secretory defect arising from AP-3 knockdown. We used lentiviral transduction of C-terminally HA-tagged IA-2, and achieved expression ~10-fold over endogenous levels (data not shown). In our initial analysis, we found that IA-2 over-expression significantly increased regulated SgII secretion in both control cells and those with AP-3 knockdown (Fig. 4 A). However, we observed that IA-2 over-expression also increased intracellular SgII levels, a finding consistent with the literature (Harashima et al., 2005; Nishimura et al., 2010). Reanalyzing the secretion data by normalizing secreted SgII to intracellular SgII (as opposed to total cellular protein) abrogated the apparent effect of IA-2 over-expression on secretion (Fig. 5). Thus, IA-2 appears to control cellular SgII levels, both in control cells and those where AP-3 has been depleted, but it does not appear to affect regulated secretion per se.

We also used RNAi to deplete IA-2 both alone and in combination with AP-3. We achieved ~90% knockdown of IA-2 at the protein level (data not shown), but saw no effect on regulated secretion when IA-2 alone was depleted. However, as with syt1, we observed a small but significant aggravating effect on the AP-3 phenotype when both proteins were knocked down together (Fig. 4 C). In addition, we attempted to silence IA-2 and IA-2β together, but this also did not affect regulated secretion (data not shown). Thus, we conclude that IA-2 is not primarily responsible for the defect in regulated secretion associated with loss of AP-3.
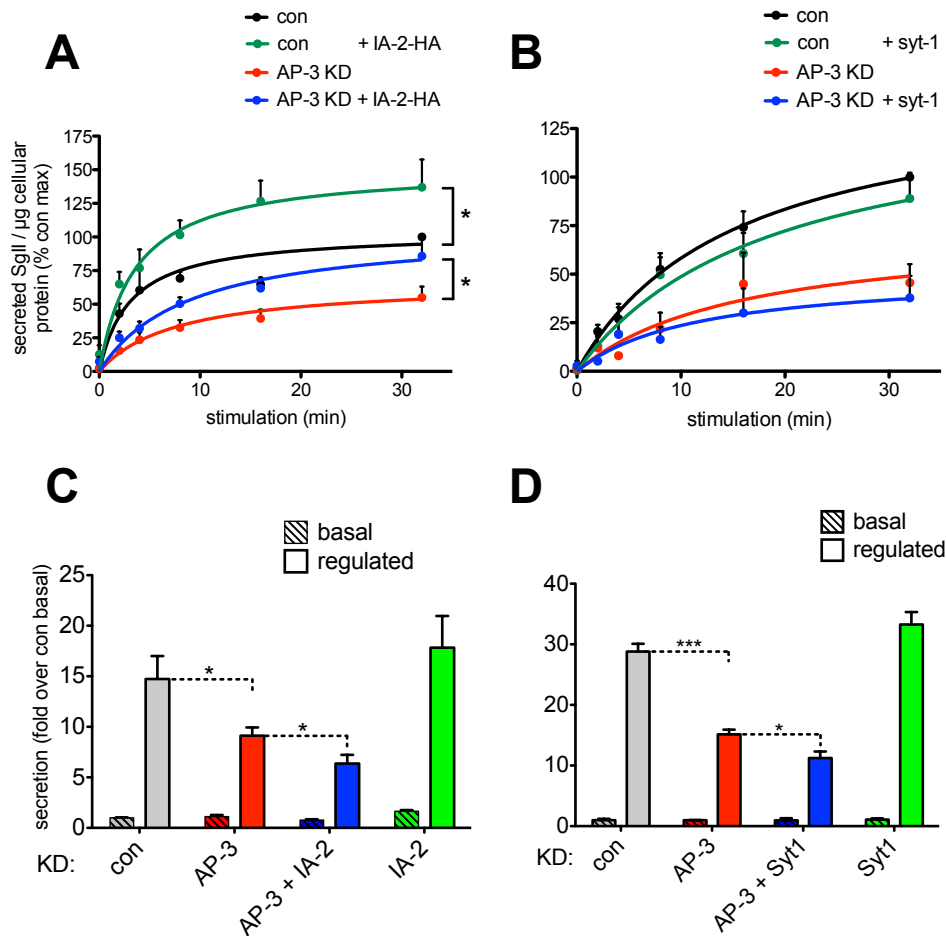
Figure 4. IA-2 and syt1 modulate the effect of AP-3 knockdown on regulated secretion
(A and B) PC12 cells were transduced with or without IA-2-HA (A) or syt1 (B) lentivirus and transiently transfected twice with AP-3 δ or control siRNA. Two days after the second siRNA transfection, cells were washed and stimulated by incubation in Tyrode's solution containing 50 mM K$^+$. Aliquots of Tyrode's were collected at the indicated time points and secreted SgII measured by quantitative fluorescent immunoblotting. At the end of the time course, cells were lysed and total protein measured for normalizing secretion data. IA-2-HA over-expression significantly increases depolarization-induced secretion in control and AP-3 knockdown cells (A). *, P < 0.04 (relative to untransduced cells by sum-of-squares F test on the regression curves; n = 4 transfections). Syt1 over-expression does not affect secretion in control or AP-3 knockdown cells (B). (C and D) Cells were transiently transfected with AP-3, IA-2 or both siRNAs (C) or with AP-3, syt1 or both siRNAs (D), washed, and incubated for 30 min in Tyrode's containing 2.5 mM (basal) K$^+$ or 50 mM (stimulated) K$^+$. Secreted SgII was measured as above, with the secreted SgII normalized to basal secretion in the control. Combined knockdown of AP-3 and IA-2 (C) or AP-3 and syt1 (D) potentiates the reduction in depolarization-induced secretion mediated by AP-3 knockdown. *, P < 0.05; ***, P < 0.005 (Newman-Keuls test, post ANOVA; n = 4 transfections). The data show mean values, and error bars indicate SEM.
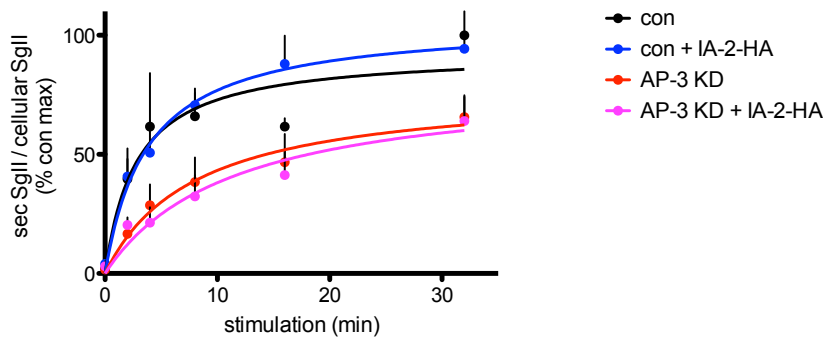
Figure 5. Increased cellular SgII accounts for secretory changes upon IA-2 over-expression
Analysis of the data in Fig. 4 A by normalization of secreted SgII to cellular SgII, rather than total cellular protein. Secreted and cellular SgII were measured by quantitative fluorescent immunoblotting. Increased cellular SgII in the IA-2-HA-transduced cells accounts for the apparent effect of IA-2 over-expression on depolarization-induced SgII secretion.

Ectopic LDCV expression of stx1A may account for AP-3's effect on regulated secretion

Since SNARE proteins are essential for the regulated exocytosis of LDCVs (Papini et al., 1995; Sadoul et al., 1995; Banerjee et al., 1996; Foran et al., 1996), we analyzed changes in all SNAREs detected in our LDCV dataset. Although we observed no changes in the vesicle-associated v-SNAREs, we were surprised to observe significant increases in the normally plasma membrane-localized t-SNAREs, stx1A and SNAP25, as well as the syntaxin-binding protein Munc18 (Fig. 6). We speculated that ectopic expression of cell surface t-SNAREs on LDCVs upon loss of AP-3 could result in the formation of cis-SNARE complexes between the t-SNAREs and LDCV-resident v-SNARE proteins such as VAMP2 (Otto et al., 1997; Lang et al., 2002), which would be expected to inhibit regulated secretion. To test this possibility, we over-expressed SNAP25 and stx1A in PC12 cells and assessed regulated secretion. SNAP25 showed no effect in this assay, but stx1A robustly inhibited regulated secretion, with no effect on basal secretion (Fig. 7). We also assessed the effect of stx1A over-expression on constitutive secretion, and found that over-expression moderately reduced this form of release as well (Fig. 8), consistent with previously published data from non-neural cells (Bittner et al., 1996; Khvotchev and Südhof, 2004).
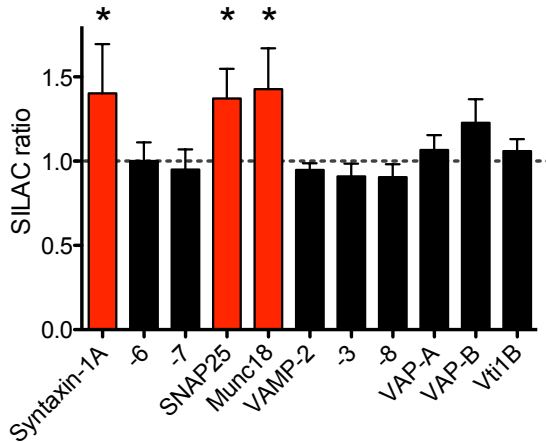
Figure 6. Analysis of SNAREs and SNARE-associated proteins reveals significant increases in syntaxin-1A, SNAP25 and Munc18 on LDCVs

SNAREs and SNARE-associated proteins detected in the initial proteomic analysis of LDCVs are shown. Two t-SNAREs, stx1A and SNAP25, and the syntaxin-binding protein Munc18 showed significant increases. *, z < -2; see Materials and Methods for a detailed description of z-score calculation. The bars show mean SILAC ratios (heavy/light), and error bars indicate SEM.
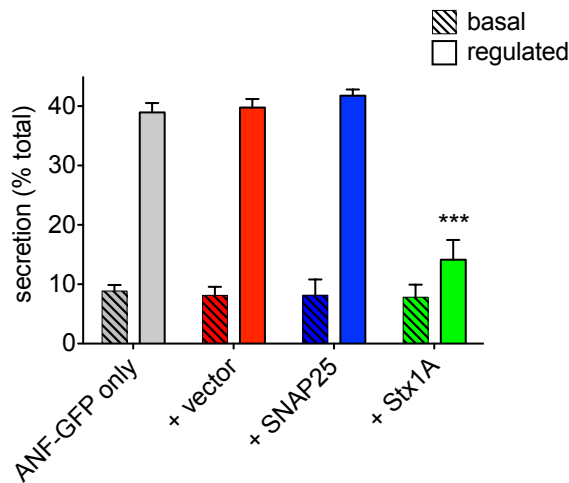
Figure 7. Over-expression of syntaxin-1A but not SNAP25 strongly impairs regulated secretion

PC12 cells were transiently transfected with ANF-GFP as a reporter for regulated secretion, with or without the addition of empty vector, SNAP25 or stx1A. Co-transfection with stx1A, but not SNAP25, strongly and specifically impairs regulated secretion. ***, P < 0.001 (Newman-Keuls test, post ANOVA; n = 4 transfections). The data show mean values, and error bars indicate SEM.
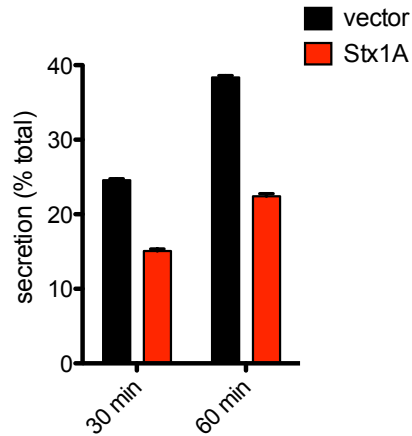
Figure 8. Over-expression of syntaxin-1A moderately impairs constitutive secretion
PC12 cells were transiently transfected with ss-GFP as a reporter for constitutive secretion, and co-transfected with empty vector or stx1A. Over-expression of stx1A moderately impairs constitutive secretion of ss-GFP at both time points assessed. The data show mean values, and error bars indicate SEM; n = 5 transfections.
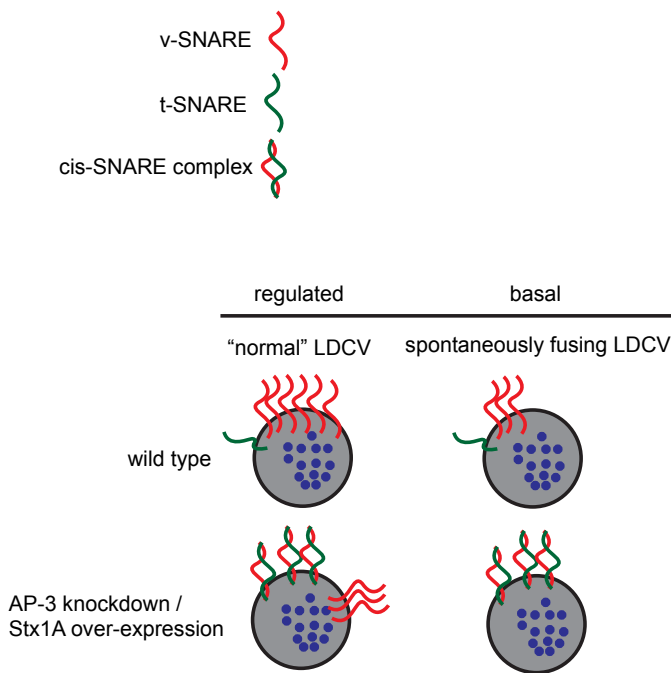
Figure 9. Model for syntaxin-mediated inhibition of regulated secretion
In this model, LDCVs destined to undergo regulated exocytosis exhibit a membrane protein composition distinct from those undergoing spontaneous fusion. In particular, LDCVs undergoing regulated exocytosis are postulated to contain a higher copy number of v-SNARE molecules than those destined to undergo spontaneous release. Loss of AP-3 or over-expression of stx1A will lead to an increased number of t-SNARE molecules on the LDCV, where they will interact with v-SNAREs, forming cis-SNARE complexes. LDCVs with a high copy number of v-SNAREs would undergo partial v-SNARE titration, while those with a low copy number would undergo full titration, thus rendering them incompetent for any form of secretion. Vesicles undergoing only partial v-SNARE titration would become spontaneously-fusing LDCVs.

Discussion

The unbiased, global assessment of changes in LDCV protein levels afforded by SILAC-based proteomics has enabled us to identify an unexpected increase in the levels of t-SNARE proteins on LDCVs after the loss of AP-3. We have tested whether simple over-expression of these t-SNAREs is sufficient to impair regulated secretion, and for stx1A, this indeed appears to be the case. We hypothesized that stx1A over-expression in wild type cells would lead to non-specific leakage of the t-SNARE into the RSP, but we have not yet excluded a role for stx1A acting more indirectly from another organelle. We propose that ectopic expression of stx1A and SNAP25 on LDCVs is likely to result in the formation of cis-SNARE complexes containing LDCV-localized VAMP2 (Fig. 9), as similar processes have been observed in other membranes (Otto et al., 1997; Lang et al., 2002). Further, we suggest that differences in v-SNARE copy number may underlie different modes of LDCV exocytosis (spontaneous vs. regulated), and thus ectopic t-SNARE expression would differentially titrate distinct pools of LDCVs. This would lead to the scenario envisioned in Figure 9, which shows that spontaneously-fusing LDCVs—containing fewer v-SNAREs—would be inactivated by ectopic t-SNARE expression, while LDCVs fusing only after stimulation (and containing more v-SNAREs) would be converted to spontaneously-fusing LDCVs, ultimately resulting in impaired regulated but intact basal secretion.

In future experiments, we will test directly whether LDCV-localized stx1A is sufficient to impair regulated secretion. In particular, we will attempt to over-express stx1A fused to the lumenal domain of IA-2—which should direct sorting to the RSP (Wasmeier et al., 2002)—and determine first whether this chimeric protein localizes to LDCVs. If so, we will ask whether expression of LDCV-restricted stx1A is sufficient to inhibit regulated secretion. In a related experiment, we will determine whether modest knockdown of stx1A is sufficient to block the effect of AP-3 knockdown, reasoning that a reduction in the overall levels of stx1A should prevent the ectopic localization of this protein to LDCVs. Potentially complicating factors for the

latter experiment are probable redundancy between the two stx1 isoforms (Gerber et al., 2008), and the fact that a large reduction in stx1 is itself likely to inhibit regulated secretion (Wang et al., 2011a).

Three potential models could explain the ectopic localization of t-SNAREs to LDCVs upon loss of AP-3. In the first model, AP-3 knockdown leads to general intermixing of the regulated and constitutive secretory pathways, thus giving rise to t-SNAREs on LDCVs. In this model, AP-3 serves as a molecular 'fence', segregating proteins at the TGN into the correct domain for entry into the appropriate pathway. This model is supported by the finding that AP-3 knockdown is associated with some SgII budding from the TGN into apparently constitutive vesicles (Asensio et al., 2010), but lacks support from the proteomic analysis, in which highly abundant constitutively secreted proteins, such as heparin sulfate proteoglycans (glypicans), were not detected in LDCVs after AP-3 knockdown. In the second model, AP-3 would sort endocytosed t-SNAREs from early endosomes to lysosomes for their degradation. In the absence of AP-3, these proteins would be available for increased recycling to the TGN, and ultimately to nascent LDCVs. This model gains appeal from its placement of AP-3 at its best-known site of action (in mammals, the early endosome), but it is less attractive due to the fact that proteins have not been shown to exhibit augmented recycling through the TGN after loss of AP-3. In the third and final model, AP-3 actively sorts t-SNAREs away from the regulated and into the constitutive secretory pathway. On its face, this model does not seem to comport with the observation that multiple membrane proteins appear to be concentrated within LDCVs by AP-3. In another sense, though, this model becomes very appealing when one looks to *S. cerevisiae*, where AP-3 is known to act at the TGN and mediate selective sorting of a syntaxin homolog directly to the vacuole (Cowles et al., 1997; Darsow et al., 1998)—thus excluding it from endosomes and the cell surface. Loss of AP-3 in this model would likely lead to increases in the levels of a relatively small number of membrane proteins on LDCVs, as we have observed here, but could nonetheless impart large effects on regulated release.

Materials and methods

Molecular biology

Stx1A and SNAP25 were amplified from PC12 cell cDNA with 5'-AgeI and 3'-SalI sites, then subcloned into pEGFP-C3 from which the EGFP coding sequence had first been excised. Syt1 and IA-2 were amplified from PC12 cell cDNA with 5'-BamHI and 3'-EcoRI sites, then subcloned into the FUGW lentiviral expression vector (again after removal of EGFP). In the case of IA-2, a C-terminal HA epitope tag was added during amplification. All constructs were verified by sequencing. ANF- and ss-GFP were prepared as described previously (Asensio et al., 2010).

Cell culture and lentivirus production

PC12 cells were maintained in DMEH-21 medium supplemented with 10% horse serum (HS) and 5% cosmic calf serum (CCS; HyClone) at 37°C. siRNA transfection was performed using Lipofectamine 2000 (Invitrogen) according to the manufacturer's instructions. HEK-293T cells were maintained in DMEH-21 medium with 10% fetal bovine serum (FBS) at 37°C. Lentivirus was produced by transfecting 293T cells with FUGW, psPAX2 and pVSVG (Lois et al., 2002) and Fugene HD (Roche) according to the manufacturer's instructions.

Antibodies

The SgII rabbit antibody was obtained from Meridian Life Science, the LAMP1 rabbit antibody from Abcam, the EEA1 mouse monoclonal antibody from BD, the TfR mouse monoclonal antibody from Zymed, the beta-COP mouse monoclonal antibody from Sigma, the p38 mouse monoclonal antibody from Chemicon, the actin mouse monoclonal antibody from Millipore.

siRNAs

siRNAs were obtained from Ambion and Dharmacon. *Silencer Select* rat Ap3d1 (antisense,

5'-UUCUUGGUCAUGAUCCAUGTG-3'), syt1 (antisense,

5'-UUUAGUCUCAAAUUUCUUCTT-3'), and corresponding non-targeting control siRNA were

from Ambion. *ON-TARGETplus* pooled rat IA-2 siRNA and non-targeting, pooled control

siRNA were from Dharmacon. The pooled IA-2 siRNA targeted the following sequences:

5'-GCUGGCAGGCUACGGAGUA-3', 5'-CCGCAGACUUUGUUCGCAU-3',

5'-CAUUCGAAACAACGGGAUA-3', 5'-GAGUAUGGCUAUAUAGUCA-3'.

Isotope labeling and LDCV isolation for proteomics

PC12 cells were maintained in *light* or *heavy* SILAC medium consisting of lysine- and arginine-

free DMEH-21 supplemented with 10% dialyzed HS and 5% dialyzed CCS. *Heavy* medium was

supplemented with $^{13}C_6$ lysine and $^{13}C_6{}^{15}N_4$ arginine (Pierce) at 0.1 mg/ml each. *Light* medium

was supplemented with normal lysine and arginine at 0.1 mg/ml each. Heavy amino acid

incorporation was checked after six passages in SILAC medium and was found to be ~99.8%

efficient.

For isolation of LDCVs, *light* and *heavy* cells were each seeded in two 15-cm plates,

transfected with negative control (*light*) or Ap3d1 siRNA (*heavy*) on days 1 and 3 after plating,

and cells harvested on day 5. LDCVs were isolated using a procedure modified from Tooze and

Huttner, 1990. Plates were put on ice, cells washed and resuspended in ice-cold PBS, then

pelleted in a clinical centrifuge at 4°C for 5 min. Cell pellets were resuspended in 250 mM

sucrose, 1 mM MgOAc, 10 mM Hepes-KOH, pH 7.2, and *Complete* protease inhibitors (Roche)

supplemented with 10 ug/ml PMSF and 2 mM EGTA. Small aliquots were taken to determine the

protein concentration of *light* and *heavy* samples. The two cell populations were then mixed in

equal proportions and a PNS prepared by homogenization with a ball-bearing device (18-μm

clearance). The PNS was then loaded onto a 0.3-1.2 M continuous sucrose gradient and LDCVs

separated from larger organelles by velocity sedimentation for 19 min at 4°C in an SW41 rotor at 25,000 rpm. 1-ml fractions were collected from the top of the gradient, and pooled fractions 3-5 were loaded onto a 0.5–2 M continuous sucrose gradient sedimented to equilibrium at 25,000 rpm and 4°C for >6 h (SW41). Three fractions spanning the peak of SgII immunoreactivity (determined by western) were pooled and LDCV proteins precipitated by chloroform/methanol precipitation. The protein pellet was dissolved in freshly prepared ice-cold 8M urea buffer with 150 mM NaCl, 100 mM Tris-HCl, pH 8.0.

Mass spectrometry

Sample Preparation. Resuspended chloroform/methanol-precipitated proteins were reduced with 4 mM TCEP for 30 minutes at room temperature then reacted with 20 mM iodoacetamide for 30 minutes at room temperature in the dark. Excess iodoacetamide was quenched with 20 mM DTT. The sample was diluted 4-fold to bring the urea concentration to 2 M, then trypsin (sequencing grade, Promega) was added at a 1:100 enzyme:substrate ratio and incubated at 37 degrees C overnight. TFA was added to 0.1% to the digested peptide mixture and the sample was desalted on a Sep-Pak Vac C18 50 mg cartridge (Waters) and lyophilized to dryness. Dried, desalted peptides were resuspended in 90% HILIC Buffer B (see below).

Hydrophilic Interaction Chromatography (HILIC) Fractionation. Buffers for HILIC fraction used were 2% ACN, 0.1% TFA (Buffer A) and 98% ACN, 0.1% TFA (Buffer B). Sample were loaded onto a 2.0 mm x 15 cm TSKgel Amide-80 column (Tosoh Biosciences) in 90% B and separated from 90% B to 50% B over one hour at a flow rate of 0.5 ml / min at room temperature using an AKTA P10 Purifier. Fractions were collected every minute (0.5 ml). The first 12 fractions containing the highest absorbance signal at 280 nm wavelength were dried down and analyzed by LC-MS/MS.

Mass Spectrometric Analysis. HILIC fractions were resuspended in 0.1% formic acid. For the first replicate analysis samples were analyzed on an LTQ Orbitrap XL mass spectrometer (Thermo Scientific) equipped with a nanoACQUITY autosampler and ultra high pressure chromatography system (Waters). 5 ul of each sample was injected onto a nanoACQUITY Symmetry C18 trap (5 um particle size, 180 um x 20 mm) in MS Buffer A (0.1% formic acid) at a flow rate of 0.4 ul/min and then separated over a nanoACQUITY BEH C18 analytical column (1.7 um particle size, 100 um x 100 mm) over 1 hour with a gradient from 2% to 25% MS Buffer B (99.9% ACN, 0.1% formic acid) at a flow rate of 0.4 ul/min. The mass spectrometer collected data in a data-dependent manner, collecting a survey scan in the Orbitrap mass analyzer at 40,000 resolution with an automatic gain control (AGC) target of $1x10^6$ followed by collision-induced dissociation (CID) MS/MS scans of the 10 most abundant ions in the ion trap with an AGC target of 5,000, a signal threshold of 1,000, a 2.0 Da isolation width, and a 30 ms activation time at 35% normalized collision energy. Charge state screening was employed to reject unassigned or 1+ charge states. Dynamic exclusion was enabled to ignore masses for 30 s that had been previously selected for fragmentation.

The second replicate was analyzed on an Orbitrap Elite mass spectrometer (Thermo Scientific) equipped with a easy-nLC II liquid chromatography system (Thermo Scientific). 5 ul of each sample was injected onto a 100 um x 2 cm C18 trap (packed with ReproSil-Pur C18-AQ 5 um particles) in MS Buffer A at a flow rate of 0.4 ul/min and then separated over a 75 um x 10 cm analytical column (packed with ReproSil-Pur C18-AQ 3 um particles) over 1 hour with a gradient from 2 to 25% MS Buffer B. The mass spectrometer collected data in a data-dependent manner, collecting a survey scan in the Orbitrap mass analyzer at 120,000 resolution with an AGC target of $1x10^6$ followed by CID MS/MS scans of the 20 most abundant ions in the ion trap with an AGC target of 5,000, a signal threshold of 500, a 2.0 Da isolation width, and a 30 ms activation time at 35% normalized collision energy. Charge state screening was employed to

159

reject unassigned or 1+ charge states. Dynamic exclusion was enabled to ignore masses for 30 s that had been previously selected for fragmentation.

The collected mass spectra were searched against all *Rattus norvegicus* sequences in the SwissProt protein sequence database concatenated to an identical database of randomized protein sequences using the Protein Prospector software suite. Randomized protein sequences were used to ensure a false positive rate less than 1% for protein identifications was achieved. Relative abundance of SILAC pairs was quantified using an in-house algorithm written in C. The algorithm calculates the ratio of area under the extracted ion chromatograms for the most abundant isotope peaks from each "light" and "heavy" SILAC pair. The algorithm also calculates three Pearson correlations the filter out low quality data: 1) the correlation of the measured and the calculated isotope distribution for the light isotope peaks, 2) the correlation of the measured and the calculated isotope distribution for the heavy isotope peaks, and 3) the correlation of the elution profiles of the light and heavy extracted ion chromatograms. Only SILAC ratios where all three correlation values were greater than 0.5 were included in the final analysis.

A Z-score metric was calculated for each protein identified and quantified by at least two different peptides using a script written in Perl. The Z-score metric is calculated as follows:

$$Z = \frac{m - M_n}{S_n}$$

where *m* is the median of log ratios for a protein detected with *n* different peptides, M_n is the median of 1000 random samplings of the median of *n* log ratios from the entire data set, and S_n is the standard deviation of 1000 random samplings of the median of *n* log ratios from the entire data set.

Secretion assays

For secretion time course experiments, PC12 cells were transduced with lentivirus at the time of plating. Cells were transfected with siRNA on days 1 and 3 after plating, then washed 2 days

later and incubated in Tyrode's solution containing 50 mM K^+ for a total of 32 min at 37°C. Aliquots of Tyrode's were removed at the time points indicated in Figs. 4 and 5, and mixed immediately with SDS-PAGE sample buffer. SgII was measured by quantitative fluorescent immunoblotting, with secreted SgII normalized to total cellular protein (Bradford assay) or cellular SgII. For other secretion assays, cells were transfected with siRNA as above, then washed 2 days later and incubated in Tyrode's solution containing 2.5 mM K^+ (basal) or 50 mM K^+ (stimulated) for 30 min at 37°C. The supernatants were collected, cell lysates prepared as previously described (Li et al., 2005), and the samples analyzed as above. In the t-SNARE over-expression experiments, ANF-GFP was used as a reporter for regulated secretion, and ss-GFP used for assessing constitutive secretion. For these experiments, secretion and storage of the reporter proteins were measured using a florescent plate reader (Tecan).

References

Asensio, C.S., Sirkis, D.W., and Edwards, R.H. (2010). RNAi screen identifies a role for adaptor protein AP-3 in sorting to the regulated secretory pathway. J Cell Biol *191*, 1173–1187.

Banerjee, A., Kowalchyk, J.A., DasGupta, B.R., and Martin, T.F.J. (1996). SNAP-25 is required for a late postdocking step in Ca2+-dependent exocytosis. J Biol Chem *271*, 20227–20230.

Bittner, M.A., Bennett, M.K., and Holz, R.W. (1996). Evidence that syntaxin 1A is involved in storage in the secretory pathway. J Biol Chem *271*, 11214–11221.

Cai, T., Hirai, H., Zhang, G., Zhang, M., Takahashi, N., Kasai, H., Satin, L.S., Leapman, R.D., and Notkins, A.L. (2011). Deletion of Ia-2 and/or Ia-2β in mice decreases insulin secretion by reducing the number of dense core vesicles. Diabetologia *54*, 2347–2357.

Chen, Z.-Y., Ieraci, A., Teng, H., Dall, H., Meng, C.-X., Herrera, D.G., Nykjaer, A., Hempstead, B.L., and Lee, F.S. (2005). Sortilin controls intracellular sorting of brain-derived neurotrophic factor to the regulated secretory pathway. J Neurosci *25*, 6156–6166.

Cool, D.R., Normant, E., Shen, F., Chen, H.C., Pannell, L., Zhang, Y., and Loh, Y.P. (1997). Carboxypeptidase E is a regulated secretory pathway sorting receptor: genetic obliteration leads to endocrine disorders in Cpe(fat) mice. Cell *88*, 73–83.

Cowles, C.R., Odorizzi, G., Payne, G.S., and Emr, S.D. (1997). The AP-3 adaptor complex is essential for cargo-selective transport to the yeast vacuole. Cell *91*, 109–118.

Darsow, T., Burd, C.G., and Emr, S.D. (1998). Acidic di-leucine motif essential for AP-3-dependent sorting and restriction of the functional specificity of the Vam3p vacuolar t-SNARE. J Cell Biol *142*, 913–922.

De Felipe, C., Herrero, J.F., O'Brien, J.A., Palmer, J.A., Doyle, C.A., Smith, A.J., Laird, J.M., Belmonte, C., Cervero, F., and Hunt, S.P. (1998). Altered nociception, analgesia and aggression in mice lacking the receptor for substance P. Nature *392*, 394–397.

Fernández-Chacón, R., Königstorfer, A., Gerber, S.H., García, J., Matos, M.F., Stevens, C.F., Brose, N., Rizo, J., Rosenmund, C., and Südhof, T.C. (2001). Synaptotagmin I functions as a calcium regulator of release probability. Nature *410*, 41–49.

Fields, H. (2004). State-dependent opioid control of pain. Nat Rev Neurosci *5*, 565–575.

Foran, P., Lawrence, G.W., Shone, C.C., Foster, K.A., and Dolly, J.O. (1996). Botulinum neurotoxin C1 cleaves both syntaxin and SNAP-25 in intact and permeabilized chromaffin cells: correlation with its blockade of catecholamine release. Biochemistry *35*, 2630–2636.

Gerber, S.H., Rah, J.-C., Min, S.-W., Liu, X., de Wit, H., Dulubova, I., Meyer, A.C., Rizo, J., Arancillo, M., Hammer, R.E., et al. (2008). Conformational switch of syntaxin-1 controls synaptic vesicle fusion. Science *321*, 1507–1510.

Gomi, H., Mizutani, S., Kasai, K., Itohara, S., and Izumi, T. (2005). Granuphilin molecularly docks insulin granules to the fusion machinery. J Cell Biol *171*, 99–109.

Harashima, S.-I., Clark, A., Christie, M.R., and Notkins, A.L. (2005). The dense core transmembrane vesicle protein IA-2 is a regulator of vesicle number and insulin secretion. Proc Natl Acad Sci USA *102*, 8704–8709.

Henquin, J.-C., Nenquin, M., Szollosi, A., Kubosaki, A., and Notkins, A.L. (2008). Insulin secretion in islets from mice with a double knockout for the dense core vesicle proteins islet antigen-2 (IA-2) and IA-2beta. J. Endocrinol. *196*, 573–581.

Khvotchev, M., and Südhof, T.C. (2004). Proteolytic processing of amyloid-beta precursor protein by secretases does not require cell surface transport. J Biol Chem *279*, 47101–47108.

Kim, T., Tao-Cheng, J.H., Eiden, L.E., and Loh, Y.P. (2001). Chromogranin A, an "on/off" switch controlling dense-core secretory granule biogenesis. Cell *106*, 499–509.

Klumperman, J., Kuliawat, R., Griffith, J.M., Geuze, H.J., and Arvan, P. (1998). Mannose 6-phosphate receptors are sorted from immature secretory granules via adaptor protein AP-1, clathrin, and syntaxin 6-positive vesicles. J Cell Biol *141*, 359–371.

Krantz, D.E., Waites, C.L., Oorschot, V., Liu, Y., Wilson, R.I., Tan, P.K., Klumperman, J., and Edwards, R.H. (2000). A phosphorylation site regulates sorting of the vesicular acetylcholine transporter to dense core vesicles. J Cell Biol *149*, 379–396.

Lang, T., Margittai, M., Hölzler, H., and Jahn, R. (2002). SNAREs in native plasma membranes are active and readily form core complexes with endogenous and exogenous SNAREs. J Cell Biol *158*, 751–760.

Li, H., Waites, C.L., Staal, R.G., Dobryy, Y., Park, J., Sulzer, D.L., and Edwards, R.H. (2005). Sorting of vesicular monoamine transporter 2 to the regulated secretory pathway confers the somatodendritic exocytosis of monoamines. Neuron *48*, 619–633.

Liu, Y., Schweitzer, E.S., Nirenberg, M.J., Pickel, V.M., Evans, C.J., and Edwards, R.H. (1994). Preferential localization of a vesicular monoamine transporter to dense core vesicles in PC12 cells. J Cell Biol *127*, 1419–1433.

Lois, C., Hong, E.J., Pease, S., Brown, E.J., and Baltimore, D. (2002). Germline transmission and tissue-specific expression of transgenes delivered by lentiviral vectors. Science *295*, 868–872.

Lowe, A.W., Madeddu, L., and Kelly, R.B. (1988). Endocrine secretory granules and neuronal synaptic vesicles have three integral membrane proteins in common. J Cell Biol *106*, 51–59.

Lynch, K.L., and Martin, T.F.J. (2007). Synaptotagmins I and IX function redundantly in regulated exocytosis but not endocytosis in PC12 cells. J Cell Sci *120*, 617–627.

Morvan, J., and Tooze, S.A. (2008). Discovery and progress in our understanding of the regulated secretory pathway in neuroendocrine cells. Histochem Cell Biol *129*, 243–252.

Murtra, P., Sheasby, A.M., Hunt, S.P., and De Felipe, C. (2000). Rewarding effects of opiates are absent in mice lacking the receptor for substance P. Nature *405*, 180–183.

Nakajima, K., Wu, G., Sakudo, A., Onodera, T., and Takeyama, N. (2011). Distinct subcellular localization of three isoforms of insulinoma-associated protein 2β in neuroendocrine tissues. Life Sci. *88*, 798–802.

Nishimura, T., Harashima, S.-I., Yafang, H., and Notkins, A.L. (2010). IA-2 modulates dopamine secretion in PC12 cells. Mol Cell Endocrinol *315*, 81–86.

Orci, L., Ravazzola, M., Amherdt, M., Perrelet, A., Powell, S.K., Quinn, D.L., and Moore, H.P. (1987). The trans-most cisternae of the Golgi complex: a compartment for sorting of secretory and plasma membrane proteins. Cell *51*, 1039–1051.

Otto, H., Hanson, P.I., and Jahn, R. (1997). Assembly and disassembly of a ternary complex of

synaptobrevin, syntaxin, and SNAP-25 in the membrane of synaptic vesicles. Proc Natl Acad Sci USA *94*, 6197–6201.

Papini, E., Rossetto, O., and Cutler, D.F. (1995). Vesicle-associated membrane protein (VAMP)/synaptobrevin-2 is associated with dense core secretory granules in PC12 neuroendocrine cells. J Biol Chem *270*, 1332–1336.

Rabin, D.U., Pleasic, S.M., Shapiro, J.A., Yoo-Warren, H., Oles, J., Hicks, J.M., Goldstein, D.E., and Rae, P.M. (1994). Islet cell antigen 512 is a diabetes-specific islet autoantigen related to protein tyrosine phosphatases. J. Immunol. *152*, 3183–3188.

Sadoul, K., Lang, J., Montecucco, C., Weller, U., Regazzi, R., Catsicas, S., Wollheim, C.B., and Halban, P.A. (1995). SNAP-25 is expressed in islets of Langerhans and is involved in insulin release. J Cell Biol *128*, 1019–1028.

Schonn, J.-S., Maximov, A., Lao, Y., Südhof, T.C., and Sørensen, J.B. (2008). Synaptotagmin-1 and -7 are functionally overlapping Ca2+ sensors for exocytosis in adrenal chromaffin cells. Proc Natl Acad Sci USA *105*, 3998–4003.

Schuldiner, O., Berdnik, D., Levy, J.M., Wu, J.S., Luginbuhl, D., Gontang, A.C., and Luo, L. (2008). piggyBac-based mosaic screen identifies a postmitotic function for cohesin in regulating developmental axon pruning. Dev Cell *14*, 227–238.

Solimena, M., Dirkx, R., Hermel, J.M., Pleasic-Williams, S., Shapiro, J.A., Caron, L., and Rabin, D.U. (1996). ICA 512, an autoantigen of type I diabetes, is an intrinsic membrane protein of neurosecretory granules. Embo J *15*, 2102–2114.

Sossin, W.S., Fisher, J.M., and Scheller, R.H. (1990). Sorting within the regulated secretory pathway occurs in the trans-Golgi network. J Cell Biol *110*, 1–12.

Tooze, S.A., and Huttner, W.B. (1990). Cell-free protein sorting to the regulated and constitutive secretory pathways. Cell *60*, 837–847.

Torii, S. (2009). Expression and function of IA-2 family proteins, unique neuroendocrine-specific protein-tyrosine phosphatases. Endocrine Journal *56*, 639–648.

Varlamov, O., and Fricker, L.D. (1998). Intracellular trafficking of metallocarboxypeptidase D in AtT-20 cells: localization to the trans-Golgi network and recycling from the cell surface. J Cell Sci *111 (Pt 7)*, 877–885.

Varlamov, O., Wu, F., Shields, D., and Fricker, L.D. (1999). Biosynthesis and packaging of carboxypeptidase D into nascent secretory vesicles in pituitary cell lines. J Biol Chem *274*, 14040–14045.

Wang, D., Zhang, Z., Dong, M., Sun, S., Chapman, E.R., and Jackson, M.B. (2011a). Syntaxin requirement for Ca2+-triggered exocytosis in neurons and endocrine cells demonstrated with an engineered neurotoxin. Biochemistry *50*, 2711–2713.

Wang, H., Ishizaki, R., Kobayashi, E., Fujiwara, T., Akagawa, K., and Izumi, T. (2011b). LOSS OF GRANUPHILIN AND OF SYNTAXIN-1A CAUSE DIFFERENTIAL EFFECTS ON INSULIN GRANULE DOCKING AND FUSION. J Biol Chem.

Wasmeier, C., Bright, N.A., and Hutton, J.C. (2002). The lumenal domain of the integral membrane protein phogrin mediates targeting to secretory granules. Traffic *3*, 654–665.

Wegrzyn, J., Lee, J., Neveu, J.M., Lane, W.S., and Hook, V. (2007). Proteomics of neuroendocrine

secretory vesicles reveal distinct functional systems for biosynthesis and exocytosis of peptide hormones and neurotransmitters. Journal of Proteome Research *6*, 1652–1665.

Wu, R.R., and Couchman, J.R. (1997). cDNA cloning of the basement membrane chondroitin sulfate proteoglycan core protein, bamacan: a five domain structure including coiled-coil motifs. J Cell Biol *136*, 433–444.

Xu, T., and Bajjalieh, S.M. (2001). SV2 modulates the size of the readily releasable pool of secretory vesicles. Nat Cell Biol *3*, 691–698.

CHAPTER 6: CONCLUSIONS AND FUTURE DIRECTIONS

Manuscripts reprinted or discussed in this dissertation which are published, under review or in preparation:

1. <u>Chapter 3</u>. Asensio, C.S., **Sirkis, D.W.**, and Edwards, R.H. (2010). RNAi screen identifies a role for adaptor protein AP-3 in sorting to the regulated secretory pathway. *Journal of Cell Biology* 191, 1173–1187.

   > In this paper we describe a large-scale RNAi screen carried out to identify factors involved in the biogenesis of the regulated secretory pathway (RSP). We identified multiple subunits of the heterotetrameric AP-3 complex, and went on characterize AP-3's role in enabling regulated secretion in neuroendocrine PC12 cells. We found that AP-3 knockdown dysregulated the release of both membrane and soluble large dense-core vesicle (LDCV) proteins, reduced the number of LDCVs and altered their morphology. In addition, we found that the loss AP-3 resulted in a defect in the formation of LDCVs at the *trans*-Golgi network (TGN), and was also associated with mis-sorting of the calcium sensor protein, synaptotagmin 1, away from LDCVs. The latter finding suggested that AP-3 might contribute to RSP formation by concentrating within nascent LDCVs the membrane proteins required for regulated release.

2. <u>Chapter 4</u>. **Sirkis, D.W.**, Asensio, C.S., and Edwards, R.H. Widespread dysregulation of peptide hormone release in mice lacking adaptor protein AP-3. Submitted to *Proceedings of the National Academy of Sciences USA* in October 2012, and currently under review.

   > In this manuscript, we ask whether loss of AP-3 *in vivo* is sufficient to dysregulate secretion from neuroendocrine cells. We find that AP-3-deficient *mocha* mice indeed exhibit dysregulated secretion of both soluble and membrane LDCV proteins from adrenal chromaffin cells. We also show that pancreatic islet cells from *mocha* mice exhibit dysregulated release of insulin and glucagon, suggesting widespread dysregulation of peptide hormone secretion. Using mouse genetics, we show that loss of both the ubiquitous and neuronal forms of AP-3 is required to impair LDCV production. In addition, we find that the marked reduction in cellular levels of secretogranin seen in AP-3-deficient neuroendocrine cells can be accounted for by augmented basal release and decreased expression, but not increased degradation. Finally, we show that loss of the related adaptor protein AP-1 alone is not sufficient to impair regulated secretion in PC12 cells, but rather that its knockdown markedly exacerbates the impairment in regulated secretion observed with AP-3 knockdown, indicating distinct roles for these two adaptors in forming the RSP.

3. Chapter 5. **Sirkis, D.W.**, Asensio, C.S., Johnson, J.R., Krogan, N.J., and Edwards, R.H. Quantitative proteomics implicates AP-3-mediated exclusion of t-SNAREs in the regulation of secretion. In preparation.

    > In this manuscript, we use quantitative proteomics to define the set of LDCV cargo proteins altered upon loss of the adaptor AP-3. We show that the levels of multiple functionally important membrane proteins are reduced after the loss of AP-3, but that knockdown of several of these identified proteins is not sufficient to perturb regulated secretion. In contrast, we find that levels of several t-SNAREs and associated proteins are increased on LDCVs after loss of AP-3, and we find that over-expression of one such protein, syntaxin-1A is sufficient to strongly impair regulated release in PC12 cells. This work has suggested several new models for AP-3's role in forming the RSP, and also implicates the exclusion of t-SNAREs as an important mechanism for enabling the regulation of secretion.

4. Asensio, C.S., **Sirkis, D.W.**, Egami, K., Brodsky, F.M., Cheng, Y., and Edwards, R.H. Self-Assembly of VPS41 Drives Formation of the Regulated Secretory Pathway. Submitted to *Developmental Cell* in October 2012, and currently under revision.

    > In this manuscript, which has not been described in detail in this dissertation, we identify the AP-3-interacting protein VPS41 as a factor essential for enabling regulated secretion in PC12 cells. Depletion of VPS41 by RNAi produces a phenotype nearly identical to that produced by loss of AP-3, and this effect occurs independently of VPS41's role in fusion at the late endosome and lysosome. In addition, we find that recombinant VPS41 self-assembles into a lattice, and this property seems to be required for regulated secretion. These findings suggest a model in which VPS41 acts as a coat protein in conjunction with adaptor protein AP-3 in the biogenesis of the RSP.

    > For this manuscript, I suggested conducting the RNAi screen for factors known to interact genetically or physically with AP-3, which led to the identification of VPS41. I was also involved in cloning rat VPS41, and frequently discussed methods and interpretation of data with C. Asensio.

In this dissertation, I have begun with a historical perspective on the morphological origins of our current understanding of regulated secretory pathway biogenesis. In the more than 50 years since vesicles of the regulated pathway were suggested to form at the Golgi apparatus, we still have only a modest appreciation of the factors involved in shaping the pathway. Thus, despite some progress, many fundamental questions remain unanswered. For example, for the membrane proteins that rely on cytosolic trafficking motifs for entry into the large dense-core vesicles (LDCVs) of the regulated secretory pathway, the identity of the machinery that directs their sorting has remained unknown. Moreover, we have not yet identified the factors involved specifically in forming LDCVs at the trans-Golgi network (TGN), as opposed to those which produce the constitutive secretory vesicles found in all cells.

By undertaking a new approach to tackle this problem, we identified the heterotetrameric adaptor protein AP-3 as an important factor in the biogenesis of the regulated secretory pathway. This result was initially surprising given that mammalian AP-3 has generally been considered to act in the endolysosomal pathway. After we identified AP-3 by screening in *Drosophila* S2 cells, we conducted an array of functional experiments in the mammalian neuroendocrine PC12 cell line. These experiments indicated that AP-3-deficient mice should also have a defect in the regulation of secretion from neuroendocrine cells, and this indeed appears to be the case. Our finding that synaptotagmin is not sorted effectively to LDCVs in the absence of AP-3 led us to formulate a model for AP-3's action (Fig. 1 A and B), and to carry out quantitative proteomic analysis, which enabled us to identify a variety of LDCV membrane proteins altered by the loss of AP-3. Strikingly, an increase in the levels of the t-SNARE, syntaxin-1A, identified in the proteomics, could apparently be responsible for AP-3's role in regulating secretion. This finding leads us to other possible models for AP-3's action in forming the RSP (Fig. 1 C). In parallel, Cédric Asensio has identified the AP-3-interacting, self-assembling protein, VPS41, as being similarly required for the regulation of secretion, and we suggest that these two proteins may act together as adaptor and coat in the formation of the regulated secretory pathway.
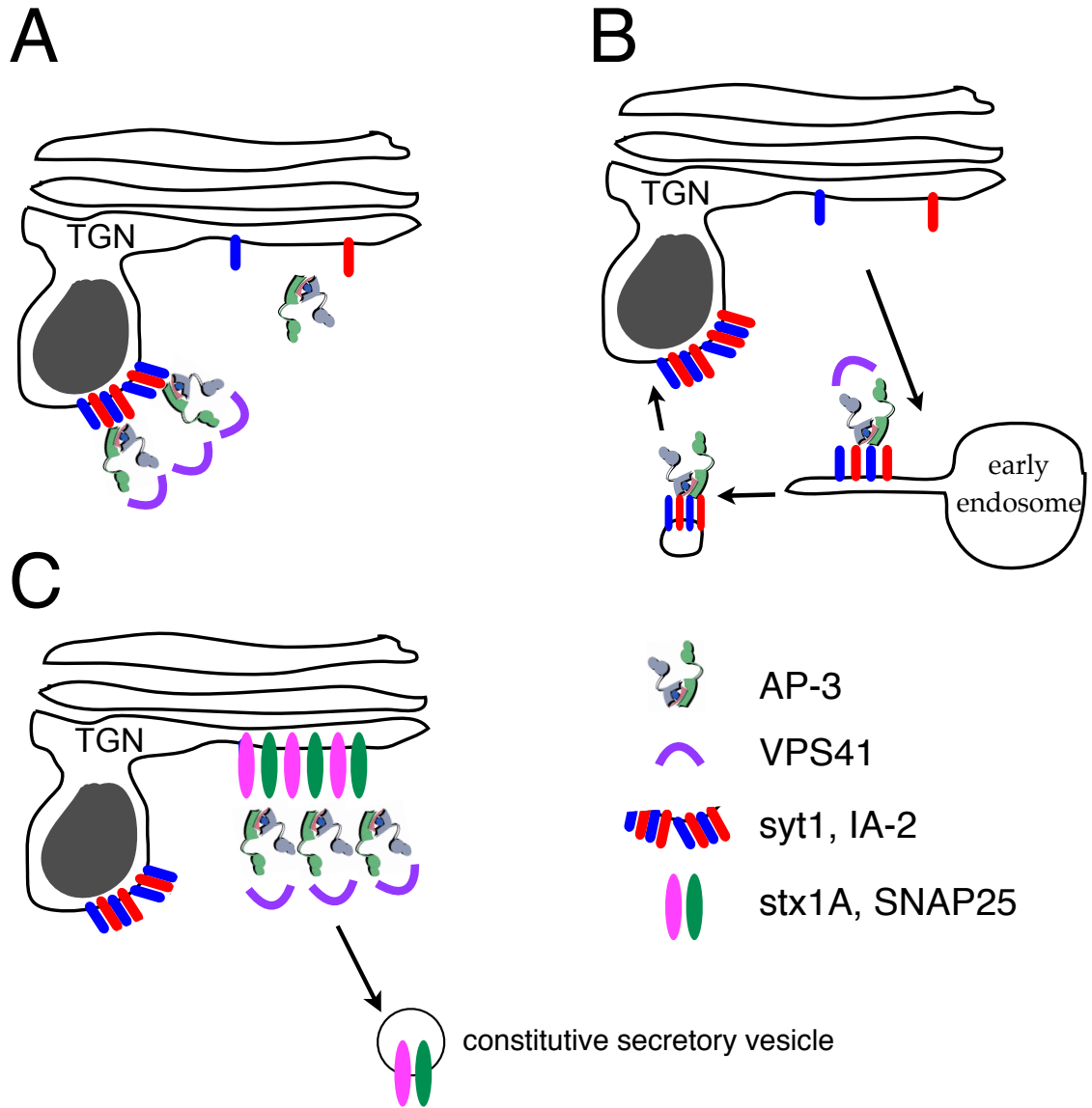
Figure 1. Models for the action of AP-3 and VPS41 in biogenesis of the regulated secretory pathway
AP-3 and VPS41 may act as adaptor and coat at either the TGN (A) or early endosome (B) to concentrate proteins for inclusion within nascent LDCVs. Model A involves only concentration of proteins at the site of LDCV formation, whereas model B requires formation of early endosome-derived transport vesicles and their subsequent fusion with newly formed LDCVs. Model A is attractive because it requires fewer speculative transport steps than model B, and in yeast, the homologs of AP-3 and VPS41 have both been shown to produce transport vesicles at the TGN. Model B, on the other hand, situates AP-3 more comfortably at its well-accepted primary location in mammalian cells, the early endosome. However, this localization has not been observed for VPS41. In addition, canonical LDCVs have not been shown to incorporate membrane proteins after their formation at the TGN. Models A and B both assume that AP-3 and VPS41 primarily act to concentrate membrane proteins for their inclusion within the RSP. Model C illustrates an alternative hypothesis, derived from the proteomic analysis, showing that AP-3 (and potentially VPS41) might instead promote the exclusion of t-SNAREs, such as stx1A, from LDCVs by sorting them into constitutive secretory vesicles for direct delivery to the cell surface. Cartoon adapted with permission from C. Asensio.
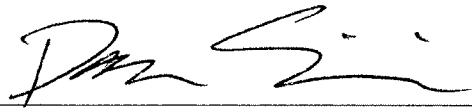
Future directions

There are several areas worthy of further exploration. First, now that we have demonstrated dysregulated peptide hormone secretion from several neuroendocrine cell types in AP-3-deficeint mice, it would be interesting to assess the function of neuropeptide- and growth factor-releasing cells in the brain. In addition, we will soon test the role of VPS41 in regulating secretion *in vivo*, using a conditional knockout mouse. In terms of the more basic mechanistic questions, we would like to determine whether AP-3 and VPS41 act directly at the TGN, the site of LDCV formation. Newer ultrastructural labeling techniques, currently being tested in the lab, may enable more-precise localization than we have been able to achieve so far. Further experiments to test whether over-expressed syntaxin-1A mediates its inhibitory effect directly from the LDCV, or from some other location, are currently underway. Along these lines, we will also ask whether the presence of stx1A is required for the effect of AP-3 knockdown on regulated secretion. Finally, with regard to the models presented in Figure 1, it will be interesting to see, as these experiments progress, whether AP-3 and VPS41 act primarily in concentrating the proteins required for regulated release, or whether they instead act primarily to prevent inappropriate inclusion of specific proteins, such as the t-SNAREs, within the regulated secretory pathway.

Publishing Agreement

It is the policy of the University to encourage the distribution of all theses, dissertations, and manuscripts. Copies of all UCSF theses, dissertations, and manuscripts will be routed to the library via the Graduate Division. The library will make all theses, dissertations, and manuscripts accessible to the public and will preserve these to the best of their abilities, in perpetuity.

Please sign the following statement:

I hereby grant permission to the Graduate Division of the University of California, San Francisco to release copies of my thesis, dissertation, or manuscript to the Campus Library to provide access and preservation, in whole or in part, in perpetuity.

_____   12/4/12

Author Signature   Date